Mathematical modelling of dog rabies transmission in N'Djamena, Chad

Inauguraldissertation

zur

Erlangung der Würde eines Doktors der Philosophie

vorgelegt der

Philosophisch-Naturwissenschaftlichen Fakultät

der Universität Basel

von

Mirjam Laager

aus

Glarus Nord (GL)

Basel, 2018

Genehmigt von der Philosophisch-Naturwissenschaftlichen Fakultät auf Antrag von

Prof. Dr. Jürg Utzinger (Fakultätsverantwortlicher)

PD Dr. Nakul Chitnis (Dissertationsleiter)

Prof. Dr. Matt Keeling (Korreferent/in)

Basel, den *22. Mai 2018*

Prof. Dr. Martin Spiess

Contents

1. Acknowledgements

This dissertation would not have been possible without the support of many people. My sincerest thanks to Nakul Chitnis, for your continuous guidance, support and useful advice. Thank you to Jakob Zinsstag, for your enthusiasm and the many inspiring discussions. Thank you to Timo Smieszek: Each skype call with you created five answers and ten new questions. Thank you to Matt Keeling for acting as external examiner in the PhD committee. The models developed in this thesis are based on hard-earned data, which would not have been accessible to me without Céline Mbilo and Monqiue Léchenne. Thank you for contributing your expertise and experience with rabies in Chad. It has been a pleasure to work with you. I would like to express my gratitude to the Swiss National Science Foundation for funding this work and the Freiwillige Akademische Gesellschaft as well as the Albert Heim Stiftung for contributing funding towards the contact sensors. Thank you to all my colleagues, mentors and friends in the Infectious Disease Modelling Unit for offering valuable advice, encouragement and chocolate. Thank you to Tom Smith for proofreading several sections of the thesis and to Christine Bürli and Jürg Furrer for helpful comments. Thank you to the Swiss TPH and its director, Jürg Utzinger. I am deeply grateful for the time I could spend at this unique institute. Finally, to my family and friends who have supported my throughout the years: Thank you.

2. Zusammenfassung

Tollwut ist eine virale Erkrankung, die durch Bisse übertragen wird und die unbehandelt zu einer fast immer tödlichen Entzündung des Gehirns führt. Alle warmblütigen Tiere können an Tollwut erkranken. Erregerreservoire umfassen eine Vielzahl von Arten unter anderem Füchse, Waschbären, Fledermäuse und Hunde. Pro Jahr sterben ungefähr 60'000 Menschen an Tollwut, vorwiegend in Afrika und Asien. Die meisten Ansteckungen von Menschen erfolgen durch Hunde. Tollwut kann durch präventive Impfungen sowie durch eine sogenannte Postexpositionsprophylaxe, die Verabreichung von Impfstoff und Immunoglobulin unmittelbar nach einem Biss, verhindert werden. Durch Impfung von Hunden kann das Risiko einer Ansteckung von Menschen reduziert werden. In West- und Zentraleuropa wurde zudem die Fuchstollwut mit oralen Impfködern ausgerottet.

In N'Djamena, der Hauptstadt des Tschad, ist Tollwut endemisch mit ca. einem Fall von Hundetollwut pro Woche. Jeder dieser Hunde beisst durchschnittlich zwei Menschen. In den Jahren 2012 und 2013 wurden zwei Hundeimpfkampagnen durchgeführt mit dem Ziel, die Hundetollwut in N'Djamena auszurotten. In beiden Kampagnen wurden 70% aller Hunde geimpft. Das führte zu einer Unterbrechung der Übertragung. Neun Monate lang traten keine Tollwutfälle mehr auf, danach etablierte sich die Übertragung jedoch wieder auf dem selben Stand wie vor den Impfkamagnen. Um das Bewegungs- und Kontaktverhalten von Hunden besser zu verstehen, wurden im Jahr 2016 in drei verschiedenen Quartieren von N'Djamena 300 Hunde mit GPS und Kontaktsensoren ausgestattet.

Wir haben drei mathematische Modelle für die Übertragung von Tollwut entwickelt und diese mit Hilfe der während den Impfkampagnen gesammelten Daten zu Hundepopulation und Tollwutfällen sowie der von den GPS und Kontaktsensoren aufgezeichneten Bewegungs- und Kontaktmessungen parametrisiert. Mit einem Modell, das auf gewöhnlichen Differentialgleichungen basiert, konnten wir zeigen, dass die Reproduktionsrate der Tollwut nach den Impfkampagnen unter 1 sank. Die Impfkampagnen haben also zu einer Unterbrechung der Übertragung geführt. Mit dem Gillespie Algorithmus haben wir eine stochastische Version des Modells implementiert und die Unterbrechung der Übertragung bestätigt. Zudem konnten wir zeigen, dass die hohe Hundesterblichkeit mehr zum Rückgang der Durchimpfungsrate nach den Kampagnen beitrug als individueller Immunitätsverlust. Verschiedene Gründe könnten dazu geführt haben, dass schon neun Monate nach den Kampagnen erneut Tollwutfälle auftraten. Erstens ist in N'Djamena die Anzahl Hunde von Quartier zu Quartier verschieden und schwankt von 300 bis zu nur 10 Hunde pro Quadratkilometer. Während den Impfkampagnen wurden nicht überall gleich viele Hunde geimpft. Diese Heterogenität könnte dazu geführt haben, dass Tollwut in manchen Quartieren schneller zurückkam. Zweitens basieren die Tollwutfalldaten auf passiver Überwachung, das heisst, Hundebesitzer können bei Tollwutverdacht ihren toten Hund für eine Untersuchung vorbeibringen. Dies ist jedoch freiwillig und daher gibt es wahrscheinlich viele Fälle, die nicht registriert werden. Drittens könnten auch infizierte Hunde von ausserhalb der Stadt die Tollwut wieder eingeschleppt haben. Mit einem Metapopulationsmodell

haben wir diese drei Gründe untersucht. Unsere Ergebnisse zeigen, dass der Import infizierter Hunde die Falldaten besser erklärt als Heterogenität oder lückenhafte Überwachung. Da der Import der wahrscheinlichste Grund für die Reetablierung der Tollwut ist, untersuchten wir die durch importierte Fälle ausgelösten Übertragungsketten. Um die Kontaktstruktur der Hundepopulation realistisch abzubilden, haben wir die Daten aus den 300 GPS und Kontaktsensoren verwendet, um ein Netzwerk aus 4000 Hunden zu generieren. Da es keine etablierte Methode für die Extrapolation eines empirisch gemessenen Netzwerks auf ein synthetisches Netzwerk mit mehr Knoten gibt, haben wir einen Netzwerkgenerierungsalgorithmus entwickelt und validiert. Mit einem individuenbasierten Modell, dessen Übertragungsrate so parametrisiert wurde, dass die Simulationsergebnisse mit den Falldaten in N'Djamena übereinstimmen, konnten wir zeigen, dass eine Impfabdeckung von 70% zwar grössere Ausbrüche verhindert, nicht aber kurze Übertragungsketten von ca. 4 bis 5 Hunden. Da stark vernetzte Hunde eine zentrale Rolle bei der Übertragung spielen, könnte das Impfen solcher Hunde die Wirkung von Impfstrategien erhöhen.

Hunde gegen Tollwut zu impfen reduziert das Risko einer Ansteckung von Menschen und hat zudem den Vorteil, dass die Risikoreduktion allen Menschen, unabhängig von ihrem sozioökonomischen Status gleichermassen zu Gute kommt. Daher sollte das Impfen von Hunden ein fester Bestandteil von Tollwutbekämpfungsprogrammen sein. Da aber bei unkontrollierten Hundepopulationen die Impfdeckung aufgrund der hohen Hundesterblickeit sehr schnell abnimmt, sind die Ergebnisse einer Impfkampagne durch Import von umgebenden Regionen oder Übertragung aus Wildtierreservoiren bedroht. Daher sollte eine hohe Durchimpfungsrate aufrecht erhalten werden, durch wiederholte Impfkampagen oder kontinuierliche Impfungen durch Veterinäre, und auch die orale Impfung von Wildtieren (die hier nicht untersucht wurde) könnte ein Bestandteil eines Tollwutbekämpfungsprogramms in N'Djamena sein.

3. Summary

Background Rabies is a viral disease that is transmitted by bite and is fatal after the onset of symptoms. All warm blooded animals are susceptible to rabies and a wide range of species including foxes, wolves, jackals, raccoons, mongooses and bats act as reservoir hosts. Approximately 60,000 people die of rabies every year, mainly in Africa and Asia. The main source of human rabies is the domestic dog. Rabies in humans is preventable by timely administration of post-exposure prophylaxis, with a reduced schedule of administration if the person was protected by pre-exposure prophylaxis. Mass vaccination of dogs is considered effective in preventing human exposure and oral vaccine baits were used to eliminate rabies from foxes in central and western Europe.

In N'Djamena, the capital of Chad, rabies is endemic with approximately one confirmed case of dog rabies per week. Each dog exposes on average two humans. In 2012 and 2013 two mass vaccination campaigns of dogs were conducted, reaching a coverage of more than 70% in both years. The campaigns interrupted transmission for nine months, but a resurgence of cases led to re-establishment of rabies at the pre-intervention endemic state. To better understand the movement and contact behaviour of dogs, 300 geo-located contact sensors were deployed on dogs in three different quarters of N'Djamena in 2016.

Methods and Results We developed three mathematical models of rabies transmission, calibrated to the incidence data and coverage levels from the campaigns and data on dog movement and contacts from the geo-located contact sensors. We used an ordinary differential equation model to assess the effect of the vaccination campaigns and found that after the campaigns, the effective reproductive ratio dropped below one. Implementing a stochastic version of the model with the Gillespie algorithm confirmed the interruption of transmission. We found that population turnover contributed more to the decrease of vaccination coverage after the campaigns than individual immunity loss. Possible reasons for the resurgence of cases after the campaigns include spatial heterogeneity of vaccination coverage and dog density, underreporting and importation of latent dogs from the surroundings of N'Djamena. We developed a deterministic metapopulation model with importation of latent dogs to investigate the potential reasons for the resurgence seen in 2014. Our results indicate that importation of latently infected dogs better explains the incidence data than heterogeneity or underreporting. Because importation seems to be the most likely reason for the resurgence in cases, we investigated the chains of transmission triggered by imported cases. In order to realistically reproduce the contact heterogeneity at individual level, we used data from 300 geo-located contact sensors to build a network of 5000 dogs. Since there is no established method for expanding a network to a network with more nodes, we have developed and validated a network construction algorithm. We developed an individual based model and calibrated the transmission rate such that the simulation results correspond to outbreak data from two quarters in N'Djamena. We have shown that 70% coverage prevents major but not minor outbreaks. Since highly connected dogs hold a critical role in rabies transmission, vaccinating such dogs could increase the effect of vaccination strategies.

Conclusions Vaccinating dogs is an effective and equitable way of reducing human exposure and should therefore be an inherent of part rabies control programmes in endemic settings. However, in the absence of dog population management, population turnover quickly reduces vaccination coverage and reintroduction from surrounding areas or spillovers from wildlife reservoirs threaten the gains of mass dog vaccination campaigns. This suggests that maintaining high vaccination coverage by either repeated mass vaccination campaigns or continuous vaccination of dogs as well as oral vaccination of reservoirs (which was not investigated here) might be part of the best intervention package for settings like N'Djamena.

4. Introduction

4.1 Rabies: The disease, its transmission and control

Rabies in the past

Rabies has frightened mankind for centuries. Dating back almost 2000 years before Christ, the Sumerian Laws of Eshnunna determined punishments for dog owners whose knowingly rabid dog bit a man and caused his death (Tarantola, 2017). The Susruta Samhita, a text of the traditional medicine Ayurveda, describes the frightening symptoms of rabies including the flow of saliva, muscular spasms, biting and fear of water (Wasik and Murphy, 2012, p. 20). Still today, these symptoms appear in names for rabies, like in Latin *hydrophobia* (fear of water), Greek *lyssa* (wolfish fury, madness) or French *rage*. The German word *Hundswuth*, which was the standard term before in the 19th-century it was replaced by *Tollwut*, even names the most common source of human rabies, the dog. Rabies is terrifying because it leads to an agonising death. It is transmitted via a bite, as in legends of werewolves (Wasik and Murphy, 2012, p. 69) and vampires (Gomez-Alonso, 1998). The symptoms seem to transform a human into a wild beast (Andry, 1780) or furious wolf (Gastaut and Miletto, 1955) and cause fear of water, a symbol of purity in many cultures. It is therefore not surprising that during rabies outbreaks the fear of rabies regularly culminated in mass dog killings. During the "Great Dog Massacre" in 1897, almost ten thousand dogs were slaughtered in the streets of Paris (Wasik and Murphy, 2012, p. 100). Less violent measures of combating rabies were taken for example in Frankfurt, where the authorities introduced dog taxes to reduce the dog population in 1803 (Steinbrecher, 2008). Dog owners were obliged to buy a tag from the knacker and attach it to the collar of their dog. Dogs without a tag were killed. Towards the end of the 19th-century control measures such as muzzling, movement restriction, tracing of rabid dogs and their contacts and strict import regulations were implemented in many European countries (Müller et al., 2012). But even though dogs were identified as the primary transmitter of rabies to humans, the cause of the disease remained invisible. The fact that not every bite from a rabid dog leads to an infection of the affected human further increased the confusion around how to prevent rabies. Rabies treatment included numerous methods ranging from cauterization to rubbing the dead dog's brain tissue on the bite wound (Tarantola, 2017).

As early as in incantations of the Old Babylonian period, the saliva of the dog was detected as the means of transmission (Cunningham, 1997), and already in 1546 the Italian physician Girolamo Fracastoro described rabies as an infective germ with an affinity for the nerves (Fracastoro, 1546, p. 65), but it was not until the 1880s that an effective treatment was discovered. In that year the German doctor Robert Koch published his famous postulates on the relationship between microbes and disease (Drews, 2015, p. 49), which could be summarized as "one disease, one microbe." After having successfully experimented with immunizations against chickenpox and anthrax, Louis Pasteur strongly agreed with this principle. Since he profoundly valued human applications, he might even have extended this slogan to "one disease, one microbe, one

vaccine" (Wasik and Murphy, 2012, p. 132). Therefore, he started to extract saliva and brain tissue from rabid dogs to find the microbe and develop a vaccine. Pasteur's son in law described the impressive laboratory work conducted by Pasteur and his coworkers in winter 1880/81: "The dog, choking with rage, its eyes bloodshot, and its body racked by furious spasms, was stretched out on a table while M. Pasteur, bending a finger's length away over this foaming head, aspirated a few drops of saliva through a thin tube." (Wasik and Murphy, 2012, p. 133). The saliva was inoculated into rabbits, whose saliva and spinal cord were used in repeated attempts to cultivate the pathogen. But unlike pneumococcus, a microbe that was discovered in the mucus of a child that was mistaken to be a rabies patient, the agent of rabies could not be cultivated nor seen under the microscope. Pasteur called this invisible agent a virus. Because it could not be isolated, it had to be preserved in live tissue. Infectious material from rabid dogs was passed on to a number of successively infected rabbits and back into a dog. In this process, Pasteur and his coworkers shortened the incubation period by applying the infective material directly to the nervous tissue, increased the virulence and attenuated the virus until they had a stable strain which could be used to immunize dogs (Wasik and Murphy, 2012, p. 135 f). The treatment was further refined until in July 1885 for the first time a human, the nine-year-old Joseph Meister, who had been bitten by a rabid dog, was successfully treated against rabies. In 1889 a virus was defined as a "microbe that is invisible under the light microscope and can pass through a filter designed to trap bacteria" (Wasik and Murphy, 2012, p 132). Five years later it was shown that rabies exactly fulfils these criteria.

Rabies today

The rabies virus is a bullet-shaped, 180 nm long lyssavirus of the family Rhabdoviridae (Mayr et al., 1984, p. 565). All warm-blooded animals are susceptible to rabies (Bano et al., 2016), and a wide range of species including foxes, wolves, jackals, raccoons, mongooses, and bats, act as reservoir hosts for lyssaviruses. The main vector for human rabies is the domestic dog (WHO, 2013), but human infections caused by other lyssaviruses such as the Australian bat lyssavirus and the European bat lyssavirus (WHO, 2018, p. 98) are increasingly being recorded. When the rabies virus enters the body via a scratch or bite of an infected host, it multiplies in the muscle cells. Through the motor endplates, it moves along the motor axons into the central nervous system at an estimated speed of 50 - 100 mm per day (Warrel and Warrel, 2004). The virus uses a "unique multilevel strategy" to escape the innate sensors and the antiviral effects of interferon (Hemachudha et al., 2013). It is also able to circumvent the immune response of the central nervous system by limiting the permeability of the blood-brain barrier (Roy et al., 2007). After infecting the brain, where it causes an encephalitis, the virus spreads in several organs and migrates to the salivary glands. From there it is delivered in high concentrations into saliva.

The incubation period ranges from weeks to years, with an average of two to three months (Singh et al., 2017). The first symptoms of rabies in humans are fever, flu-like symptoms, and pain at the site of the bite. About two-thirds of rabies patients develop the furious form with fluctuating consciousness, hydrophobia, and spasms. The paralytic form is characterized by ascending pure motor weakness (Hemachudha et al., 2013). Since by the time of the onset of symptoms the virus is already broadly distributed in the central nervous system, rabies was until

recently always fatal after the onset of symptoms. Death occurs within 7 to 11 days. In 2004 a 15-year-old unimmunized girl who had been bitten by a bat showed symptoms of rabies. After the confirmation of the rabies diagnosis, the treating clinicians induced a coma and carried out an ad hoc treatment with different drugs which ended in the survival of the girl (Willoughby, 2007). However, when this so-called Milwaukee protocol was applied to other rabies patients, only 5 out of 35 survived. Therefore rabies remains the disease with the highest fatality rate among all viral encephalitides (Hemachudha et al., 2013).
Before the onset of symptoms, rabies is preventable. Pre-exposure prophylaxis, which consists of four doses of vaccination (WHO, 2010), can be administered before a bite. In the case of a contact with a rabid animal, the post-exposure prophylaxis consists of vaccination and depending on the type of the exposure and the previous vaccination status the injection of immunoglobulins (WHO, 2010). Timely administration of post-exposure prophylaxis together with wound management and injection of immunoglobulins are highly effective in preventing the disease (WHO, 2010). Mass vaccination of dogs is considered effective in preventing human rabies (Hemachudha et al., 2013) and oral vaccine baits were used to eliminate rabies from foxes in central and western Europe (Freuling et al., 2013).

Taming rabies: elimination or control?

In spite of the existence of effective prophylactic and treatment measures, an estimated number of 60,000 people die of dog-mediated human rabies every year (Hampson et al., 2015). Most of these deaths occur in low-income regions with low dog-vaccination coverage and limited access to post-exposure prophylaxis (Hampson et al., 2015). Rabies is a neglected tropical disease, which is why it is often under-reported. Charles Rupprecht, who has been the chief of the rabies programme of the Center for Disease Control and Prevention for many years, has summarized the consequences of this neglect: "We don't have an effective surveillance system because there are no resources. And there are no resources because there are no cases!" (Wasik and Murphy, 2012, p.230). However, this vicious cycle has begun to be broken as more and more voices advocate for rabies elimination. The successes with oral vaccinations of foxes in Europe and dog-vaccination campaigns in Latin America encouraged a growing number of experts to consider rabies elimination a reachable goal (Lankester et al., 2014; Fooks et al., 2014; Lembo et al., 2010; Hampson et al., 2016; Fahrion et al., 2017; Anyiam et al., 2016). This confidence was further favoured by a general atmosphere of optimism concerning disease elimination: out of the 17 neglected tropical diseases in 2012 two were targeted for eradication and five for elimination by the World Health Organization (WHO, 2012). So when the WHO presented their global framework for eliminating dog-mediated human rabies by 2030 at the 2015 rabies global conference (WHO, 2015) the Director-General, Margaret Chan, proclaimed: "Rabies belongs in the history books. This event will help put it there." (Chan, 2015). The framework established five pillars of rabies elimination: socio-cultural, technical, organization, political and resources. The activities promoted in the framework include raising awareness of rabies as a preventable disease, promoting responsible dog ownership, facilitating dog population management, dog vaccination and bite prevention, increasing access to post-exposure prophylaxis and improving diagnostics and surveillance. The following two examples show that the interplay of all these factors is essential for successful rabies control.

From 2010 to 2015 a rabies elimination demonstration project was implemented in 28 districts of Tanzania. Mass vaccination campaigns of dogs and improved access to post-exposure prophylaxis led to a local elimination of rabies from Pemba island and a reduction of cases on the mainland (Mpolya et al., 2017). Furthermore, a mobile phone-based surveillance system was deployed. Effective surveillance for reporting of post-exposure prophylaxis demands, animal rabies cases and progress of dog vaccination campaigns was identified as being crucial (Mtema et al., 2016). When a case was introduced to Pemba island in 2016, a strong outbreak response could be initiated only because rabies incursion detected early (Mpolya et al., 2017).
In Morocco rabies has been a notifiable disease since 1913. Starting in the 1980s three national rabies control plans have been conducted based on free mass vaccination campaigns of dogs with a maximum of 450,917 dogs vaccinated in 2005. The control plans also included the opening of new treatment centres to increase access to post-exposure prophylaxis. Despite these interventions, animal rabies cases between 1986 and 2015 remained constant at approximately 300 cases per year. Human cases did not decrease below 20 cases per year. Darkaou et al. (2017) claim that the lack of dog population management combined with decreased vaccination of dogs during livestock crises led to the limited success of rabies control. Furthermore, they highlight, that while dog vaccination is mandatory, the law does not take into account responsible dog ownership.
The WHO framework explicitly states that mass vaccination of dogs is the most cost-effective intervention to achieve elimination of dog-mediated human rabies. At the same time, improved access to post-exposure prophylaxis is promoted. This is because even though it is clear that both vaccination of dogs and vaccination of humans are important tools for averting dog-mediated human rabies, the question of which combination of these tools is the best strategy is controversial. Is a combination of rabies control in the dog population together with post-exposure prophylaxis in humans more adequate than trying to eliminate rabies by mass vaccination campaigns of dogs? How this question is answered will have a substantial impact on the planning, implementation and possibly the success of efforts towards the goal of eliminating dog-mediated human rabies. In this setting mathematical models provide useful tools to assess the impact of different interventions on the disease dynamics and to compare proposed control strategies.

4.2 Mathematical modelling of rabies

How modelling motivated fox vaccination

Starting in the 1950s, a rabies epidemic spread across Europe from east to west with foxes as the main host (Bogel et al., 1976). At the same time WHO held a series of expert meetings on rabies. The reports of these meetings recommended gassing, poisoning, trapping and shooting of foxes, with the aim of reducing the population level below a threshold that would no longer be able to support transmission (WHO, 1957). These recommendations were implemented until the 1980s, sometimes even with concrete targets of reducing foxes to 0.2 to 0.5 animals per square kilometer (Mayr et al., 1984, p. 569). In 1981 Anderson and May developed a mathematical model of rabies transmission and concluded that because of the high reproduction and dispersal potential of foxes, culling is unlikely to be an effective intervention (Anderson et al., 1981). They recommended vaccination of foxes and referred to field trials of oral vaccination baits,

which had been conducted for example in Switzerland since 1978. Oral vaccination was then broadly applied (Müller et al., 2015) and eliminated fox rabies from central and western Europe (Freuling et al., 2013). This example shows that mathematical models can give useful insights into transmission dynamics and assess the impact of interventions. Even though it is difficult to know to what extent the modelling work of Anderson and May truly influenced the actual change of strategies it is instructive to observe that using a rather simple transmission model they were able to derive conclusions that pointed towards a successful strategy.

Modelling the spatial spread of rabies in wildlife

Models of rabies in wildlife have extensively investigated the spatial dynamics of the epidemics. The model by Anderson et al. (1981) was based on ordinary differential equations (ODEs) describing the population dynamics of foxes and the transitions from susceptible to exposed and from exposed to infective. Murray et al. (1986) expanded that model by adding a diffusion term to incorporate the spatial dispersal of rabid foxes. This yielded a system of partial differential equations with a travelling wave solution. They determined the minimal speed of the travelling wavefront for different diffusion coefficients and argued that reducing the density of foxes in a zone ahead of the wave could hinder the spread of rabies. Killing foxes would leave territories empty and would therefore enhance the spread of rabies through juvenile foxes recolonizing these territories, so Murray et al. (1986) advocated establishing a protective barrier by vaccinating and not by killing them. Since the different movement behaviour of adult and juvenile foxes is relevant for rabies transmission, Ou and Wu (2006) further expanded the model of Murray et al. (1986) by introducing age-dependent diffusion rates. This yielded a system of reaction-diffusion equations with delayed nonlinear interactions, allowing the population dynamics of foxes to be linked the spatial spread of rabies, via the relationship between the minimal wave speed and the maturation time.

Keller et al. (2013) studied the spread of raccoon rabies in New York state. Using finite elements for the space discretization of a partial differential equation (PDE) model they established a fine spatial grid and locally varied the diffusion coefficient. This allowed them to incorporate landscape heterogeneities such as rivers, forests, and highways. They found that rivers substantially influence the disease spread. Starting from a similar PDE model of raccoon rabies, Neilan and Lenhart (2011) applied optimal control theory to investigate the optimal spatial and temporal distribution of oral vaccine baits, and found that the optimal strategy is to place a vaccination belt in front of the epidemic wave. Natural barriers like rivers or forests can aid this strategy considerably by fortifying or even replacing vaccination belts. They also investigated the impact of long-distance translocations and found that such movements of rabid raccoons ahead of the wave-front can produce additional transmission foci which have to be rapidly reduced with high concentrations of vaccination. Furthermore, associating higher costs for vaccination leads to a considerably lower optimal amount of vaccine used, which results in optimal schemes that hinder but not entirely contain the spread of rabies.

Models based on differential equations reproduced the wavelike spread of rabies that was observed in foxes in Europe and raccoons the United States. But a rabies epidemic wave can also be generated by individual-based models combining local dispersal with long-distance translocations, as has been shown by Jeltsch et al. (1997). Smith et al. (2001) investigated the role

of long-distance translocations with a stochastic spatial rabies model for raccoon rabies in Connecticut. They linked local transmission dynamics on the level of townships with movement of infection between adjacent townships incorporating landscape features and long-distance movements of incubating raccoons. They found that translocation of raccoons can establish new foci and highlighted the importance of surveillance for rabies control.

Modelling dog rabies control

In models of rabies in domestic dogs the spatial aspect is generally less important than with wildlife because the movement of owned dogs is likely to be centered around the house of the owner. Since most humans contracting rabies are infected by dogs, models for dog rabies often put a strong focus on control. Coleman and Dye (1996) estimated the growth rate using outbreak data from four rabies epidemics and found that vaccinating 70% of the dog population would prevent outbreaks. The model they used to link the growth rate to the required coverage was an ODE model without population dynamics. Since dog densities, reproduction and death differ substantially across different settings, many studies have fitted the parameters of ODEs to specific dog demographies in different countries, including Kenya (Kitala et al., 2002), China (Chen et al., 2015; Ruan, 2017), Tanzania (Fitzpatrick et al., 2014; Bilinski et al., 2016) and the Philippines (Tohma et al., 2016). In this thesis, an ODE model was adopted to the dog population of N'Djamena (chapter 5).

The importance of host contact structures for disease transmission

Differential equation models capture transmission in the form of a term that multiplies the number or the density of the susceptibles with the number or density of the infectives and a transmission rate. The underlying assumption is that any individual is equally likely to encounter any other individual. But assuming homogeneous mixing of the population neglects the social structure among the hosts. Contacts are usually not random but highly structured. Many studies have highlighted the importance of including host contact structure into infectious disease modelling (Newman, 2003; Pastor-Satorras et al., 2015; Silk et al., 2017). Watts and Strogatz (1998) studied rewired regular networks and showed that infectious diseases spread more easily in these highly clustered systems. Andersson (1999) considered stochastic epidemic processes on graphs and derived an expression for the basic reproductive ratio, which depends not only on the expected value but also on the standard deviation of the degree distribution of the graph. Because the variance of some power law distributions is not well defined, this has implications for the spread of diseases on scale free networks. Pastor-Satorras and Vespignani (2001) found the absence of an epidemic threshold for scale-free networks and concluded that on these networks diseases can spread and persist independently of the spreading rate. Albert et al. (2000) showed that scale free-networks are very robust against random errors but are rapidly fragmented under targeted attacks that remove high degree nodes, a property with consequences for vaccination. These theoretical insights have led to a better understanding of disease transmission dynamics for a range of different diseases, including pertussis (Rohani et al., 2010), influenza (Barclay et al., 2014), SARS (Meyers et al., 2005), HIV (Morris and Kretzschmar, 1995) and gonorrhea (Yorke et al., 1978) and have also inspired new control measures such as acquaintance immunization (Cohen et al., 2003), contact tracing (Kretzschmar et al., 1996), and

ring vaccination (Greenhalgh, 1986; Müller et al., 2000).
Several models of rabies transmission have included the contact structure among animals. The network structure underlying these models has been established based on radio-tracking of foxes (White et al., 1995), proximity loggers for raccoons (Hirsch et al., 2013; Reynolds et al., 2015) and GPS devices on dogs (Dürr and Ward, 2015; Johnstone-Robertson et al., 2017). In this thesis, data from contact sensors on 300 dogs are used to build a contact network and simulate rabies transmission on that network (chapter 7).

4.3 Rabies in N'Djamena

Endemic rabies in N'Djamena

N'Djamena, the capital of Chad, is located south of Lake Chad at the border with Cameroon. The city consists of 10 districts of which one is located south of the Chari river. Approximately 1,300,000 people live in N'Djamena. In the wet season from June to September some areas within the city are flooded. Using a capture-mark-recapture model the total number of dogs in N'Djamena has been estimated at around 30,000, with an estimated percentage 14% of ownerless dogs (Léchenne et al., 2016b). A household survey on dog ownership in N'Djamena found that the main purpose of keeping a dog is the usage as watchdogs (Mindekem et al., 2005b). These dogs are mostly kept inside compounds during the night and are fed by the owners but can roam freely during the day. Dog density varies strongly across the city, with high density in predominantly Christian districts and low density in predominantly Muslim districts. That dog ownership is less likely in Muslim households has also been observed in rural areas (Mbilo et al., 2016). The dog population is characterized by a low average life expectancy and a male:female ratio of 3:1 (Mindekem et al., 2017a), possibly due to the practice of killing female puppies as a way of population control. As of 2012 weekly rabies incidence was reported through passive surveillance. There was approximately one case of confirmed dog rabies per week. On average one rabid dog bit approximately two humans (Zinsstag et al., 2009). The demand for post-exposure prophylaxis was estimated to be around 25 treatments per month (Mindekem et al., 2017b) which substantially exceeds the number of confirmed rabies cases. While there could be more rabies cases than reported, it is also likely that many of the post-exposure treatments are administered to persons who have been bitten by healthy dogs. A post-exposure treatment recommendation is often issued based on the severity of the bite wound rather than the status of the biting animal (Léchenne et al., 2017).

Vaccination campaigns

Because of the substantial cost of post-exposure prophylaxis, an alternative way of preventing rabies was considered. The results of a deterministic ODE model together with a cost calculation indicated that dog vaccination could eliminate dog rabies in N'Djamena. Zinsstag et al. (2009) estimated that the high initial cost for dog vaccination campaigns would pay off after approximately five years due to the decreased demand for post-exposure prophylaxis. Therefore, in 2012 and 2013 two mass dog vaccination campaigns were conducted. Vaccination posts were set up, five days a week for 13 weeks. Dogs were brought to the vaccination posts from the surrounding areas by the owners. Vaccination was free to the owner because pilot surveys had

shown that charging owners for vaccination results in decreased coverage (Dürr et al., 2008b). In the first campaign, from October 2012 to January 2013, a total number of 18,182 dogs were vaccinated. In the second campaign, from October 2013 to January 2014, the number of vaccinated dogs was 22,306 (Léchenne et al., 2016b). This corresponds to a coverage of more than 70 % in both years.

Resurgence

After the vaccination campaigns, a resurgence in cases was observed. The first case appeared in September 2014, only eight months after the end of the second campaign. After this first case, some more cases followed and one year after the campaigns the rabies incidence was equal to the incidence before the vaccination campaigns. Possible reasons for this early resurgence include heterogeneity, underreporting and importation of latent dogs from the surroundings of the city. Dog densities varied across the city and vaccination coverage was not homogeneous due to different levels of participation during the campaigns. It is possible that the spatial heterogeneity facilitated the fast reestablishment. Rabies cases are also frequently underreported (Hampson et al., 2015) and the introduction of infections into cities has been observed for example in Bangui (Bourhy et al., 2016).

Available data

Before, during and after the vaccination campaigns, dog rabies incidence was monitored by passive surveillance. An immune antibody fluorescence test (IFAT) was used to analyse brain samples of suspected rabid dogs brought to a permanently installed laboratory. This surveillance was started in 2012 and is still ongoing. During the campaigns vaccination coverage, and dog densities were recorded. Furthermore, repeated serological measurements were conducted on 105 vaccinated dogs to determine the duration of the vaccine induced immunity. To better understand the movement and contact behaviour of dogs, 300 geo-located contact sensors were deployed on dogs in three different quarters of N'Djamena. These data can be used to develop and parametrise rabies transmission models.

4.4 Goals and objectives

The goal of this project was to use modelling approaches to gain new insights into dog rabies transmission dynamics using the data from the N'Djamena studies, to help improve vaccination strategies. The aim was to identify core elements of the transmission process and to provide a tool to compare different interventions such as pre- and post-exposure prophylaxis of humans and vaccination of dogs. In order to achieve this goal, the following objectives were pursued:

Objective 1 Parameterise a deterministic transmission model using the data from the vaccination campaigns in 2012 and 2013, to understand if transmission was interrupted and whether individual immunity loss or population turnover contribute more to the decreasing vaccination coverage.

Objective 2 Develop a further model for dog rabies transmission in N'Djamena that captures heterogeneity and use this model to determine whether recent rabies cases in N'Djamena are due to reintroduction or due to ongoing transmission.

Objective 3 Develop a model for the movement and contact behaviour of dogs, parameterise it using the data collected in N'Djamena in 2016, and use the model to understand how the contact structure among dogs influences the spread of rabies.

5. Vaccination of dogs in an African city interrupts rabies transmission and reduces human exposure

Jakob Zinsstag[1,2], Monique Lechenne[1,2], Mirjam Laager[1,2], Rolande Mindekem[3], Service Naïssengar[4], Assandi Oussiguéré[4], Kebkiba Bidjeh[4], Germain Rives[1,2], Julie Tessier[1,2], Seraphin Madjaninan[3], Mahamat Ouagal[4], Daugla D. Moto[3], Idriss O. Alfaroukh[4], Yvonne Muthiani[1,2], Abdallah Traoré[5], Jan Hattendorf[1,2], Anthony Lepelletier[6], Lauriane Kergoat[6], Hervé Bourhy[6], Laurent Dacheux[6], Tanja Stadler[7,8], Nakul Chitnis[1,2]

[1]Swiss Tropical and Public Health Institute, P.O. Box, 4002 Basel, Switzerland

[2]University of Basel, Petersplatz 1, 4003 Basel, Switzerland

[3]Centre de Support en Santé Internationale, BP 972, N'Djamena, Chad

[4]Institut de Recherche en Elevage pour le Développement, BP 433, N'Djamena, Chad

[5]Laboratoire Central Vétérinaire, BP2295, Bamako, Mali

[6]Institut Pasteur, Unit Lyssavirus Dynamics and Host Adaptation, WHO Collaborating Centre for Reference and Research on Rabies, 28 Rue du Docteur Roux, 75724 Paris Cedex 15, France

[7]Department of Biosystems Science and Engineering, Federal Institute of Technology (ETH), Mattenstrasse 26, 4058 Basel, Switzerland

[8]Swiss Institute of Bioinformatics, Lausanne, Switzerland

This manuscript has been published in Science Translational Medicine, December 2017.

5.1 Abstract

Despite the existence of effective rabies vaccines for dogs, dog-transmitted human rabies persists and has reemerged in Africa. Two consecutive dog vaccination campaigns took place in Chad in 2012 and 2013 (coverage of 71% in both years) in the capital city of N'Djamena, as previously published. We developed a deterministic model of dog-human rabies transmission fitted to weekly incidence data of rabid dogs and exposed human cases in N'Djamena. Our analysis showed that the effective reproductive number, that is, the number of new dogs infected by a rabid dog, fell to below one through November 2014. The modeled incidence of human rabies exposure fell to less than one person per million people per year. A phylodynamic estimation of the effective reproductive number from 29 canine rabies virus genetic sequences of the viral N-protein confirmed the results of the deterministic transmission model, implying that rabies transmission between dogs was interrupted for 9 months. However, new dog rabies cases appeared earlier than the transmission and phylodynamic models predicted. This may have been

due to the continuous movement of rabies-exposed dogs into N'Djamena from outside the city. Our results show that canine rabies transmission to humans can be interrupted in an African city with currently available dog rabies vaccines, provided that the vaccination area includes larger adjacent regions, and local communities are informed and engaged.

5.2 Introduction

Dog rabies has been eliminated in large parts of the industrialized countries in Europe and North America. In the last few decades, a concerted effort by South and Central American countries has reduced dog rabies transmission close to elimination (Hampson et al., 2007). Despite the existence of effective vaccines for dogs, dog-transmitted human rabies persists and has even reemerged in Asia and Africa, where still more than 59,000 people die annually from this preventable disease. The largest part of the burden is borne by India followed by Africa, China, and Southeast Asian countries (Hampson et al., 2015). Because of rabies' low propensity to transmit secondary infections beyond a bitten individual, it appears feasible to eliminate dog-mediated human rabies through the mass vaccination of dogs (Cleaveland et al., 2014; Hampson et al., 2009). However, reaching this goal in partnership with the World Health Organization (WHO), the Food and Agriculture Organization of the United Nations (FAO), the World Organization for Animal Health (OIE), and the Global Alliance for Rabies Control (GARC; www.rabiesalliance.org) requires a rigorous scientific approach (Zinsstag, 2013).

Reaching sufficient coverage to interrupt dog rabies virus transmission and prevent reintroduction requires an in-depth understanding of dog ecology (Mindekem et al., 2005a), dog-human interactions, and the social and cultural determinants of vaccine acceptability, as well as the effective deployment of vaccines with a highly sensitive surveillance system (Hampson et al., 2009; Kayali et al., 2003b; Obrist et al., 2007; Dürr et al., 2008a; Talbi et al., 2010). It requires scientists to closely collaborate with authorities and communities as partners, in a transdisciplinary way, between human and animal health (Hadorn et al., 2008; Charron, 2012). Concomitant mathematical and economic frameworks can yield new insights into fundamental properties of pathogen transmission (Townsend et al., 2013b) and comparative cost-effectiveness (Zinsstag et al., 2009) but do not explain sufficiently how this effectiveness can be achieved (Klepac et al., 2013).

In 2003, a small-scale study showed the feasibility of dog rabies control in an African city (Kayali et al., 2003b) with low cost of $2 to $3 per vaccinated dog (Mindekem et al., 2017c). However, in some African countries, dog owners cannot afford inoculations and depend on mass vaccination campaigns that are free of cost (Dürr et al., 2008a; Jibat et al., 2015). Analysis of pre- and post-vaccination rabies cases and economic data showed that a single simulated dog vaccination campaign was able to interrupt transmission and was less costly than human post-exposure prophylaxis (Zinsstag et al., 2009). A proof of the feasibility of dog rabies elimination in an African city would have far-reaching consequences for a regionally concerted effort to eliminate rabies in Africa.

Previously, a citywide dog rabies mass vaccination campaign was set up in partnership with the Chadian authorities, the Institut de Recherche en Elevage pour le Développement, the Centre de Support en Santé Internationale, and the Swiss Tropical and Public Health Institute (Léchenne

et al., 2016b). The Chadian government paid for the costs of personnel and logistics, and a philanthropic donor paid for the costs of dog vaccines and research. Passive dog rabies and human exposure surveillance started before the campaigns and is still ongoing. Here, we analyze the passive surveillance data taken from dogs brought to the diagnostic laboratory during this previous work using mathematical transmission models and phylodynamic analyses of dog-related rabies virus. We investigate the impact of the vaccination campaigns for interrupting transmission and the potential for maintaining elimination.

5.3 Results

Field data from mass vaccinations show reduced rabies incidence in dogs and humans

The vaccination campaign operations are described in detail in a previous publication (Léchenne et al., 2016b) and summarized in Materials and Methods. Vaccination coverage surveys followed each sequence to assess the achieved coverage and the deficit to reach 70% target coverage. In both campaigns, 71% of all dogs were vaccinated (95% confidence interval, 69 to 76%) (Léchenne et al., 2016b).

We obtained results about the weekly incidence of dogs newly infected with rabies (Figure 5.1) and the incidence of related human exposure (Figure 5.1). These data were collected through passive surveillance, that is, from dogs that were suspected to be infected and brought for testing to the rabies laboratory in N'Djamena and through collection of rabies virus strains from rabid dogs. Recorded numbers of vaccinated dogs were used for the estimation of vaccination coverage (18). The data suggested that mass dog vaccination campaigns in 2012 and 2013 reached sufficient coverage to interrupt transmission from January 2014 to October 2014. Per capita dog rabies incidence in the city of N'Djamena, estimated from passive surveillance, dropped from 0.33 dogs/10,000 per week before the mass vaccination campaign to 0.016 dogs/10,000 per week in 2014 (Figure 5.1). Similarly, the per capita incidence of human exposure to rabid dogs, as estimated from passive surveillance, dropped from 1/1,000,000 humans exposed to rabies virus per week before the mass vaccination to less than 0.002/1,000,000 per week in 2014, which is less than one person per year (Figure 5.1).

Transmission modeling indicates extensive vaccination interrupted dog-to-dog rabies transmission

We used a deterministic, population-based model of ordinary differential equations to model rabies transmission among dogs as well as between dogs and humans (Table 5.2). The surveillance field data were used to estimate the effective reproductive number R_e (the number of new rabid dogs infected by one rabid dog at any time, accounting for immunity and interventions) and the threshold population density of susceptible dogs using mathematical models. The transmission model showed that between the two campaigns in 2012 and 2013, effective recorded vaccination coverage decreased from a peak of 67% (December 2012) (Léchenne et al., 2016b) to a trough of 33% (October 2013), assuming an exponential distribution for the persistence of immunity, which was estimated from 105 immunized dogs undergoing repeated serological measurements.

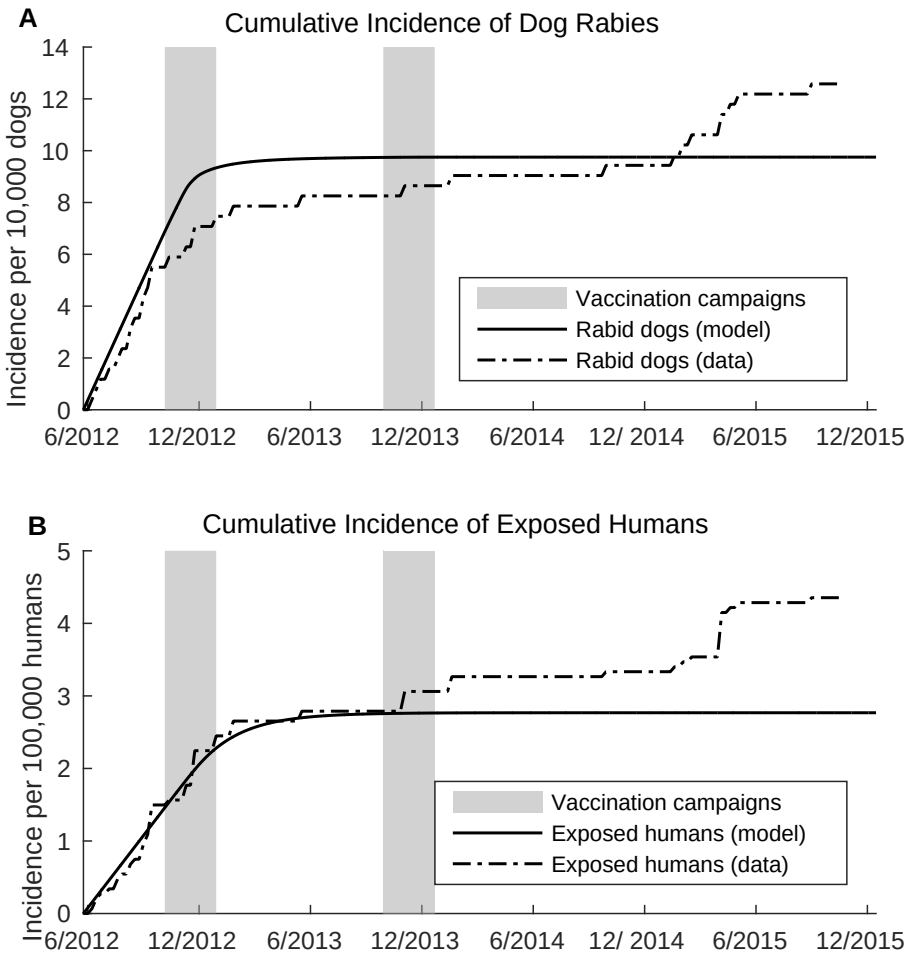

Figure 5.1: Cumulative incidence of dog rabies and human exposure. (A) Cumulative incidence of recorded cases of dog rabies (infectious dogs) and simulated incidence of dog rabies in N'Djamena from 6 June 2012 to the end of October 2015. (B) Cumulative incidence of recorded human exposure to rabid dogs and simulated incidence of human exposure to rabid dogs in N'Djamena from 6 June 2012 to the end of October 2015.

This represents a 51% relative coverage loss (Figure 5.2). The model suggested that population replacement by the birth of susceptible dogs accounted for 29% of the relative coverage loss, whereas individual dog immunity loss accounted for 22% of this relative coverage loss.

The effectively vaccinated surface area in our campaign of 240 km^2 (2012) was much lower than the 770 km^2 assumed in an earlier simulation (Zinsstag et al., 2009). The empirical data from the current study provide a better estimate of parameter values, the threshold density of susceptible dogs, and the basic reproductive number, that is, the number of secondary infections resulting from a typical case in a completely susceptible population, as $R_0 = 1.14$, instead of $R_0 = 1.01$. This means that rabies is potentially more infectious in N'Djamena than previously reported (Zinsstag et al., 2009). The effective reproductive number, R_e , decreased from the equilibrium value of 1 at the start of the first vaccination campaign and remained below 1 through November 2014, implying that the conditions for rabies virus persistence were not maintained since the start of the vaccination campaigns. Simulations of a deterministic ordinary differential equation model (Figure 5.1), fitted to rabies case data from N'Djamena, and a stochastic extension (Figure 5.3) suggested that dog-to-dog rabies transmission was interrupted from early 2013 onward.

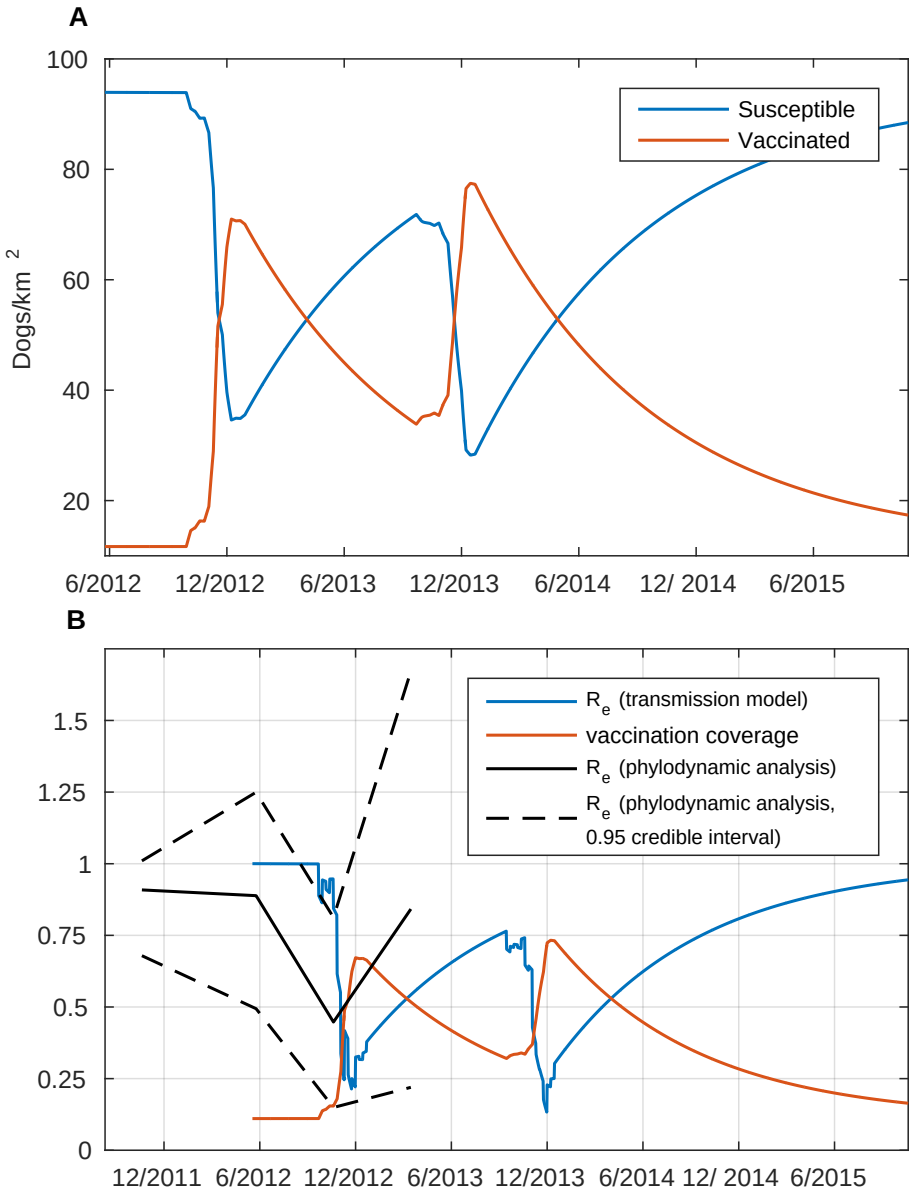

Figure 5.2: Density of vaccinated and unvaccinated dogs in relation to the effective reproductive number. (A) Density of susceptible (blue lines) and vaccinated (orange lines) dogs against time since 6 June 2012. The solid lines show the simulated values from an ordinary differential equation transmission model from June 2012 to October 2015. (B) Effective reproductive number, R_e , and vaccination coverage against time. The solid orange line shows the vaccination coverage and the solid blue line shows the effective reproductive number - both estimated from the ordinary differential equation transmission model. The solid black line is the median R_e obtained from the phylogenetic sequencing data, with upper and lower 95% credible intervals as black dashed lines.

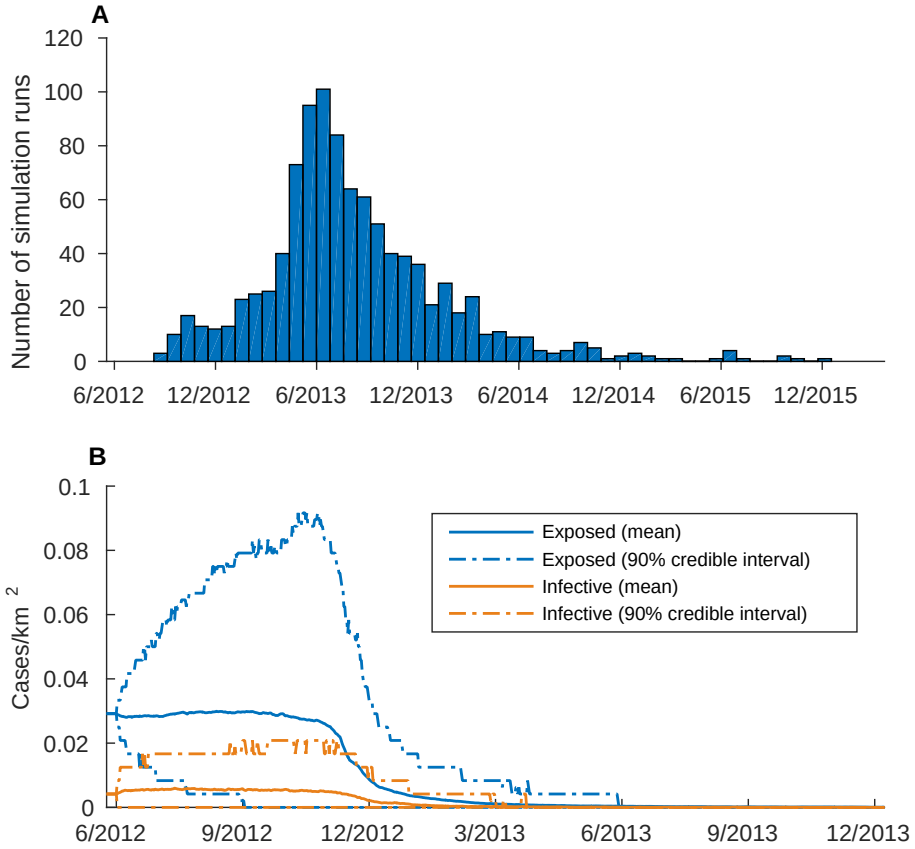

Figure 5.3: Stochastic simulations of the interruption of transmission. (A) Distribution of the simulated expected date of interruption of transmission from 1000 simulation runs of the stochastic model of dog rabies transmission. (B) Mean and 90% credible interval for exposed and infectious dogs from 500 runs of the stochastic model.

Rabies reintroduction may be due to an influx of dogs into the city from neighboring areas

Because our model did not include importation of infections, we wondered whether dog rabies cases seen from October 2014 onward (Figure 5.1) were due to imported cases (with subsequent local transmission) rather than sustained ongoing transmission from the end of 2013 or the beginning of 2014. To test this hypothesis, we performed a maximum likelihood (ML) phylogeny of nucleoprotein sequences from rabies virus isolates collected in Chad (from N'Djamena and other regions) from August 2011 to January 2015. The dog rabies cases from 2014 onward were phylogenetically distinct from those previously circulating in N'Djamena (Figure 5.4). We therefore suspected that domestic dogs from surrounding peri-urban and rural areas were the more likely source of reinfection rather than ongoing transmission in dogs or wild animals. Consistent with this, only dog-related rabies virus strains and no wildlife-related strains were found in a previous rabies virus phylogenetic analysis performed in N'Djamena (Dürr et al., 2008c).

Transmission model inferences regarding viral dynamics are robust to parameter choice

We performed sensitivity analysis to determine whether the simulation results were robust compared to our estimates of parameter values. Figure 5.5 shows simulation results of the density

of infectious dogs over 6 years, allowing for uncertainty in each of the parameter values (varied one at a time). In each simulation run, the dog transmission rate, β_{dd} , was refitted for that set of parameter values. The results were robust to uncertainty in the parameter values, and except for low vaccine efficacy values, the simulations predicted that transmission would be interrupted after the first campaign. Figure 5.6 shows a similar sensitivity analysis of the simulated number of infectious dogs but with a fixed value for the dog transmission rate, β_{dd}, estimated from the baseline set of parameter values (Table 5.3). The ranges of the parameter values were greater than in Figure 5.5, and the results showed the importance of that parameter on the expected number of rabid dogs over time. Most parameters had little effect, but similar to the sensitivity analysis for R_c, high values for the carrying capacity of dogs, the probability of an exposed dog developing rabies, and low values for the rabies-induced death rate led to a high number of infectious dogs. Figure 5.7 shows the simulated densities of infectious dogs and exposed humans depending on the probability of detection of infectious dogs, p_d, and of exposed humans, p_h, used to fit the dog-to-dog and dog-to-human parameters, β_{dd} and β_{hd}, respectively. Low values of these detection probabilities result in higher numbers of infectious dogs and exposed humans, leading to higher estimates for the β_{dd} and β_{hd} transmission parameters. The results indicated that the simulation data were robust regarding these detection probabilities, unless the probabilities were very low and that underreporting of rabies cases was unlikely to have a substantial effect on our results (Figure 5.7). This, in turn, suggested that underreporting of cases did not play a large role in the persistence of rabies transmission. Even accounting for heterogeneity in underreporting, it was unlikely that unreported transmission persisted for 9 months and more likely that a reintroduction occurred, either from wildlife or from dogs with ongoing transmission outside the city of N'Djamena.

Phylodynamic analyses support rabies transmission interruption by the mass vaccination campaigns

We conducted a phylodynamic analysis to estimate the transmission potential of rabies in N'Djamena. We simulated the evolutionary relationships between 29 nucleotide sequences encoding the N-protein from dog-related rabies virus isolates [collected between August 2011 and June 2013 (Talbi et al., 2010, 2009)] under the assumption of the transmission model to estimate the viral reproductive number. Although the 95% highest posterior density (HPD) intervals were wide because of the small number of sequences, the effective reproductive number estimated from the genetic data showed the same pattern as the R e estimated from the incidence data (Figure 5.2). This corroborated the results of the deterministic transmission model, which estimated the transmission potential from the time series of the number of weekly cases. We therefore demonstrate by two different methods, analyzing two different kinds of data, that dog rabies transmission can be interrupted by the mass vaccination of dogs in the African city of N'Djamena.

5.4 Discussion

The models and data presented here show that the period with no rabies transmission in N'Djamena was longer after mass vaccination campaigns than in the absence of such cam-

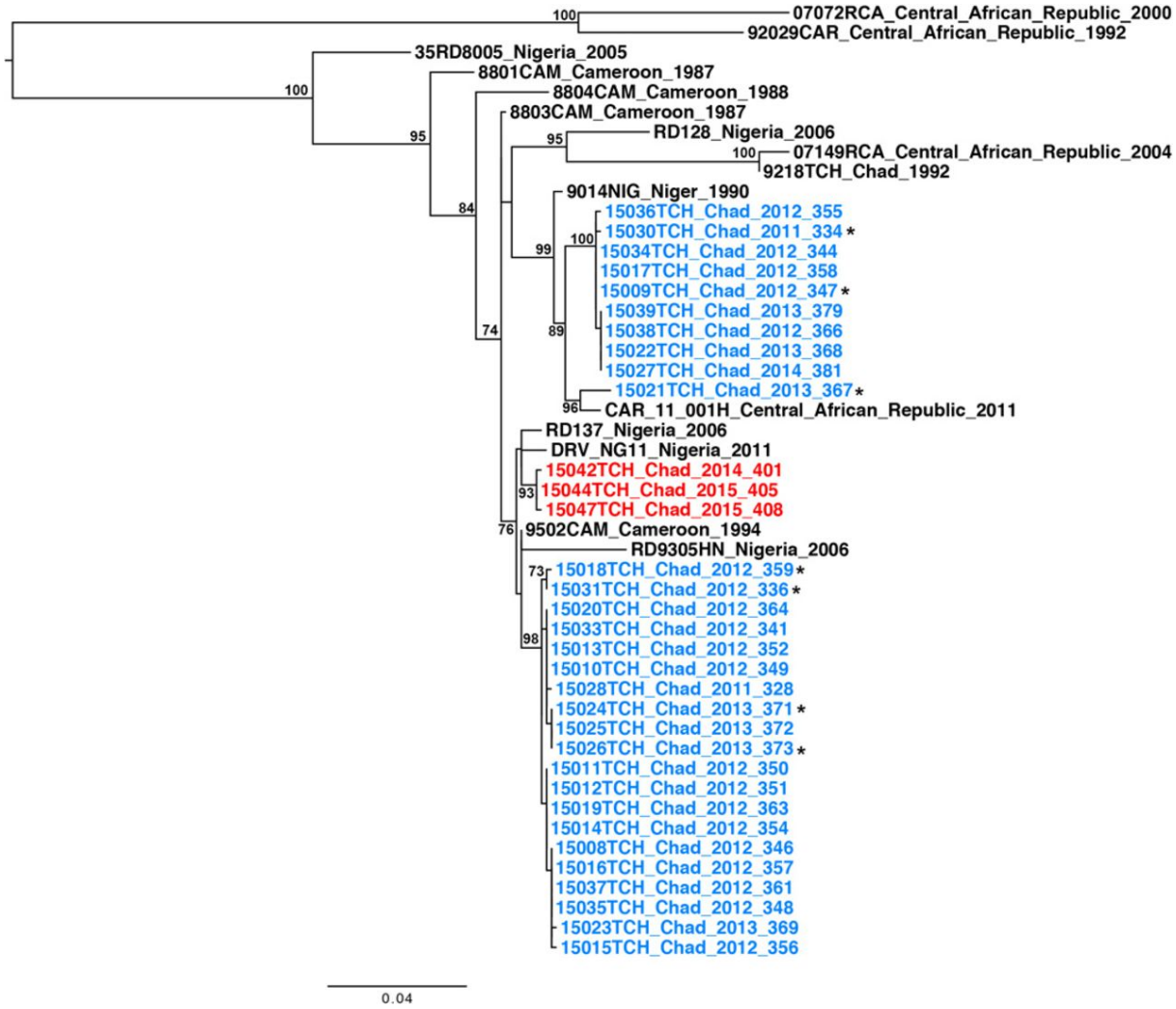

Figure 5.4: Phylogeny of rabies strains isolated during and after the mass vaccination campaign. ML phylogeny of nucleoprotein sequences from rabies virus isolates collected in Chad from August 2011 to January 2015 and from sequences of previous isolates originating from Chad and from other neighboring countries. Sequences in blue were obtained from isolates collected in N'Djamena, Chad, during the period from August 2011 to January 2014, except for the sequences with an asterisk, which correspond to isolates collected outside of N'Djamena or without any precise origin (for one isolate) during the same period. Sequences in red are those obtained from isolates collected in N'Djamena from February 2014 to January 2015. Only bootstrap values > 70 are indicated on selected nodes. A scale, indicating genetic distance, is presented by the horizontal bar. The tree is midpoint rooted for clarity only.

paigns, suggesting that dog rabies virus transmission in this African city could be interrupted, and consequently, human rabies exposure could be reduced. However, the duration of transmission interruption in our study was shorter than our model predictions presented here and in earlier work (Zinsstag et al., 2009), indicating that there was likely to be a reintroduction of infection from latently infected dogs from the adjacent peri-urban areas, similar to what was reported in a recent study on rabies transmission in Bangui (Bourhy et al., 2016). Our study suggested that urban centers may not be hotspots of dog rabies transmission, leading to spillover cases in rural areas, as previously thought. Dog rabies transmission is ongoing in peri-urban and rural African areas and is likely to be continuously transmitted into urban areas through human-mediated transport of dogs (Talbi et al., 2010). Sustainable elimination of dog rabies therefore will require action over a much larger geographical area. We have proposed a development impact bond financing scheme for dog rabies elimination in the entire country of Chad (Anyiam et al., 2017). There is still considerable uncertainty surrounding the role of

density and spatial heterogeneity to external reintroduction in the transmission of dog rabies (Morters et al., 2013). A meta-population or contact network modeling approach may better represent the observed heterogeneity of the dog population in N'Djamena (Figure 5.8). Further research is needed to assess how dog density and the spatial heterogeneity of dog populations influences the dynamics of dog rabies elimination (Morters et al., 2013; Begon et al., 2002). Our study is limited by the low number of rabies virus strains that were isolated during the rabies mass vaccination campaigns. For this reason, the confidence intervals of the phylodynamically estimated basic reproductive number are wide. Another limitation is that we could not identify the source of the rabies viruses that were reintroduced from outside the city. Further ongoing research will compare the isolated strains in this study with strains that will be collected countrywide. Determining the optimal timing of vaccination campaigns in N'Djamena to maintain elimination requires knowledge of the rabies importation rate into the city. Our results are in line with a recent study in Bangui, Central African Republic, showing that rabies is continuously reintroduced in towns by human-mediated transport of dogs from surrounding peri-urban areas (Bourhy et al., 2016) and rapidly dispersed between cities (Talbi et al., 2010). Therefore, we suggest that dog rabies control in African cities should be planned for larger areas, including suburban and rural areas, and be coordinated regionally between neighboring countries for effective elimination of dog rabies in Africa (Hampson et al., 2007). In particular, movement of dogs with or without their owners should be restricted to limit the dispersal of dog-associated rabies virus. Dog vaccination campaigns should also be complemented by affordable compulsory dog registration. Our study supports the need for improvements in and reinforcement of rabies surveillance in rural and more remote areas to achieve inclusive and comprehensive rabies reporting that can then be used to guide vaccination decisions. New rapid tests for rabies could be used in a decentralized manner and may enable collection of data about rabies epidemiology in remote locations (Léchenne et al., 2016a). In contrast to previous reports (Durrheim et al., 2015a), our study suggests that mass vaccination of dogs, coupled with post-exposure prophylaxis, could be sufficient to eliminate rabies transmission in an African city, in both dogs and humans, as long as vaccination is extended to a larger area beyond the city itself. In the long term, eliminating the infectious rabies reservoir in dogs will be more cost-effective than perpetual post- or pre-exposure prophylaxis in humans (Mindekem et al., 2017c). Dog vaccination campaigns will need to be adapted to local conditions to reach sufficient coverage (Mosimann et al., 2017; Muthiani et al., 2015), a regional approach similar to the well-coordinated dog rabies control efforts among Latin American countries (Hampson et al., 2007). The recent creation of the Pan African Rabies Control Network (PARACON; paracon.rabiesalliance.org) is an important first step toward the goal of eliminating dog rabies from Africa by 2030.

5.5 Materials and methods

Study design

The objective of this study was to test the hypotheses (i) that dog rabies transmission in an African city could be interrupted by the mass vaccination of dogs and (ii) that cities are potential hotspots of dog rabies transmission and reintroduction of rabies after vaccination would be slow. Given that we observed the reintroduction of dog rabies after the mass vaccination of dogs (in

N'Djamena, Chad; see below), we hypothesized that rabies was reintroduced from outside the city. The research subjects were the weekly number of routinely recorded suspected rabid dogs and the number of exposed humans per rabid dog. The design of the present study is composed of four main components covering the city of N'Djamena, Chad: (i) An ongoing passive dog rabies surveillance system. Suspected rabid dogs (dead or alive) were brought to the rabies diagnostic laboratory. No active collection of suspected dogs was done. For every dog suspected to be infected with rabies, information on exposed humans was collected on a routine basis. (ii) A dog rabies mass vaccination campaign was undertaken from October to December each in 2012 and 2013 (18). Blood was taken from 104 dogs in 2012 before the start of the mass vaccination campaign to assess the proportion of existing vaccination antibodies. The fluorescent antibody virus neutralization test was used for this purpose (30). Data on rabid dogs and exposed humans were collected up to the end of 2015 for this study. (iii) A mathematical model of dog-to-dog and dog-to-human rabies transmission was parameterized from the weekly number of rabid dogs and exposed humans collected before, during, and after the mass vaccination campaign. (iv) A phylogenetic and phylodynamic analysis of the rabies virus strains collected during the campaigns was used to assess their genetic closeness and to estimate the basic reproductive number of the rabies transmission in dogs independently from the mathematical transmission model.

Surveillance of dog rabies and human exposure

Passive routine dog rabies surveillance started on 4 June 2012 and is currently ongoing in N'Djamena at the Institut de Recherche en Elevage pour le Développement by standard immunofluorescence as described in (Zinsstag et al., 2009; Kayali et al., 2003a). Before the mass vaccination campaign, the average weekly incidence of dog rabies was of 0.33 dogs per 10,000. For every laboratory-confirmed rabid dog, on average, 1.6 humans were reported to be exposed (ascertained by questioning the dog owner), leading to a weekly incidence of 0.11 per 100,000 people.

Dog rabies mass vaccination campaign 2012 and 2013

A citywide mass dog vaccination campaign including all 10 districts of N'Djamena took place in 2012 and was repeated in 2013 (Léchenne et al., 2016b). In both campaigns, the objective was to vaccinate 70% of the total dog population of N'Djamena with the dog rabies vaccine Rabisin (Merial Inc.). The vaccination campaigns began in the first week of October 2012 and 2013 and lasted for a total of 13 weeks until the first week of January of the next year. Vaccination took place only on Friday to Sunday due to availability of staff and participation of the public during these days (as evaluated in previous studies) (Kayali et al., 2003b). Every Friday to Sunday, 10 fixed post-vaccination teams were set up in 1 of 12 (13 in 2013) areas of the city corresponding to administrative boundaries. Over the 3-day period, these teams vaccinated on average 1433 dogs (minimum, 24; maximum, 6460) in 2012 and 1709 dogs (minimum, 67; maximum, 4591) in 2013, depending on the sociocultural and ecological context of the city district (Table 5.1). Details of the operational performance and the results of the vaccination campaigns are published elsewhere (Léchenne et al., 2016b).

Vaccination week	Vaccinated dogs (2012)	Vaccinated dogs (2013)
1	834	722
2	181	468
3	376	330
4	24	434
5	793	67
6	901	1173
7	6460	928
8	1393	4215
9	3074	4372
10	1698	3424
11	311	4591
12	385	979
13	209	525

Table 5.1: Number of dogs vaccinated in each week of the vaccination campaigns. The campaign in 2012 started on 8 October 2012 (week 19) and in 2013 started on 30 September 2013 (week 70), as described in (Léchenne et al., 2016b)

Coverage assessment

A coverage assessment was carried out each week after vaccination in the previously vaccinated area (Figure 5.8). Vaccination zones and their analysis perimeter corresponded in most cases to a district. The coverage assessment was composed of a household survey in randomly selected geographical locations within the analysis perimeter to estimate the proportion of owned vaccinated dogs. In addition, random transects (where the field team traveled in straight lines to count the number of owned and ownerless dogs) were carried out with a car in the same zone to estimate the dog density in the street and the proportion of ownerless dogs. Data from both studies were then combined in one Bayesian statistical model as reported elsewhere (Léchenne et al., 2016b).

Description of mathematical model of dog-dog and dog-human transmission

We use a deterministic population-based model of ordinary differential equations extended from a previously published model for dog-to-dog rabies transmission (Zinsstag et al., 2009)

$$\frac{dS_d(t)}{dt} = b_d N_d(t) + \lambda_d V_d(t) - r_d \beta_{dd} S_d(t) I_d(t) - (\nu_d \alpha_d(t) + m_d + \gamma_d N_d(t)) S_d(t), \tag{5.1a}$$

$$\frac{dE_d(t)}{dt} = r_d \beta_{dd} S_d(t) I_d(t) - (\sigma_d + \nu_d \alpha_d(t) + m_d + \gamma_d N_d(t)) E_d(t), \tag{5.1b}$$

$$\frac{dI_d(t)}{dt} = \sigma_d E_d(t) - (\mu_d + m_d + \gamma_d N_d(t)) I_d(t), \tag{5.1c}$$

$$\frac{dV_d(t)}{dt} = \nu_d \alpha_d(t)(S_d(t) + E_d(t)) - (\lambda_d + m_d + \gamma_d N_d(t)) V_d(t), \tag{5.1d}$$

where the state variables and parameters are defined in Tables 5.2 and 5.3, respectively. The total dog population size is

$$N_d(t) = S_d(t) + E_d(t) + I_d(t) + V_d(t) \tag{5.2}$$

and the density-dependent death rate is

$$\gamma_d = \frac{b_d - m_d}{K_d} \tag{5.3}$$

where K_d is described in Table 5.3 and b_d is required to be greater than m_d. We note here that we assume density-dependent transmission and that, in general, (Eq. 5.1) is a nonautonomous model where $\alpha_d(t)$ varies with time

$$\alpha_d(t) = \alpha_d^* + \alpha_0^{(i)}(t) + \alpha_1^{(i)}(t)e^{-\varphi t} \tag{5.4}$$

where α_d^* is the (assumed) constant background vaccination rate, $\alpha_0^{(i)}(t)$ and $\alpha_1^{(i)}(t)$ are campaign-dependent vaccination values for the ith week, and φ is a saturation parameter. Outside of the campaigns, $\alpha_d(t) = \alpha_d^*$. We further restrict the values of $\alpha_0^{(i)}$ and $\alpha_1^{(i)}$ to ensure that $\alpha_d(t)$ is continuous so that the system for rabies transmission (Eq. 5.1) has a unique solution that exists for all time.

We similarly use an ordinary differential equation model for dog-to- human transmission based on (Zinsstag et al., 2009)

$$\frac{dS_h(t)}{dt} = b_h N_h(t) - \beta_{hd} S_h(t) I_d(t) + a_h E_h(t) - m_h S_h(t), \tag{5.5a}$$

$$\frac{dE_h(t)}{dt} = \beta_{hd} S_h(t) I_d(t) - (a_h + \sigma_h + m_h) E_h(t), \tag{5.5b}$$

$$\frac{dI_h(t)}{dt} = \sigma_h E_h(t) - (\mu_h + m_h) I_h(t), \tag{5.5c}$$

where the total human population size is

$$N_h(t) = S_h(t) + E_h(t) + I_h(t) \tag{5.6}$$

σ_h is the rate of progression from the exposed to the infectious state depending on the site of the bite

$$\sigma_h = \frac{P_2 P_6}{i_{head}} + \frac{P_3 P_7}{i_{arm}} + \frac{P_4 P_8}{i_{trunc}} + \frac{P_5 P_9}{i_{leg}} \tag{5.7}$$

a_h is the abortive rate of progression from the exposed back to the susceptible state

$$a_h = \frac{P_2(1 - P_6)}{i_{head}} + \frac{P_3(1 - P_7)}{i_{arm}} + \frac{P_4(1 - P_8)}{i_{trunc}} + \frac{P_5(1 - P_9)}{i_{leg}} \tag{5.8}$$

and the probabilities of biting different parts of the body (P_2 through P_5), the probabilities of subsequent progression to rabies (P_6 through P_9), and the average time to do so ($1/i_\xi$, where ξ is head, arm, trunk, or leg) are described in more detail in the previous formulation of the model (Zinsstag et al., 2009). Figure 5.9 shows a schematic of the model system. We note that the dynamics for rabies transmission in humans is dependent on rabies transmission in dogs, but the transmission in dogs is independent of transmission in humans.

Mathematical analysis

In the absence of vaccination campaigns [$\alpha_d(t) = \alpha_d^*$], the autonomous mathematical model for rabies transmission in dogs (Eq. 5.1) has a trivial disease-free equilibrium point

$$S_d = \frac{(b_d + \lambda_d)K_d}{b_d + \lambda_d + \nu_d\alpha_d^*}, \tag{5.9a}$$

$$E_d = 0, \tag{5.9b}$$

$$I_d = 0, \tag{5.9c}$$

$$V_d = \frac{\nu_d\alpha_d^* K_d}{b_d + \lambda_d + \nu_d\alpha_d^*}, \tag{5.9d}$$

The control reproductive number for the dog rabies model is the number of dogs that one newly introduced rabid dog would infect, assuming no disease in the population (with only background vaccination)

$$R_c = \frac{r_d\beta_{dd}\sigma_d K_d}{(\sigma_d + \nu_d\alpha_d^* + b_d)(\mu_d + b_d)} \tag{5.10}$$

We show that with only background vaccination (no vaccination campaigns), when $R_c < 1$, the disease-free equilibrium point (Eq. 5.9) is locally asymptotically stable, and when $R_c > 1$, the disease-free equilibrium point is unstable, and there exists a locally asymptotically stable endemic equilibrium point where rabies persists in the population. In addition, if there is no background vaccination, the control reproductive number reduces to the basic reproductive number

$$R_0 = \frac{r_d\beta_{dd}\sigma_d K_d}{(\sigma_d + b_d)(\mu_d + b_d)} \tag{5.11}$$

At any time, t, allowing for vaccination campaigns, the effective reproductive number, $R_e(t)$, represents the expected number of new infections caused by one infectious dog

$$R_e(t) = \frac{r_d\beta_{dd}\sigma_d S_d}{(\sigma_d + \nu_d\alpha_d(t) + m_d + \gamma_d N_d(t))(\mu_d + m_d + \gamma_d N_d(t))} \tag{5.12}$$

If we assume that the total dog population is at carrying capacity (which is reasonable because the density of rabid dogs is low, so it has a minimal impact on the population density of dogs), the effective reproductive number simplifies to

$$R_e(t) = \frac{r_d\beta_{dd}\sigma_d S_d}{(\sigma_d + \nu_d\alpha_d(t) + m_d)(\mu_d + m_d)} \tag{5.13}$$

The threshold density of susceptible dogs at which transmission occurs, S_d^* , is the density at which $R_e = 1$. From (Eq. 5.13), outside of vaccination campaigns, this is

$$S_d^* = \frac{(\sigma_d + \nu_d\alpha_d(t) + b_d)(\mu_d + b_d)}{r_d\beta_{dd}\sigma_d} \tag{5.14}$$

The threshold vaccination coverage reached in a campaign to eliminate transmission, ψ^*, is given by

$$\psi^* = 1 - \frac{1}{R_c} \tag{5.15}$$

when background vaccination takes place outside the campaign. Equivalently, this is

$$\psi^* = \frac{K_d - S_d^*}{K_d} \tag{5.16}$$

After the vaccination campaigns, the coverage of protected dogs decreases exponentially due to population loss of susceptible dogs [proportionally, b_d/l_d+b_d: 57% for parameter values in Table 5.3] and due to loss of vaccine efficacy [proportionally, l_d/l_d+b_d: 43% for parameter values in Table 5.3].

Parameter estimation

The values for most parameters are taken from the previous model (Zinsstag et al., 2009) except where new published results or new data have allowed for revised values. The parameter values and their sources are summarized in table 5.3. The birth and death rates of dogs were calculated as in previous work, but the carrying capacity of dogs was revised to reflect a total population of 25,103 dogs in an area of 240 km^2, as estimated in the 2012 coverage assessment. The vaccination rate of dogs and the transmission rates from dogs to dogs and dogs to humans were estimated as described below.

Dog vaccination rate

We found that 12% ($n = 105$) of all owned dogs had antibodies (and so could be considered effectively vaccinated), implying that there was some ongoing background vaccination outside of the two campaigns conducted in 2012 and 2013. The coverage assessment estimated that for every 10 owned dogs, there was one unowned dog. Assuming that the background vaccination rate was constant and the proportion of vaccinated dogs was at equilibrium (Eq.5.9), with demographic and other vaccination parameters as in table 5.3, the per capita background vaccination rate was 2.96×10^{-3}/week. The number of dogs marked as vaccinated in each campaign is shown in Table 5.1. We estimated the vaccination rate parameters, $\alpha_0^{(i)}$ and $\alpha_1^{(i)}$, using a simple model of vaccination for each campaign

$$\frac{dU^{(i)}}{dt} = b_d(K_d - U^{(i)}) - \overline{\alpha_d}^{(i)}(t)U^{(i)}, \tag{5.17a}$$

$$\frac{dV^{(i)}}{dt} = \overline{\alpha_d}^{(i)}(t)U^{(i)}, \tag{5.17b}$$

where $U^{(i)}$ is the density of all unmarked dogs, $V^{(i)}$ is the density of dogs marked in campaign week i, and $\overline{\alpha_d}^{(i)}(t)$ the rate of marking dogs during campaign week i. We define time, t, as varying from 0 at the start of each campaign week to 1 at the end of each campaign week. The coverage assessment could only determine whether dogs were marked as vaccinated or not and did not determine the immune status of dogs. We therefore ignore the efficacy of

the vaccination and do not consider background vaccination, because these dogs would not be marked as campaign-vaccinated dogs, so

$$\overline{\alpha_d}^{(i)}(t) = \alpha_0^{(i)}(t) + \alpha_1^{(i)}(t)e^{-\varphi t} \tag{5.18}$$

For simplicity, we ignore rabies transmission, assume that the dog population is at carrying capacity, and ignore the death of marked dogs or the loss of marking collars during the campaign week. Because the coverage assessment was conducted within 3 days of the vaccination campaign, these assumptions are reasonable. We assume that the markings from the 2012 campaign do not last until 2013, so for both campaigns, the initial density of unmarked dogs is equal to the carrying capacity

$$U^{(1)}(0) = K_d \tag{5.19}$$

and from continuity

$$U^{(i)}(0) = U^{(i-1)(1)for i>1} \tag{5.20}$$

The initial density of dogs marked during a campaign week is zero

$$V^{(i)}(0) = 0 for i \leq 1 \tag{5.21}$$

We fix $\varphi = 100$. To ensure that $\alpha_d(t)$ is continuous, we set

$$\alpha_0^{(1)} + \alpha_1^{(1)} = 0, \tag{5.22a}$$

$$\alpha_0^{(i)} + \alpha_1^{(i)} = \alpha_0^{(i-1)} + \alpha_1^{(i-1)}e^{-\varphi} \text{ for } i > 1 \tag{5.22b}$$

The final density of dogs marked in a campaign week, $V^{(i)}$, is set equal to the number of marked dogs estimated from the coverage assessment for that week (Table 5.1) divided by the campaign area for that year (240 km^2 in 2012 and 285 km^2 in 2013). Condition (Eq. 5.22) and the ordinary differential equations for the vaccination model (Eq. 5.17) with its boundary conditions provide two sets of equations for each campaign week. For other parameter values as provided in table 5.3, we numerically simulate the vaccination model using an adaptive step-size Runge-Kutta method (ode45) and then use a root-finding algorithm (fzero) to calculate $\alpha_0^{(i)}$ and $\alpha_1^{(i)}$ (in MATLAB, version 8.5) for each campaign week. Figure 5.10 shows the final estimated vaccination rates during the two campaigns.

Rate of loss of vaccine immunity

In 2012, before the vaccination campaigns were conducted, a total of 105 dogs in N'Djamena were tested for antibody titers, vaccinated, and then followed up over a period of 1 year. Of these dogs, 58 had initial antibody titers that showed no previous vaccination and were successfully

followed up over the entire year. After 1 year, 44 dogs had antibody titers above 0.5 IU, which, as a conservative estimate, we considered protective (Moore and Hanlon, 2010). We calculated the rate of loss of vaccine decay, λ_d , assuming exponential decay and a relative value of 0.76 after 52 weeks.

Rabies transmission rates

The number of rabid dogs and exposed humans recorded per week since 4 June 2012 are shown in the additional file RabiesData1.txt. Recording of both human and dog cases is ongoing, but the analysis only included cases until the end of October 2015. We divide the numbers of dogs and humans by the area estimated in the coverage assessment of the 2012 vaccination campaign (240 km^2) to provide the densities of rabid dogs and exposed humans. We first fit the dog-to-dog transmission rate, β_{dd}, for the model with transmission only in dogs (Eq. 5.1) with the data for the number of rabid dogs with other parameter values as described in table 5.3 and the vaccination rate as described above. We then use this value for β_{dd} to estimate the dog-to-human transmission rate, β_{hd}, for the full model with transmission between dogs (Eq. 5.1) and to humans (Eq. 5.5) with the data for number of exposed humans. To fit β_{dd}, we numerically simulate Eq. 5.1 using an adaptive step-size Runge-Kutta method and minimize the Euclidean distance between the simulated incidence of infectious dogs (from the first term of the right-hand side of Eq. 5.1) and the observed weekly incidence of infectious dogs in MATLAB. We assume that the probability of detecting a rabid dog is $p_d = 0.5$ so that, on average, there were twice as many rabid dogs as those detected. There are few data on this parameter, but our sensitivity analysis showed that unless p_d is very low, the estimated values for β_{dd} did not change much (Figure 5.9). We assume that the initial condition for the ordinary differential equations in June 2012 is at the unique endemic equilibrium [with $\alpha_d(t) = \alpha_d^*$] and the dog density is at carrying capacity. We similarly fit β_{hd} by numerically simulating Eqs. 5.1 and 5.5 and minimizing the Euclidean distance between the simulated density of exposed humans, $E_h(t)$, and the observed density of exposed humans on a weekly time step in MATLAB. Here, we assume perfect detection of exposed humans ($p_h = 1$) and that the initial condition in June 2012 is at the unique endemic equilibrium with a population density of humans of 4833 humans/km^2 (from a total population size of 1.16 million in 2012 estimated from the 2011 population size of 1.079 million using a growth rate of 7.5%).

Phylogenetic importation analysis

To investigate the hypothesis of a reintroduction of dog rabies in N'Djamena from outside of the city after the vaccination campaigns, we performed a phylogenetic analysis using the previously described 29 complete nucleoprotein sequences of rabies virus isolates collected between August 2011 and January 2014, with the inclusion of one supplementary sequence of an isolate collected during this period (GenBank accession number KY124541), in addition to the sequences of the three first isolates collected in the city after this period (from February 2014 to January 2015, GenBank accession numbers MF53862931) and to published available sequences from Chad (n = 1) and from neighboring countries (n = 14). Using jModelTest2 (Darriba et al., 2012; Guindon and Gascuel, 2003), the best-fit model of nucleotide substitution according to the Bayesian Information Criterion was the general time reversible model with proportion of invariable sites plus

gamma-distributed rate heterogeneity (GTR+I+Γ4). A phylogenetic tree was then estimated using the ML method available in PhyML 3.0 (Guindon et al., 2010) using subtree-pruning-regrafting branch-swapping. The robustness of individual nodes on the phylogeny was estimated using 1000 bootstrap replicates and using the approximate likelihood ratio test with Shimodaira-Hasegawalike supports (Anisimova and Gascuel, 2006). GenBank accession numbers of published sequences used in this tree are as follows: EU853590 (07072RCA), EU853651 (07149RCA), EU038107 (35RD8005), KT119773 (8801CAM), KX148243 (8803CAM), U22635 (8804CAM), EU853654 (9014NIG), KX148208 (92029CAR), KT119779 (9218TCH), KT119784 (9502CAM), KF977826 (CAR_11_001h), KC196743 (DRV_NG11), EU038108 (RD128), EU038096 (RD137), and EU038093 (RD9305HN).

Sensitivity analysis

We conducted local and global sensitivity analysis of the control reproductive number, R_c (Eq. 5.10), to the model parameters (Figure 5.11). We used the normalized forward sensitivity index for the local analysis (Chitnis et al., 2008; Arriola and Hyman, 2009) at the parameter values defined in table S2 and the partial rank correlation coefficients for the global analysis (Wu et al., 2013), assuming that all parameters were uniformly distributed in the intervals: $r_d \in [0.049, 1]$, $\beta_{dd} \in [0.00292, 0.0614]$, $K_d \in [10.5, 221]$, $\sigma_d \in [0.0239, 0.504]$,$b_d \in [0.0013, 0.0273]$, $\mu_d \in [0.123, 2.59]$, $\nu_d \in [0.094, 1]$, and $\alpha_d^* \in [0.000296, 0.00622]$. Both the local and global analysis showed that the probability of developing rabies, r_d , the transmission rate, β_{dd}, the carrying capacity, K_d , and the rabies-induced mortality rate, μ_d , had a strong impact on the threshold for sustained transmission, R_c , whereas the other parameters had minimal impact.

Stochastic model simulations

We derived and numerically simulated a stochastic dog-to-dog transmission model based on Eq. 5.1, with the master equation

$$\frac{dP(n,t)}{dt} = \sum_i [W_i(n|m_i)P(m_i,t) - W_i(m_i|n)P(n,t)] \tag{5.23}$$

where n is any state of the system at time t, and W_i are the transmission rates deduced from the parameters in table 5.3 using the Gillespie algorithm with the tau-leaping simulation method (Gillespie, 1977; Cao et al., 2006). Figure 5.12 shows a sample stochastic simulation of the density of exposed and infectious dogs with the corresponding simulation of the deterministic model and the underlying data for the number of infectious dogs. Figure 5.3 shows that the mean of 500 simulation runs of the stochastic model declines after the first vaccination campaign in a similar manner to the deterministic model.

Pylodynamic analysis

Twenty-nine sequences of canine rabies viruses, collected between August 2011 and June 2013, were analyzed with Beast v2 (Bouckaert et al., 2014). We chose a Hasegawa-Kishino-Yano model for substitutions with a relaxed log-normal clock (Drummond et al., 2006). We assumed an exponential (0.001) prior for the mean rate, an exponential (0.3333) prior for the SD, and a log-normal (1,1.25) prior for kappa. For the epidemiological model, we chose the birth-death skyline

model (Stadler et al., 2013). We used a log-normal (0,1) prior for the effective reproductive number, R_e , and allowed R_e to change in January 2013, August 2012, and April 2012 (that is, every 4.8 months before the last sample in June 2013). We assumed a uniform prior on the interval (9.44,9.5) for the dog removal rate [corresponding to an expected infection time of exposed and active rabies between (1/9.5,1/9.44) years, which is about 1.1 months]. The sampling probability of a rabid dog was assumed to be 0 before the first sample and uniform on (0.4,0.6) between the first and last sample. The time of the initial case in that transmission chain was assumed to be a uniform prior on (0,20) before the most recent sample. We ran the Markov chain Monte Carlo simulations for 10 9 steps. We neglected the first 10% of the states as a burn-in period. The effective sample size of all parameters was 350 or higher (determined within Tracer v1.6.0, http://tree.bio.ed.ac.uk/software/tracer/), implying that we obtained substantial mixing. To investigate sensitivity toward our assumption of a constant sampling proportion, we performed a second analysis allowing the sampling proportion to change at the same time points as when the R_e changes. As above, sampling was assumed to be 0 before the oldest sample. Further sampling was assumed to be uniform on (0.2,0.6) in each interval [compared to uniform on (0.4,0.6) above]. As shown in Figure 5.13, the results do not change qualitatively.

5.6 Supplementary materials

$S_d(t)$	Susceptible dog density at time t
$E_d(t)$	Exposed dog density at time t
$I_d(t)$	Rabid dog density at time t
$V_d(t)$	Vaccinated dog density at time t
$S_h(t)$	Susceptible human density at time t
$E_h(t)$	Exposed human density at time t
$I_h(t)$	Rabid human density at time t

Table 5.2: State variables of dog rabies transmission model.

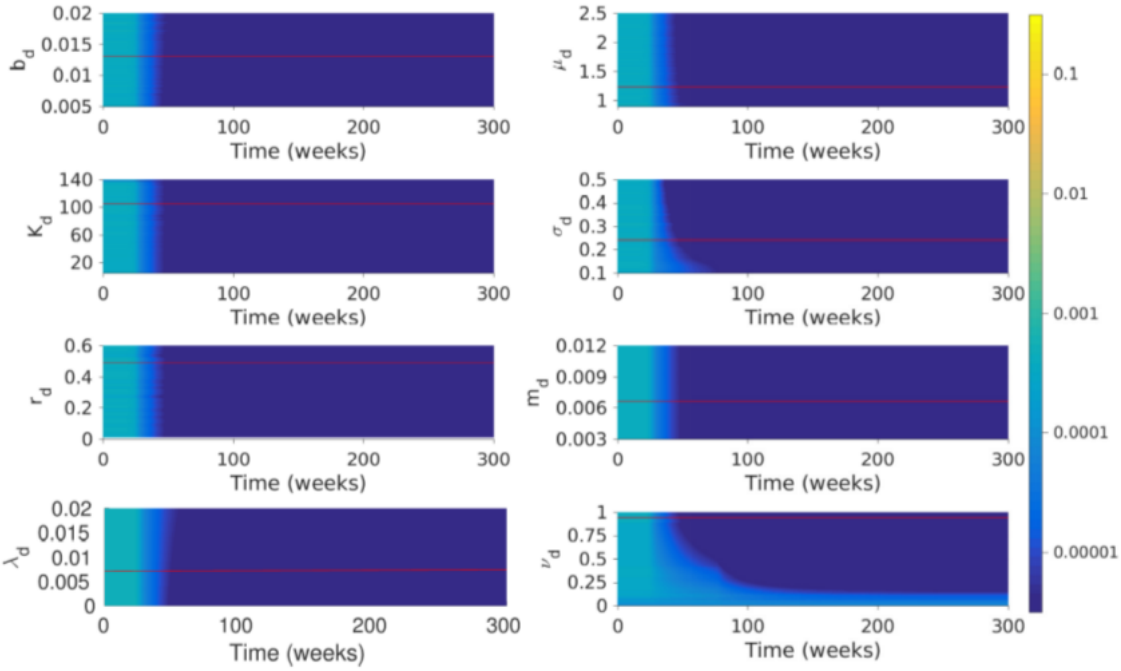

Figure 5.5: One-dimensional sensitivity analysis of simulation results on parameter values. The plots show simulations of the density of infectious dogs over 6 years (300 weeks) where all parameters are fixed at values described in table 5.3 except for the parameter being varied and β_{dd}. The x-axis shows the time in weeks and y-axis shows the value of the parameter (in its corresponding units). The color of each pixel represents the density of infectious dogs. The horizontal red lines correspond to the parameter values in table 5.3 and the solution plotted in Figure 5.1.

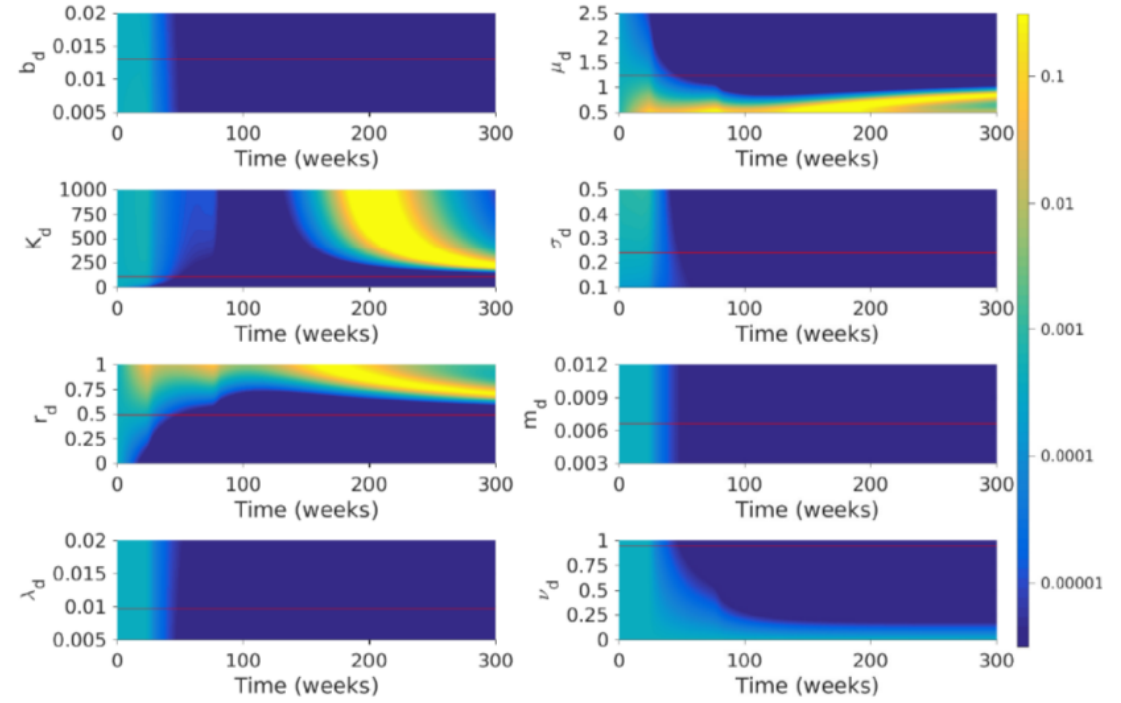

Figure 5.6: One-dimensional sensitivity analysis of simulation results on parameter values with dog-to-dog transmission fixed as constant. The plots show simulations of the density of infectious dogs over 6 years (300 weeks) where all parameters are fixed at values described in Table 5.3 except for the parameter being varied (β_{dd} is fixed at 0.0292). The x-axis shows the time in weeks and y-axis shows the value of the parameter (in its corresponding units). The color of each pixel represents the density of infectious dogs.

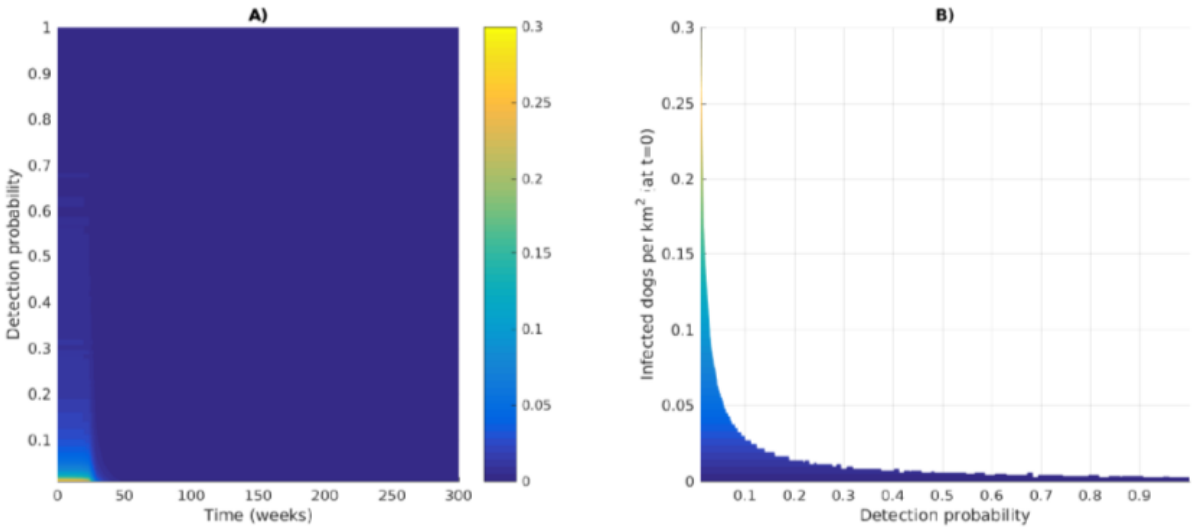

Figure 5.7: Sensitivity analysis of the simulation results on the probability of detecting rabid dogs. (A) The simulated density of infectious dogs depending on the detection probability of rabid dogs, p_d, over time. The x-axis corresponds to time (measured in weeks) and the y-axis to the detection probability. The color of each pixel corresponds to the density of infectious dogs. (B) The endemic equilibrium value for density of infectious dogs (in the absence of vaccination campaigns) depending on p_d. The x-axis corresponds to to the detection probability, p_d and the y-axis (and color of the pixel) correspond to the endemic equilibrium density of infectious dogs.

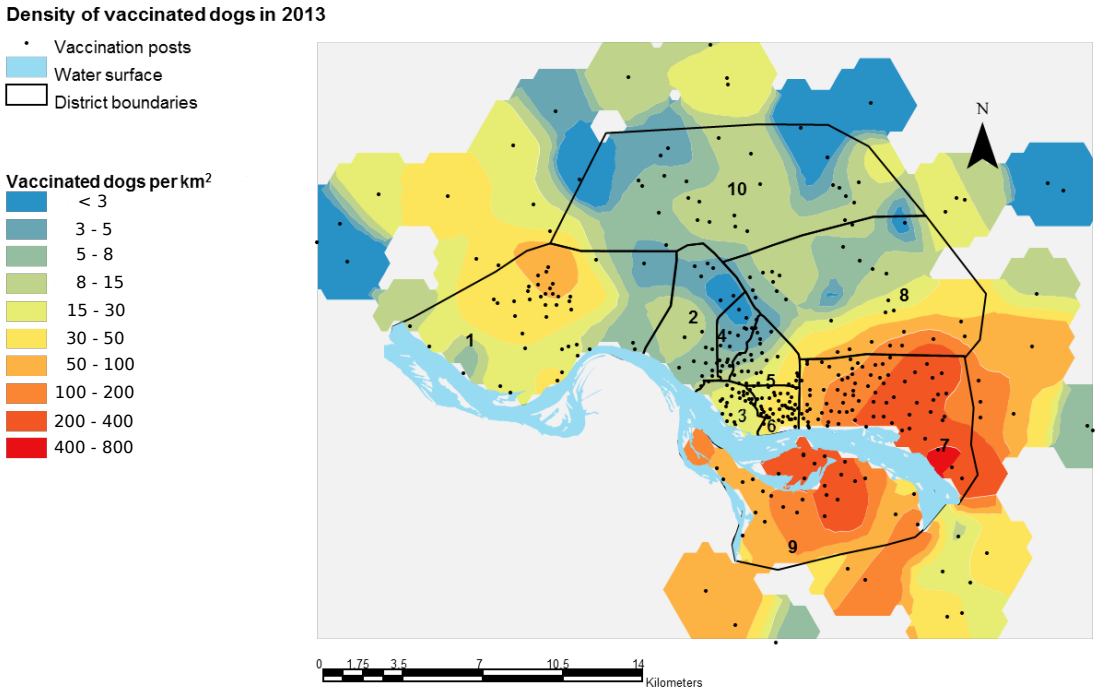

Figure 5.8: Density of vaccinated dogs in N'Djamena in 2013 calculated on the basis of the data presented by Léchenne et al. (2016b). Black dots indicate the locations of the fixed vaccination posts. It is assumed that dogs diffuse from these locations after vaccination in a homogeneous way. We used a diffusion kernel prediction map with a bandwidth of 1040 m (which is the diameter of a circle of 0.86 km^2, the area per post of 331 posts in a total area of 285km^2). The water surface was included as a barrier function.

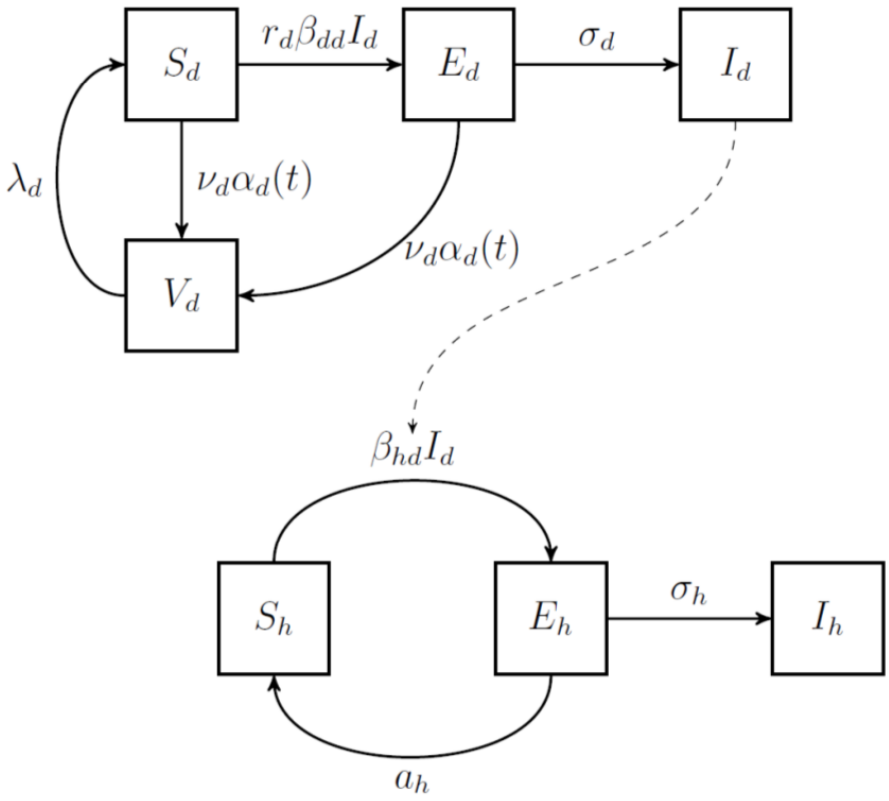

Figure 5.9: Schematic of mathematical model of rabies. Birth and death rates of humans and dogs are not shown.

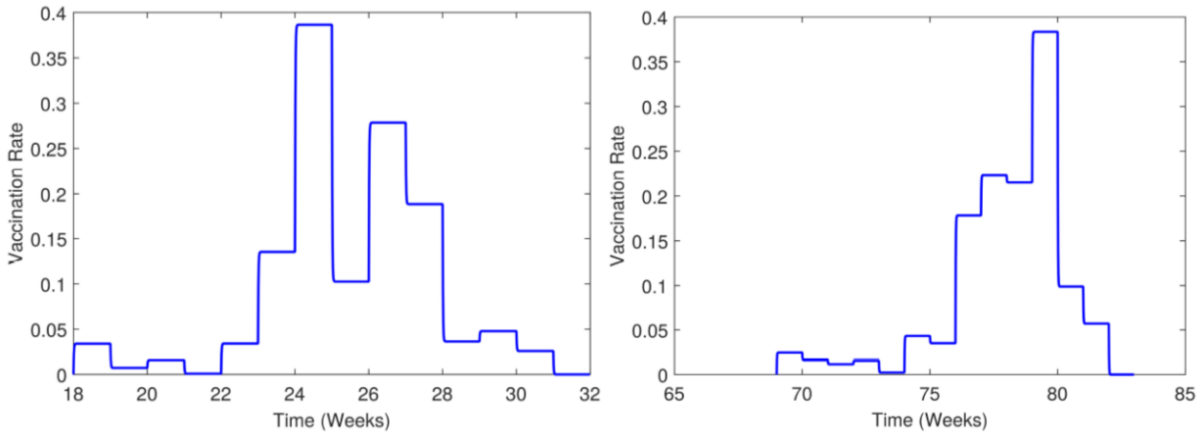

Figure 5.10: Vaccination rates during the two campaigns in 2012 and 2013. The weeks are labelled starting from 4 June 2012.

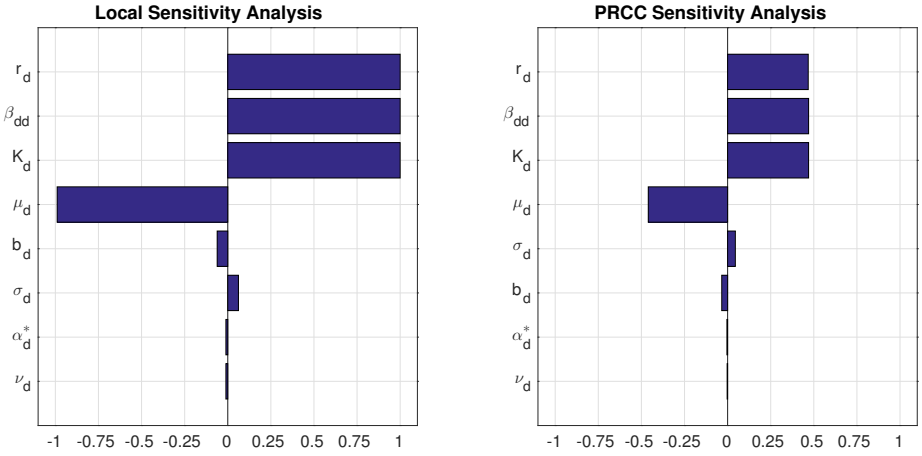

Figure 5.11: Local and global sensitivity indices of the control reproductive number, R_c , to the model parameters.

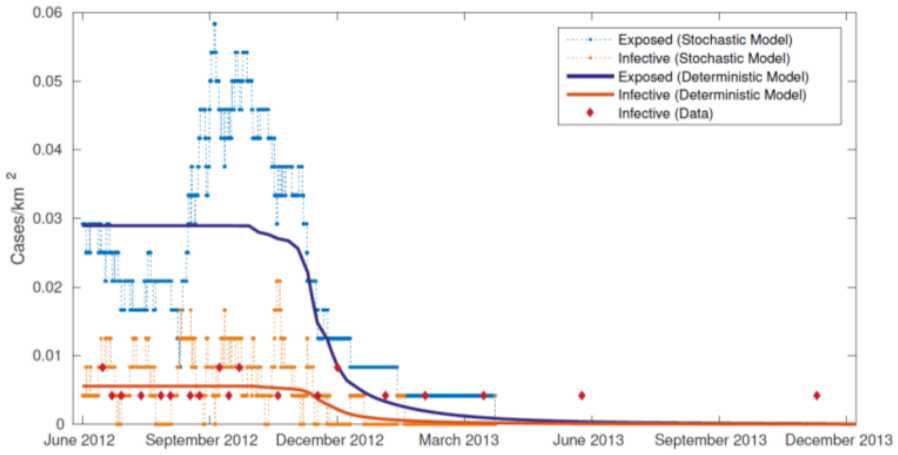

Figure 5.12: Sample simulation of the stochastic model, including the deterministic result.

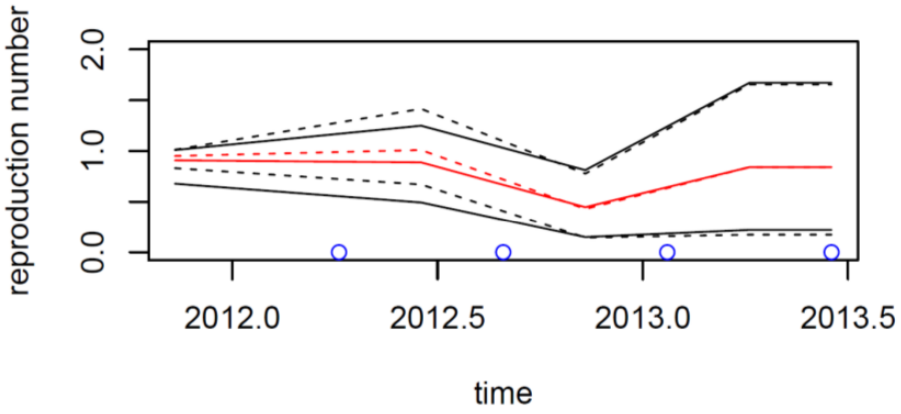

Figure 5.13: Results of the phylodynamic analysis showing median (red) and 95% HPD interval (black) for R_e through time. Solid lines correspond to the constant sampling proportion assumption, and dashed lines to the changing sampling proportion assumption. Blue points indicate the change of R_e and sampling proportion. We plot the R_e estimate for each interval at the midpoint of the interval, and interpolate linearly in between.

Symbol	Description	Source	Value	Unit
b_d	Dog birth rate	Household survey (Mindekem et al., 2005a)	0.013	week^{-1}
m_d	Dog natural death rate	Household survey (Mindekem et al., 2005a)	6.64 x 10^{-3}	week^{-1}
K_d	Dog carrying capacity	estimated from dog population size and area from coverage survey 2012 (Léchenne et al., 2016b)	105	animals km^2
β_{dd}	Dog to dog transmission rate	Estimated for this study	0.0292	km^{2}week^{-1}animals $^{-1}$
σ_d	Dog rate of progression from exposed to infectious state	Previous model (Zinsstag et al., 2009)	0.239	week^{-1}
r_d	Probability of exposed dog developing rabies	Previous model (Zinsstag et al., 2009)	0.49	1
μ_d	Death rate due to rabies in dogs	Previous model (Zinsstag et al., 2009)	1.23	week^{-1}
α_d^*	Background dog vaccination rate	Estimated for this study	2.96 x 10^{-3}	week^{-1}
ν_d	Efficacy of vaccine in dogs	Previous model (Zinsstag et al., 2009)	0.94	1
λ_d	Rate of loss of vaccine efficacy in dogs	Estimated assuming exponential decay based on data from 105 dogs vaccinated during the campaign in 2012	5.5 x 10^{-3}	week^{-1}
b_h	Human birth rate	Previous model (Zinsstag et al., 2009)	7.6 x 10^{-4}	week^{-1}
m_h	Human mortality rate	Previous model (Zinsstag et al., 2009)	2.9 x 10^{-4}	week^{-1}
β_{hd}	Dog to human transmission rate	Estimated for this study	2.34 x 10^{-5}	
σ_h	Human rate of progression to rabies	Calculated with parameter values from the probability tree of the location of human exposure (Zinsstag et al., 2009) using equation 5.7	0.0967	week^{-1}
μ_h	Death rate due to rabies in humans	Previous model (Zinsstag et al., 2009)	1	week^{-1}

Table 5.3: Parameters of the rabies transmission model with estimated values and sources. Most parameters have the same value as in the previous model (Zinsstag et al., 2009), but some have been updated from more recent publications or from new data from the current study (as described in the section on parameter estimation).

6. A metapopulation model of dog rabies transmission in N'Djamena, Chad

Mirjam Laager[1,2], Monique Léchenne[1,2], Kemdongarti Naissengar[3], Rolande Mindekem[4], Assandi Oussiguere[3], Jakob Zinsstag[1,2], Nakul Chitnis[1,2]

[1]Swiss Tropical and Public Health Institute, Socinstrasse 57, 4051 Basel, Switzerland

[2]University of Basel, Petersplatz 1, 4001 Basel, Switzerland

[3]Institut de Recherches en Elevage pour le Développement, BP 433, Farcha, N'Djamena

[4]Centre de Support en Santé Internationale, BP 972, Moursal, N'Djamena, Chad

This manuscript has been submitted to the Journal of Theoretical Biology, July 2017

6.1 Abstract

Rabies transmission was interrupted for several months in N'Djamena, the capital city of Chad, after two mass vaccination campaigns of dogs. However, there was a resurgence in cases, which was not predicted by previous models of rabies transmission. We developed a deterministic metapopulation model with importation of latent dogs, calibrated to four years of weekly incidence data from passive surveillance, to investigate possible causes for the early resurgence. Our results indicate that importation of latently infective dogs better explains the data than heterogeneity or underreporting. Stochastic implementations of the model suggest that the two vaccination campaigns averted approximately 67 cases of dog rabies (out of an estimated 74 cases without vaccination) and 124 human exposures (out of an estimated 148 human exposures without vaccination) over two years. Dog rabies vaccination is therefore an effective way of preventing rabies in the dog population and to subsequently reduce human exposure. However, vaccination campaigns have to be repeated to maintain the effect or reintroduction through importation has to be prevented.

6.2 Introduction

Rabies is a viral disease that is transmitted by bite and can affect any mammal. After the onset of symptoms, rabies is fatal. Approximately 59,000 people die of rabies every year (Hampson et al., 2015), mainly in developing countries with children most at risk. The main vector for human rabies is the domestic dog. Rabies in humans can be prevented by vaccinating dogs or by post exposure treatment of humans, which consists of vaccination and injection of immunoglobulin (WHO, 2010). Pre-exposure vaccination is also available, which simplifies the post exposure regimen and has been recommended in places with high dog bite incidence, incomplete rabies

control in the animal reservoir and limited access to immunoglobulin (Kessels et al., 2017; WHO, 2013).

Detailed analysis of rabies transmission biology suggests that rabies has a low reproductive ratio (Hampson et al., 2009) and that with a sufficiently high dog rabies vaccination coverage, rabies could be eliminated (Lembo et al., 2010; Lankester et al., 2014; Fooks et al., 2014; Fahrion et al., 2017). Dog rabies vaccination can be an effective path of preventing human exposure, avoiding the very expensive post exposure treatment. However maintaining vaccination coverage over a longer time is crucial, as has been seen in the recent case of rabies reintroduction in Arequipa (Castillo-Neyra et al., 2017).

Mathematical models offer a framework to compare the effect of different interventions on disease transmission dynamics, with a long history of application to rabies. Anderson et al. (1981) developed a deterministic ordinary differential equation model to simulate the dynamics of rabies transmission among foxes in Europe, assuming density dependent transmission and logistic population dynamics of foxes. They concluded that culling is unlikely to be an effective intervention and recommended compulsory vaccination of cats and dogs. Murray et al. (1986) modified the model by Anderson *et al.* by adding a diffusion term to incorporate spatial dispersal of rabid foxes. They determined the minimal speed of the travelling wavefront for different diffusion coefficients and applied these results to a hypothetical fox rabies outbreak in the south of England. Ou and Wu (2006) introduced a distinct movement behaviour of adult and juvenile foxes, which yields a system of reaction diffusion equations with delayed nonlinear interactions. Using finite elements for space discretization of a system of partial differential equations, Keller et al. (2013) simulated the spread of raccoon rabies on a fine grid incorporating landscape heterogeneities such as rivers, forests and highways.

While models for rabies in wildlife populations such as foxes and raccoons often use random diffusion to incorporate space in the model and are interested in movement over large areas, models of transmission in dogs have to take into account that movement of domestic dogs is likely to be centred around the residences of the owners. Several models of dog rabies transmission have addressed this. Dürr *et al.* collected detailed geopositioning system (GPS) data on dog movement in Australia (Dürr and Ward, 2014) and developed an individual based, stochastic transmission model where the transmission probability between two dogs decreased with distance between the owners households according to a function that was estimated from the movement behaviour data (Dürr and Ward, 2015). Beyer et al. (2011) fitted a stochastic metapopulation model of 75 villages in Tanzania to incidence data, assuming that transmission probability decreases exponentially with distance between households. Chen et al. (2015) modelled the spread of rabies in Mainland China by using a deterministic compartmental model in each province and assuming movement of dogs between the provinces.

In N'Djamena, the capital of Chad, two mass vaccination campaigns of dogs were conducted in 2012 and 2013, reaching a vaccination coverage of 70% in both years, as described in more detail in a previous publication (Léchenne et al., 2016b). During a period of 13 weeks, from October to January, vaccination posts were set up in all districts of N'Djamena (Figure 6.1). Dogs were brought to the vaccination posts by the owners and were vaccinated free of charge. After the vaccination, a certificate was issued and the vaccinated dogs were marked with a collar. The weekly number of vaccinated dogs ranged from 24 to 4402 dogs and the total number of

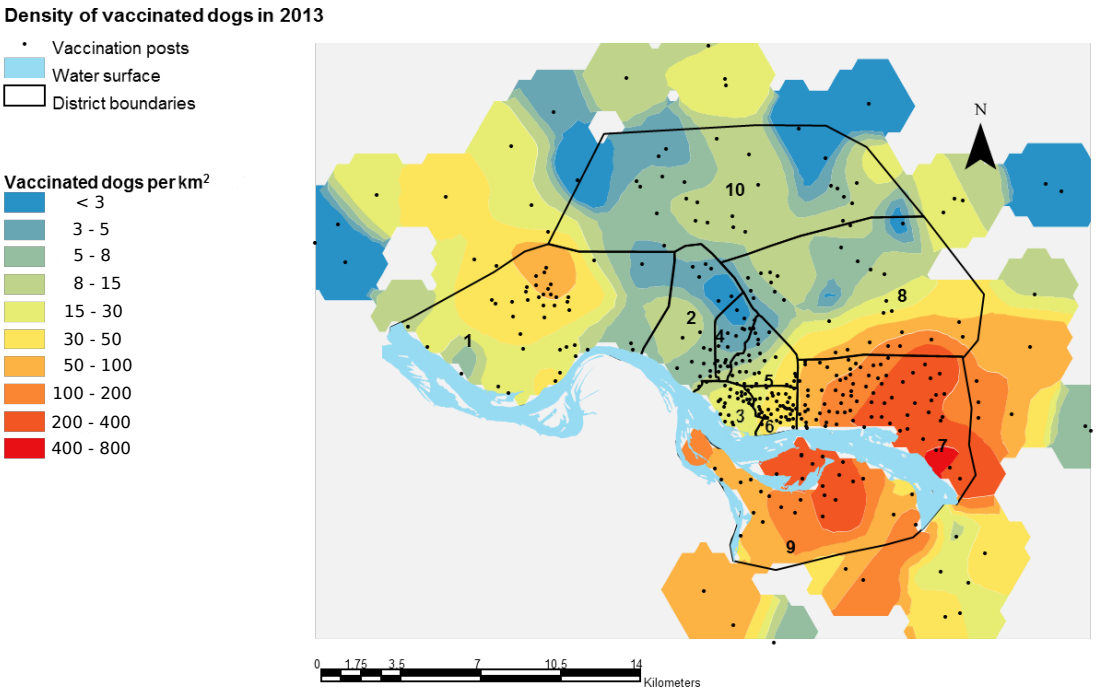

Figure 6.1: Districts of N'Djamena and density of vaccinated dogs in 2013. (Figure reproduced from (Zinsstag et al., 2017))

vaccinated dogs after 13 weeks was 17,538 in 2012 and 21,340 in 2013. Coverage was assessed with a capture-mark-recapture model. Since 2012, weekly incidence of rabies in dogs was reported through passive surveillance. Before the campaigns, there was on average one confirmed case of dog rabies per week. The campaigns interrupted transmission for 8 months, but there was a resurgence in cases, which was not predicted by a previous model of rabies transmission (Zinsstag et al., 2017). Possible reasons for the early resurgence include heterogeneity, reintroduction and underreporting. Dog densities and vaccination coverage varied largely across the different districts of N'Djamena (Figure 6.1) and this heterogeneity could facilitate early re-establishment of rabies in the population in higher transmission districts. A previous study in Bangui showed that reintroduction of strains from outside the city occurs frequently (Bourhy et al., 2016), which could also explain the early resurgence seen in N'Djamena. Rabies cases are also frequently underreported (Hampson et al., 2015). Each case in the passive surveillance data was confirmed by an immunofluorescence antibody test (IFAT) which implies that all recorded cases are true cases. However, since passive surveillance is based on voluntary reporting, there could be many additional cases. The resurgence seen in the data could therefore also be explained by unreported ongoing transmission.

We develop a deterministic ordinary differential equation model to explore which one of these reasons best explains the resurgence. We incorporate heterogeneity by dividing the city into patches, with a homogeneous model in each patch and some movement of infections between patches and allow for the importation of latent dogs from the surroundings of the city. We fit the model parameters to the four years of weekly incidence data and conduct a sensitivity analysis to assess the effect of underreporting on the estimated transmission rates. A stochastic version of the model, implemented via the Gillespie algorithm, yields a distribution of the time to elimination.

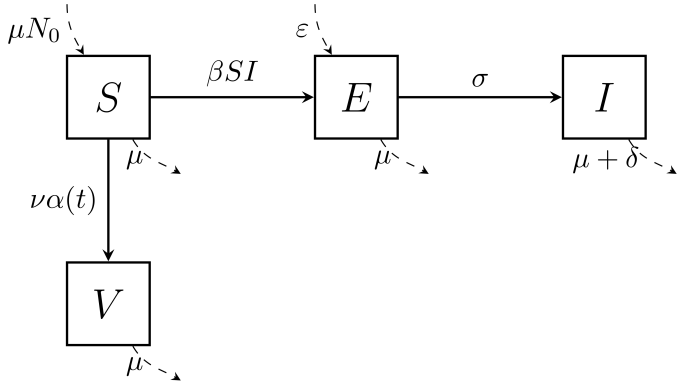

Figure 6.2: Schematic of the homogeneous model.

6.3 Model description

Homogeneous model We use a deterministic ordinary differential equation model, based on a previous model (Zinsstag et al., 2009, 2017), where the population is divided into susceptible (S), exposed (E), infective (I) and vaccinated (V) dogs. As in the previous model and in many deterministic models of rabies transmission (Anderson et al., 1981; Murray et al., 1986; Ou and Wu, 2006; Chen et al., 2015), dogs become exposed via density dependent transmission and die from rabies according to a per capita disease induced death rate. The previous model assumed logistic population dynamics of dogs with a quadratic death rate. We simplified the model by assuming a constant birth and a constant per-capita death rate. We also removed the vaccination of exposed dogs, since we found no evidence that dogs can still be successfully protected after an infectious bite. A study showed that 88% of dogs vaccinated with a single dose against rabies still survived a challenge with live rabies virus after three years (Lakshmanan et al., 2006), so we assume that vaccinated dogs stay protected for the rest of their lives. We also allowed for the importation of latent dogs into the population.

The equations for the homogeneous model are given by

$$\frac{dS(t)}{dt} = \mu N_0 - (\nu\alpha(t) + \mu)S(t) - \beta S(t)I(t), \tag{6.1a}$$

$$\frac{dE(t)}{dt} = \beta S(t)I(t) - (\sigma + \mu)E(t) + \varepsilon, \tag{6.1b}$$

$$\frac{dI(t)}{dt} = \sigma E(t) - (\delta + \mu)I(t), \tag{6.1c}$$

$$\frac{dV(t)}{dt} = \nu\alpha(t)S(t) - \mu V(t). \tag{6.1d}$$

The description of the state variables and parameters can be found in the Tables 6.1 and 6.2 (ignoring the indices of the patches). A schematic of the model is shown in Figure 6.2. All rates are constant in time, except for the vaccination rate, which is given by

$$\alpha(t) = \alpha^* + \alpha_0^{(i)}(t) + \alpha_1^{(i)}(t)e^{-\varphi_\alpha t}, \tag{6.2}$$

where α^* is a background vaccination rate and $\alpha_0^{(i)}$ and $\alpha_1^{(i)}$ are fitted to the number of vaccinated dogs in each week i of the two vaccination campaigns in N'Djamena .

Variable	Description
$S_k(t)$	Number of susceptible dogs in patch k at time t
$E_k(t)$	Number of exposed dogs in patch k at time t
$I_k(t)$	Number of rabid dogs in patch k at time t
$V_k(t)$	Number of vaccinated dogs in patch k at time t

Table 6.1: State variables of the transmission models. For the homogeneous model, state variables have no subscript k.

Metapopulation model We expand the homogeneous model described above to a metapopulation model with n subpopulations. In each subpopulation the population dynamics are described by

$$\frac{dS_k(t)}{dt} = \mu N_{0,k} - (\nu\alpha_k(t) + \mu)S_k(t) - \beta_k S_k(t)\sum_{j=1}^{n} m_{kj} I_j(t), \tag{6.3a}$$

$$\frac{dE_k(t)}{dt} = \beta_k S_k(t)\sum_{j=1}^{n} m_{kj} I_j(t) - (\sigma + \mu)E_k(t) + \varepsilon_k, \tag{6.3b}$$

$$\frac{dI_k(t)}{dt} = \sigma E_k(t) - (\delta + \mu)I_k(t), \tag{6.3c}$$

$$\frac{dV_k(t)}{dt} = \nu\alpha_k(t)S_k(t) - \mu V_k(t), \tag{6.3d}$$

The state variables and the parameters are described in Tables 6.1 and 6.2.

	Description	Dimension	Conditions
μ	Birth/death rate	1/time	$\mu > 0$
$N_{0,k}$	Stable dog population in patch k in the absence of rabies	animals	$N_0 > 0$
β_k	Transmission rate in patch k	1/(animals $\times$ time)	$\beta_k > 0$
σ	Rate of progression from exposed to infectious state	1/time	$\sigma > 0$
δ	Disease induced death rate	1/time	$\delta > 0$
$\alpha_k(t)$	Vaccination rate in patch k at time t	1/time	$\alpha_k(t) \geq 0$
ν	Efficacy of vaccine	dimensionless	$0 \leq \nu \leq 1$
ε_k	Rate of importation of exposed dogs into patch k	animals	$\varepsilon_k \geq 0$
m_{kj}	Proportion of time a dog from patch j spends in patch k	dimensionless	$0 \leq m_{kj} \leq 1$

Table 6.2: Parameters of the transmission models. Time is measured in weeks. For the homogeneous model, the parameters $N_{0,k}, \beta_k, \alpha_k(t)$ and ε_k have no subscript k.

Since we consider a population of owned dogs we assume Lagrangian movement, which means that there is no exchange of dogs between the patches, but only movement of infection (unlike the model in Chen *et al.* (Chen et al., 2015)). All dogs live in their home patch, but infected dogs can infect susceptible dogs in adjacent patches. These between patch dynamics are captured by the matrix $M = (m_{kj})_{k,j=1}^{n}$, where m_{kj} describes the proportion of time an infected dog from patch j spends in patch k. We impose the following three conditions on M:

(C I) $m_{kj} = m_{kj}$ for all k, j,

(C II) $m_{kk} \geq m_{kj}$ for all j,

(C III) $\sum_{j=1}^{n} m_{kj} = 1$ for all k.

The first and second condition imply that a dog from patch k spends as much time in patch j as any dog from patch j spends in patch k and that a dog spends most time in the patch where its owner lives. The third condition is a normalization that assures, that the sum of the

proportional time spent in all patches is one. In the case of no movement this model simplifies to n homogeneous models like the ones described by equations (6.1).

Stochastic implementation of the model We use the Gillespie algorithm (Gillespie, 1977) to simulate the time evolution of the stochastic counterpart of the model described by equations (6.1). For transition rates dependent on the parameter values and state variables at any point in time the algorithm randomly draws a time step based on the sum of all the transition rates and then selects one of all the possible events according to their relative probabilities. Implementing the transitions between the states of the model as a stochastic process allows us to account for unlikely events, to model the importation of exposed dogs as discrete importation events at random points in time and to gain insight into the distribution of the time to elimination.

6.4 Model analysis

Homogeneous model without importation

Disease free equilibrium and reproductive number In the absence of importation ($\varepsilon = 0$) and with a constant vaccination rate $\alpha(t) = \alpha^*$ the disease free equilibrium of the homogeneous model is given by

$$S^* = \frac{\mu}{\mu + \nu\alpha^*} N_0, E^* = I^* = 0 \text{ and } V^* = \frac{\nu\alpha^*}{\mu + \nu\alpha*} N_0. \tag{6.4}$$

We use the next generation matrix approach described by (Diekmann et al., 2010) and define the basic reproductive ratio, R_0, as the number of secondary infections, one infectious individual produces over the course of its infectious period in the absence of interventions (also excluding vaccination ($\alpha^* = 0$)). In the homogeneous model the basic reproductive ratio is given by

$$R_0 = \frac{\beta\sigma N_0}{(\sigma + \mu)(\delta + \mu)},$$

and the disease free equilibrium is

$$S^* = N_0, E^* = I^* = V^* = 0. \tag{6.5}$$

Theorem 1. *The disease free equilibrium (6.5) is locally asymptotically stable if $R_0 < 1$ and unstable if $R_0 > 1$.*

Proof. The eigenvalues of the Jacobian of the homogeneous model (6.1) evaluated at the disease free equilibrium in the absence of vaccination are the roots x of the characteristic equation

$$(\mu + x)\left[x^3 + a_2x^2 + a_1x + a_0\right] = 0 \tag{6.6}$$

with $a_2 = \sigma + \delta + 3\mu, a_1 = (\sigma + \mu)(\delta + \mu) + (\sigma + \mu)\mu + (\delta + \mu)\mu - \sigma\beta N_0$ and $a_0 = (\sigma + \mu)(\delta + \mu)\mu - \sigma\mu\beta N_0$. From the Routh-Hurwitz criterion we know, that these eigenvalues all have negative real parts if and only if $a_2 > 0, a_0 > 0$ and $a_2a_1 > a_0$ which is true if and only if $R_0 < 1$.

□

Endemic equilibrium The endemic equilibrium is given by

$$S^* = \frac{(\sigma+\mu)(\delta+\mu)}{\sigma\beta}, \tag{6.7a}$$

$$E^* = \frac{\delta+\mu}{\sigma}\left(\frac{\sigma\mu N_0}{(\sigma+\mu)(\delta+\mu)} - \frac{\nu\alpha^*+\mu}{\beta}\right), \tag{6.7b}$$

$$I^* = \frac{\sigma\mu N_0}{(\sigma+\mu)(\delta+\mu)} - \frac{\nu\alpha^*+\mu}{\beta}, \tag{6.7c}$$

$$V^* = \frac{\nu\alpha^*(\sigma+\mu)(\delta+\mu)}{\sigma\beta\mu}. \tag{6.7d}$$

Theorem 2. *In the absence of vaccination ($\alpha^* = 0$) the endemic equilibrium (6.7) is locally asymptotically stable if and only if $R_0 > 1$.*

Proof. The eigenvalues of the Jacobian of the homogeneous model (6.1) evaluated at the endemic equilibrium in the absence of vaccination are the roots x of the characteristic equation

$$(\mu + x)\left[x^3 + a_2x^2 + a_1x + a_0\right] = 0 \tag{6.8}$$

with $a_2 = 2\mu+\sigma+\delta+\frac{\sigma\beta\mu N_0}{(\sigma+\mu)(\delta+\mu)}$, $a_1 = (2\mu+\sigma+\delta)\frac{\sigma\beta\mu N_0}{(\sigma+\mu)(\delta+\mu)}$ and $a_0 = \mu(\sigma\beta N_0-(\sigma+\mu)(\delta+\mu))$. From the Routh-Hurwitz criterion we know, that these eigenvalues all have negative real parts if and only if $a_2 > 0, a_0 > 0$ and $a_2a_1 > a_0$ which is true if and only if $R_0 > 1$.

□

Homogeneous model with importation

The homogeneous model with importation has no disease free equilibrium. To calculate the endemic equilibrium, we simplify the system of equations (6.1) to the quadratic equation

$$aI^2 + bI + c = 0$$

with $a = -\beta(\sigma+\mu)(\delta+\mu)$, $b = \sigma\beta\mu N_0 + \sigma\beta\epsilon - (\alpha+\mu)(\sigma+\mu)(\delta+\mu)$ and $c = \sigma\epsilon(\alpha+\mu)$. Since $a < 0$ and $c > 0$, there is exactly one positive solution I^*.

Metapopulation model without importation

Disease Free equilibrium and reproductive number In the absence of importation and with a constant vaccination rate $\alpha_k(t) = \alpha_k^*$ the disease free equilibrium of the metapopulation model is given by

$$S_k^* = \frac{\mu}{\nu\alpha_k^*}N_{0,k}, E_k^* = I_k^* = 0 \text{ and } V_k^* = \frac{\nu\alpha_k^*}{\nu\alpha_* + \mu}N_{0,k}. \tag{6.9}$$

The basic reproductive ratio is given by the largest eigenvalue of the next generation matrix K. We find that

$$K = \frac{\sigma}{(\sigma+\mu)(\delta+\mu)}\begin{bmatrix} \beta_1N_{0,1} & & 0 \\ & \ddots & \\ 0 & & \beta_nN_{0,n} \end{bmatrix} M.$$

In the absence of movement, where each patch is isolated and therefore $M = I$, the identity matrix, the basic reproductive ratio is given by

$$R_0 = \max_k R_0^k,$$

where $R_0^k = \frac{\sigma\beta_k N_{0,k}}{(\sigma+\mu)(\delta+\mu)}$ is the basic reproductive ratio of patch k.
In the case of homogeneous mixing, where the movement from each patch to any other patch equals one divided by the number of patches and therefore $M = \frac{1}{n}\mathbf{1}$, where $\mathbf{1}$ is a matrix where each entry equals 1, the basic reproductive ratio is given by

$$R_0 = \frac{1}{n}\sum_{k=1}^{n} R_0^k.$$

Theorem 3. *For any migration matrix M satisfying the conditions (C I), (C II) and (C III)*

$$\frac{1}{n\sqrt{n}}\sum_{k=1}^{n} R_0^k \leq R_0 \leq \max_k R_0^k.$$

Proof. For any nonnegative $n \times n$ matrix A consider the unique matrix G with

$$G \star G = A \star A^T,$$

where $\star$ denotes the element-wise product of two matrices. G is called geometric symmetrization of A. It has been shown ((Schwenk, 1986)) that

$$\rho(A) \geq \rho(G).$$

Since all the entries of K are real and nonnegative, the geometric symmetrization of K is given by $G = (g_{ij})$ with

$$g_{ij} = \sqrt{R_0^i R_0^j m_{ij} m_{ji}}.$$

Since G is symmetric,

$$\rho(G) = ||G||_2,$$

where $||\,||_2$ is the spectral norm. The spectral norm is compatible with the Euclidean norm, which yields

$$||G||_2 \geq \frac{1}{||x||_2}||Gx||_2,$$

for all $x \in \mathbb{R}^n$ with $||x|| \neq 0$. With $x_j := {}^1\!/_{m_{jj}}$ and $||Gx||_2 \geq ||Gx||_\infty$, this yields

$$\begin{aligned}
\frac{1}{||x||_2}||Gx||_2 &\geq \frac{1}{||x||_2}\max_k\left(\sum_{j=1}^{n}\sqrt{R_k R_j m_{kj} m_{jk}}\frac{1}{m_{jj}}\right)\\
&\geq \frac{1}{||x||_2}\sum_{j=1}^{n}\max_k\left(\sqrt{R_k R_j m_{kj} m_{jk}}\frac{1}{m_{jj}}\right)\\
&\geq \frac{1}{||x||_2}\sum_{j=1}^{n} R_j.
\end{aligned}$$

Since ${}^1\!/_{m_{jj}} \leq n$ we get

$$\frac{1}{||x||_2} \geq \frac{1}{n\sqrt{n}},$$

which yields

$$\rho(K) \geq \rho(G) \geq \frac{1}{n\sqrt{n}} \sum_{j=1}^{n} R_j.$$

For the upper bound we use that

$$R_0 = \rho(K) \leq ||K||,$$

for any norm $||\ ||$. The basic reproductive number, R_0, is therefore bounded from above by

$$\begin{aligned} ||K|| &= \max_{||x||_\infty=1} ||Ax||_\infty \\ &= \max_k \left\{ \frac{\sigma\beta_k C_k}{(b+\delta)(b+\sigma)} \sum_{j=1}^{N} |m_{kj}| \right\} \\ &= \max_k R_0^k \end{aligned}$$

□

Metapopulation model with importation

The metapopulation model with importation has no disease free equilibrium point. We cannot explicitly calculate the endemic equilibrium point, although we expect that there is a unique endemic equilibrium point which is locally asymptotically stable when $R_0 > 1$. We use the mean of the weekly number of cases from the incidence data collected in the 14 weeks before the vaccination campaigns (Table 6.4) to estimate the pre-intervention weekly incidence of cases ϕ_k^*. We use ϕ_k^* to estimate the endemic equilibrium in each district given by

$$I^* = \frac{1}{\delta}\phi_k^*, \tag{6.10a}$$

$$E^* = \frac{\delta+\mu}{\sigma} I_k^*, \tag{6.10b}$$

$$S^* = \frac{\mu N_{0,k}}{\mu + \beta_k \sum_{j=1}^{m} m_{kj} I_j^*}, \tag{6.10c}$$

$$V^* = 0. \tag{6.10d}$$

6.5 Model calibration

We calibrate the homogeneous and metapopulation model to data on the dog population of N'Djamena, using four years of weekly incidence data, numbers of vaccinated dogs for each district and demographic information. The incidence data (Table 6.4) comes from passive surveillance of the rabies diagnostic laboratory in N'Djamena. Each case is confirmed with an immunofluorescence antibody test (IFAT) and entered into a database together with basic information on the owner, the status of the animal and the number of bite victims. The data on the total number of dogs and the number of vaccinated dogs was collected during the vaccination campaigns as explained in more detail in a previous publication (Léchenne et al., 2016b) and is summarized in Table 6.3. A recent study (Mindekem et al., 2017a) collected data on the number of puppies per litter, the proportion of female dogs with puppies and the age structure

of the dogs in N'Djamena. The dog population dynamics in N'Djamena are distinguished by a low average lifespan (approximately 3 years) and a high mortality of dogs of less than 3 months of age. A common method for estimating birth rates is counting the number of puppies per litter. Death rates are commonly deduced from the average lifespan of dogs. In a population with a high mortality in young age classes, a birth rate estimated from the number of puppies per litter is higher than the death rate estimated from the average lifespan of dogs, which would suggest an exponential increase of the dog population. However, since the dog population is only partially shaped by natural resource availability but mainly by human demand and the number of dogs has remained stable between 2001 (Mindekem et al., 2017a) and 2011 (Léchenne et al., 2016b), it is reasonable to assume a more or less constant dog population size. When calibrating a model to demographic data, this can be achieved by introducing a carrying capacity, which yields an additional death rate and a subsequent increased population turnover. However, since young dogs are often not vaccinated this leads to an over estimation of the overall immunity loss of the population after a vaccination campaign. We therefore use a constant birth and death rate μ, deduced from the average lifespan of 3 years.

For the metapopulation model, we divide the city into 10 patches, where the patches correspond to the districts that are shown in Figure 6.1, since the incidence data we use is aggregated at district level. The stable population size in each district, $N_{0,k}$, is estimated in a recent publication (Léchenne et al., 2016b) and summarised in Table 6.3. We estimate the entries of the migration matrix M assuming equal movement between any two adjacent patches, no direct movement between patches that share no border and, based on the results in (Smith et al., 2001), a 7-fold reduction of movement across the river. This yields the following migration matrix:

$$M = \begin{bmatrix} m_{1,1} & p & 0 & 0 & 0 & 0 & 0 & 0 & 0 & p \\ p & m_{2,2} & p & p & 0 & 0 & 0 & p & 0 & p \\ 0 & p & m_{3,3} & p & p & p & 0 & 0 & rp & 0 \\ 0 & p & p & m_{4,4} & p & 0 & 0 & p & 0 & 0 \\ 0 & 0 & p & p & m_{5,5} & p & p & p & 0 & 0 \\ 0 & 0 & p & 0 & p & m_{6,6} & p & 0 & rp & 0 \\ 0 & 0 & 0 & 0 & p & p & m_{7,7} & p & rp & 0 \\ 0 & p & 0 & p & p & 0 & p & m_{8,8} & 0 & p \\ 0 & 0 & rp & 0 & 0 & rp & rp & 0 & m_{9,9} & 0 \\ p & p & 0 & 0 & 0 & 0 & 0 & p & 0 & m_{10,10} \end{bmatrix}$$

with $r = 1/7$, $m_{ii} = 1 - \sum_{j \neq i} m_{ij}$ and p bounded above so that conditions (C I), (C II) and (C III) are satisfied. We fit a separate transmission rate, β_k, and importation rate, ε_k, for each district and the proportion of dogs moving, p, to the four years of weekly incidence data from N'Djamena, by minimising the squared Euclidean distance between the simulated weekly incidence and the data. For the initial fitting we assume no underreporting. Other rabies biology parameters, such as the incubation period, $1/\sigma$, are taken from literature. The data on number of dogs, dog rabies cases and vaccinated dogs for each district is displayed in Table 6.3. The baseline parameter values are summarised in Table 6.5. The fitted parameter values for each district are shown in Table 6.6.

cases:

District	Number of dogs, $N_{0,k}$	Number of vaccinated dogs	Time of vaccination (Week,Year)
1	1933	925 / 1325 / 62	(42,2012) / (46,2013) / (47,1013)
2	217	64 / 123	(43,2012) / (44,2013)
3	811	376 / 468	(44,2012) / (42,2013)
4	175	24 / 67	(45,2012) / (45,2012)
5	579	311 / 330	(52,2012) / (43,2013)
6	1535	919 / 1044	(46,2012) / (41,2013)
7	17273	3342 / 6683 / 503 5507 / 4372 / 2699	(47,2012) / (48,2012) / (49,2012) (48,2013) / (49,2013) / (50,2013)
8	1399	413 / 741	(52,2012) / (51,2013)
9	5672	1929 / 1929 / 4402	(50,2012) / (51,2012) / (51,2013)
10	482	120 / 200	(52,2012) / (51,2013)

Table 6.3: Data used to calibrate the models. For the metapopulation model the number of dogs, number of dog rabies cases and number of vaccinated dogs per week are used for each district. For the homogeneous model the respective values are aggregated over the districts.

2012														
week	26	27	28	30	32	33	35	36	38	39	40	44	47	50
dog rabies cases	1	1	1	1	1	1	1	1	2	2	1	1	1	1
human exposures	1	2	1	1	2	1	2	1	3	2	6	1	3	7
2013														
week	3	7	23	47										
dog rabies cases	1	1	1	1										
human exposures	3	3	2	4										
2014														
week	6	42												
dog rabies cases	1	1												
human exposures	3	1												
2015														
week	6	8	10	17	21	38								
dog rabies cases	1	1	1	2	1	1								
human exposures	1	1	1	9	1	1								
2016														
week	8	15	16	17	19	20	23	24	28	29	30			
dog rabies cases	1	1	1	1	2	2	1	2	3	2	3			
human exposures	1	2	1	2	2	4	3	3	8	6	9			

Table 6.4: Weekly number of dog rabies cases and subsequent human exposures over time.

	Description	Value	Unit	Range	Source
μ	Birth rate	0.0066	1/time	[0.0013, 0.0192]	field study
σ	Inverse incubation period	0.239	1/time	[0.01, 1]	previous model
δ	Disease induced death rate	1.23	1/time	[1, 7]	previous model
ν	Efficacy of vaccine	0.95	dimensionless	[0.8, 1]	previous model

Table 6.5: Parameter values of the rabies transmission model. Time is measured in weeks. Field study: Mindekem et al. (2017a), previous model: Zinsstag et al. (2009)

We fit the vaccination rates, $\alpha_k(t)$, to the data from the vaccination campaigns as described in more detail in a previous publication (Zinsstag et al., 2017). In each patch the vaccination rate, $\alpha_k(t)$, is given by

$$\alpha_k(t) = \alpha_k^* + \alpha_{0,k}^{(i)}(t) + \alpha_{1,k}^{(i)}(t)e^{-\varphi_\alpha t}, \tag{6.11}$$

where α_k^* is a constant background vaccination rate, $\alpha_{0,k}^{(i)}$ and $\alpha_{1,k}^{(i)}$ are fit to the number of vaccinated dogs in patch k in week i and φ_α is a constant auxiliary parameter, that we set to $\varphi_\alpha = 100$. We assume that in each patch k and each week i the number of unvaccinated dogs, U, and vaccinated dogs, V, satisfy the following equations

	Metapopulation model, importation			**Metapopulation model, no importation**		**Homogeneous model, importation**		**Homogeneous model, no importation**
k	$\beta_k(10^{-4})$	$\varepsilon_k(10^{-2})$	$p(10^{-4})$	$\beta_k(10^{-4})$	$p(10^{-2})$	$\beta(10^{-5})$	$\varepsilon(10^{-1})$	$\beta(10^{-5})$
1	4.855	7.21		4.73				
2	0.029	0		1.88				
3	0.745	0		2.48				
4	3.040	0		3.02				
5	20.87	0.36	2.21	0	4.05	3.45	1.362	4.26
6	0.140	0		60.03				
7	0.713	4.03		0.702				
8	0.437	0		0.01				
9	1.400	6.26		2.39				
10	6.631	0		2.65				

Table 6.6: Values for the fitted transmission rates, β_k, importation rates, ε_k, and movement proportions, p, for the different models. Values displayed over a whole column apply to all districts.

$$\frac{dU}{dt} = bN_{0,k} - \alpha_k^{(i)} - bU, \tag{6.12a}$$

$$\frac{dV}{dt} = \alpha_k^{(i)} U, \tag{6.12b}$$

with $\alpha_k^{(i)} = \alpha_{0,k}^{(i)} + \alpha_{1,k}^{(i)} e^{-\varphi_\alpha t}$. For the weeks during the vaccination campaigns we fit $\alpha_{0,k}^{(i)}$ and $\alpha_{1,k}^{(i)}$ by minimising the squared Euclidean distance between the simulated number of vaccinated dogs and the data on the number of vaccinated dogs collected during the campaigns that are summarised in Table 6.3. For all other weeks $\alpha_k^{(i)} = 0$. For the homogeneous model the same procedure can be applied by fitting $\alpha_0^i(t)$ and $\alpha_1^i(t)$ to the sum of the number of vaccinated dogs over all the patches.

6.6 Numerical simulations and sensitivity analysis

Simulation results of the deterministic models

We numerically solve the model equations (6.1) and (6.3) using MATLAB (with the Runge-Kutta solver `ode45`). We use the pre-intervention endemic equilibrium calculated from the incidence data before the vaccination campaigns as an initial condition and fit the transmission rates, β_k, the movement parameter, p, and the importation rates, ε_k, by minimising the squared Euclidean distance between the simulated weekly incidence and the data. The simulated cumulative incidence by the best fitting parametrization are shown in Figure 6.3. Both models without importation show an interruption of transmission after the first vaccination campaign. We therefore conclude that in our model framework, heterogeneity alone does not explain the resurgence of cases. The models with importation perform similarly well and capture the resurgence of cases after the campaigns that is seen in the data.

Stochastic implementation of the models

Deterministic models are useful to provide analytical results and to derive equilibria and threshold conditions. However, they do not capture random events which can be important in a system with low numbers of cases. We therefore implement a stochastic version of our model which allows us to capture random events and to explore the distribution of the time to elimination.

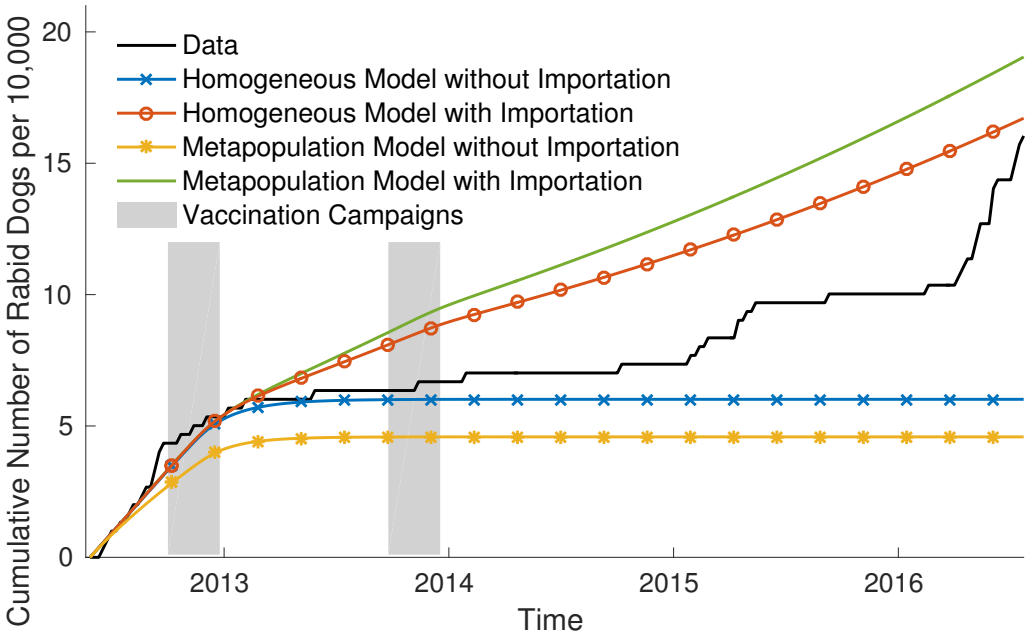

Figure 6.3: Incidence data from N'Djamena (black line) and cumulative number of rabid dogs in the four different models.

Simulations of elimination without importation In the absence of importation, the weekly incidence declines after the first vaccination campaign. We used the stochastic implementation of the homogeneous and the metapopulation model without importation to explore the distribution of the time to elimination. The stochastic simulations in Figure 6.4 show that it is likely that rabies could die out even without vaccination, because of the low number of cases. This further suggests that importation is necessary for persistence of rabies transmission.

Simulations of cases averted with importation In the model with importation, there can be interruption of transmission but no permanent elimination. We used the stochastic version of the homogeneous model with importation to estimate the average number of dog rabies cases per year in the case of no vaccination. We incorporated parameter uncertainty using a Bayesian sampling resampling approach. We created an initial sample of 10,000 parameter sets in a subset of $\mathbb{R}^5$, using Latin hypercube sampling with values for μ, σ, δ and ν drawn from uniform distributions with ranges shown in Table 6.5 and ε uniformly drawn from the range $[0, 0.1]$. For each set of parameter values, we computed the likelihood of the simulation results of the model with the vaccination campaigns to the data using a Poisson likelihood given by

$$\mathcal{L}(\theta|x) = \prod_{i=1}^{n} \frac{\theta_i^{x_i}}{x_i!} e^{-\theta_i}, \tag{6.13}$$

where x_i is the incidence data in week i and θ_i is the simulated incidence in week i. We resampled 1,000 sets of parameter values (with replacement) based on their likelihood from the initial 10,000 samples. We simulated the stochastic model for these 1,000 parameter sets assuming no vaccination campaigns. We found that in the absence of vaccination campaigns, the average number of cases per year was 37, with an interquartile range of (34,42). In the years 2013 and 2014, after the first and the second vaccination campaign, there were 7 cases of dog rabies in N'Djamena. This implies that over two years, 67 cases of rabies were averted by the vaccination campaigns.

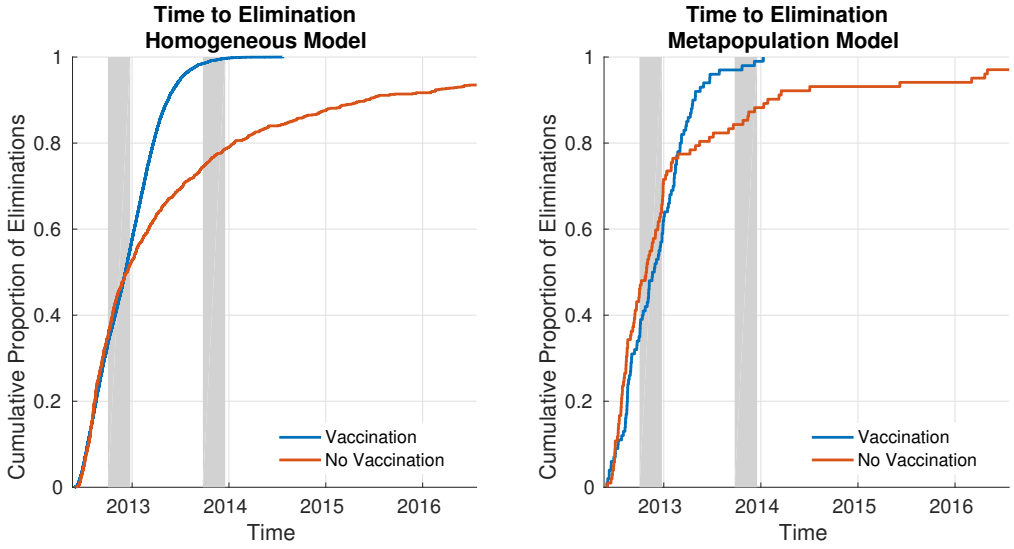

Figure 6.4: Time to elimination in the stochastic implementation of the homogeneous and the metapopulation model in the absence of importation with vaccination (blue line) and without vaccination (red line).

The surveillance data also includes the number of human exposures for each rabid dog (Table 6.4). We use the MATLAB function `poissfit` to fit a Poisson distribution to the number of humans bitten by each rabid dog, yielding an estimated mean of 2.0159 human exposures per dog. We translated the number of dog rabies cases averted, for each simulation run, to the number of human exposures averted by sampling a number of human exposures for each dog rabies case from this distribution. We estimate that the vaccination campaigns averted approximately 124 (82, 214) human exposures over two years.

Underreporting

To assess the impact of underreporting on the transmission dynamics, we assumed that each true rabies case is reported to the rabies diagnostic laboratory with a detection probability p. The rabies diagnostic laboratory conducting the immunofluorescence antibody test (IFAT) is situated in district 1 in the west of N'Djamena, whereas most cases are reported from districts 7 and 9 at the north-east of the city. We therefore assume that reporting cases is not dependent on the distance to the laboratory and assume a homogeneous rate of underreporting across all districts. We ran 10,000 simulations of the homogeneous model sampling the detection probability p from a uniform distribution in the range $[0.01, 1]$ and used it to estimate the true number of cases from the reported cases, which we then used for fitting the transmission rate, β. While the absolute number of cases depends on the detection probability, p, the overall dynamics of the cumulative incidence curve are not affected by the underreporting as shown in Figure 6.5.

Simulations with an incidence dependent disease induced death rate

An alternative explanation for the early resurgence could be that the cases in the data are produced by a series of small epidemics that are repeatedly ended by a raised alertness in the population and a subsequent increased death rate of rabid dogs. To investigate the impact of this assumption we conduct a theoretical exercise with the following equations:

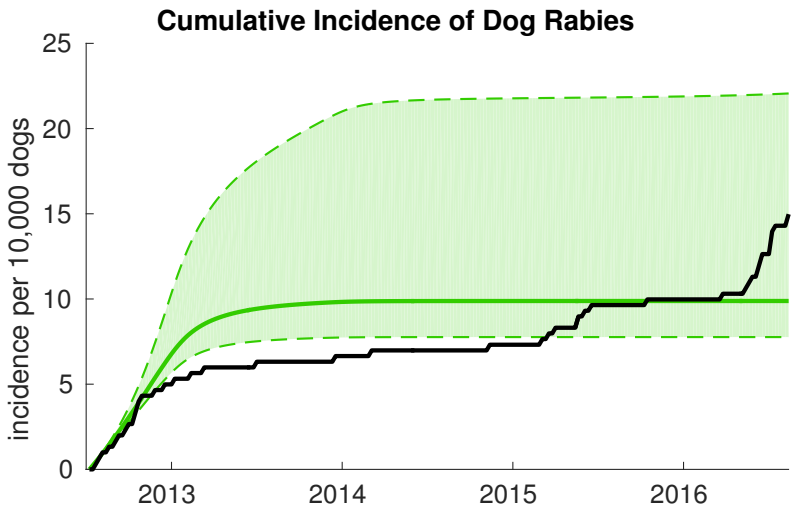

Figure 6.5: Sensitivity analysis of the cumulative number of cases with respect to detection probability. The black line is the reported number of cases. The green line and interval represents the median and the 95% credible interval of the estimated number of cases for different reporting probabilities.

$$\frac{dS(t)}{dt} = \mu N_0 - (\nu\alpha(t) + \mu)S(t) - \beta S(t)I(t), \tag{6.14a}$$

$$\frac{dE(t)}{dt} = \beta S(t)I(t) - (\sigma + \mu)E(t), \tag{6.14b}$$

$$\frac{dI(t)}{dt} = \sigma E(t) - (\delta(I(t)) + \mu)I(t), \tag{6.14c}$$

$$\frac{dV(t)}{dt} = \nu\alpha(t)S(t) - \mu V(t). \tag{6.14d}$$

where

$$\delta(I(t)) = \delta_0 + (\delta_1 - \delta_0)(1 - e^{-\varphi_\delta I(t)}).$$

The parameters δ_0 and δ_1 correspond to the upper and lower bound of the disease induced death rate. We assume that if rabies is not present in the population the disease induced death rate is equal to the baseline value ($\delta_0 = 1.23$). As rabies incidence increases the disease induce death rate, $\delta(I(t))$, approaches a hypothetical value of $\delta_1 = 7$, which corresponds to a scenario where each infected dog is killed on average one day after it first shows symptoms. We choose a hypothetical value for the saturation parameter ($\varphi_\delta = 0.5$) and a high transmission rate ($\beta = 1.0 \cdot 10^{-4}$). Although we cannot analytically compute the endemic equilibrium point for this system, we can numerically simulate the time evolution of the system. The incidence over time of the homogeneous model with and without importation, and with the incidence dependent death rate are shown in Figure 6.6. The model with the incidence dependent death rate also shows the observed resurgence in cases after the vaccination campaigns. The hypothesis that transmission is in fact higher than estimated from the incidence data and that rabies is kept under control by small scale local interventions could therefore also be a potential explanation of the pattern we see in the data.

Sensitivity analysis

We conducted global sensitivity analysis of the cumulative number of cases over four years to four model parameters (δ, σ, μ and ν) for the homogeneous and metapopulation models,

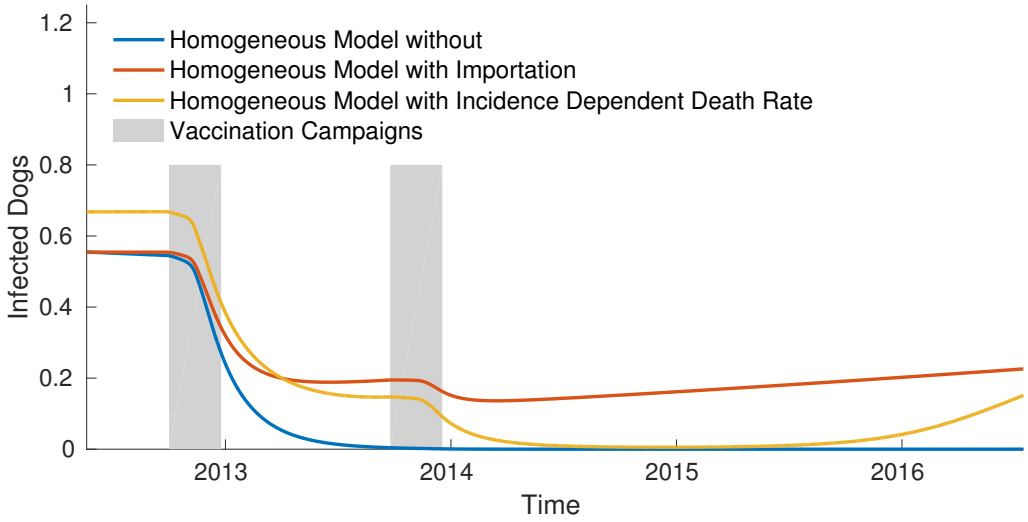

Figure 6.6: Infective dogs over time for homogeneous models without importation (blue line, $\beta = 4.26 \cdot 10^{-5}, \varepsilon = 0$), with importation (red line, $\beta = 3.45 \cdot 10^{-5}, \varepsilon = 0.1362$) and without importation but with an incidence dependent disease induced death rate (yellow line, $\beta = 1.0 \cdot 10^{-4}, \varepsilon = 0$).

with and without importation. We ran 10,000 simulations, drawing values for the parameters with ranges given in Table 6.5 assuming uniform distributions, and fit the transmission rates β_k for each simulation run. We calculated the partial rank correlation coefficients (PRCC) of the cumulative incidence over four years to the model parameters. The results in Figure 7.8 show that all models are very sensitive to the disease induced death rate, δ. This is because the disease induced death rate determines for how long a dog is infectious and therefore has a crucial impact on the transmission dynamics. If the transmission rate, β_k, were constant, the sensitivity to the incubation period, $1/\sigma$, would be positive in all models, because as σ increases, the duration of the incubation period decreases, and the probability that a dog survives the exposed period increases, leading to a higher number of cases. However, because we fit the transmission rates, β_k, for each set of parameter values, the best fitting β_k for models without importation were lower for higher values of σ, leading to a lower number of cases. In the models with importation, the introduction of exposed dogs compensates for this and leads to a higher number of cases. The mortality and birth rate, μ, mainly influences the transmission dynamics via the loss of vaccination coverage in the population after a campaign due to the death of vaccinated dogs and the birth of unvaccinated dogs. However the cumulative number of cases is not very sensitive to this population turnover of dogs.

6.7 Discussion and conclusion

After two mass vaccination campaigns of dogs in N'Djamena in 2012 and 2013, rabies transmission was interrupted for several months. However, there was a resurgence in dog rabies cases, which was not predicted by previous models of rabies transmission. We used deterministic compartmental models to explore different reasons for this early resurgence. These hypotheses include heterogeneity, importation of exposed dogs and underreporting of rabies cases with higher levels of ongoing transmission in certain districts. Dog densities and vaccination coverage varied substantially across the districts of N'Djamena (Figure 6.1) because of differences in attitudes towards dog ownership depending on the sociocultural backgrounds (Léchenne et al.,

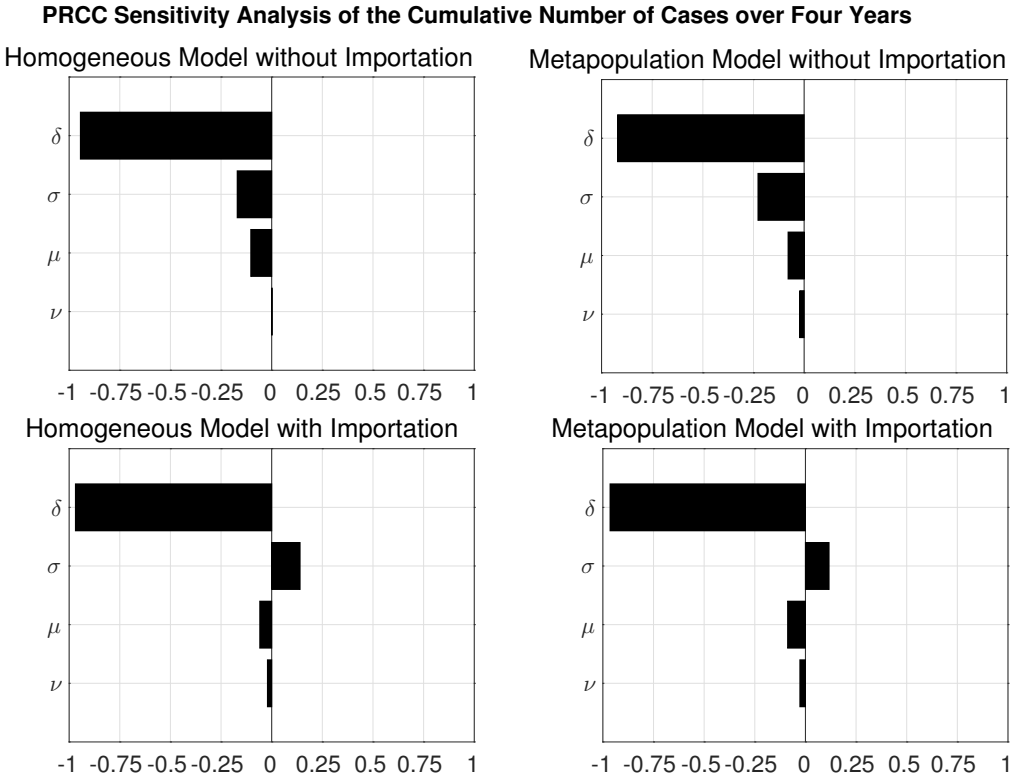

Figure 6.7: Partial rank correlation coefficient analysis of the cumulative number of cases over four years for the four different models.

2016b). Our results suggest that heterogeneity alone does not explain the resurgence in cases, whereas importation of cases is a plausible explanation of the incidence data. Our analysis of underreporting suggests that while it alters the number of cases, it does not affect the transmission dynamics, so it is an unlikely explanation of the resurgence. Simulations of the stochastic versions of our models estimated that the vaccination campaigns averted approximately 67 cases of dog rabies over two years.

Since our models suggest importation of cases was the likely cause of resurgence within the city, preventing the introduction of latent dogs, possibly by monitoring the vaccination status of incoming dogs, would help to maintain a longer duration without rabies. Alternatively, longer lasting vaccination coverage could be achieved by repeated mass vaccination campaigns or continuous vaccination through the veterinary health system to lengthen the period of herd immunity. Since the dog population turnover substantially influences the overall immunity loss of the population, increasing the lifespan of vaccinated dogs would also be beneficial. Furthermore, interventions that target rabid dogs and quickly remove them from the system could suppress transmission. An efficient surveillance system could therefore substantially contribute to rabies control.

Our models assumed density dependent transmission of rabies and a homogeneous dog population within each patch of the metapopulation model. Even though this approach captures the heterogeneity in dog densities and vaccination coverage at district level, it does not account for the fine scale contact structure among the dogs in each district. Future work is needed to show how this contact structure among the dogs could influence the transmission dynamics of rabies.

Our analyses estimated that the dog vaccination campaigns averted about 124 human exposures over two years. Dog vaccination is therefore an effective tool to reduce human cases and can contribute to the goal of zero rabies deaths by 2030.

Acknowledgements

This work was supported by the Swiss National Science Foundation under grant number 310030 160067. The authors thank Peter Pemberton-Ross, Timo Smieszek and Thomas Smith for helpful comments and discussions.

7. The importance of contact structures of dog populations for rabies transmission

Mirjam Laager[1,2], Céline Mbilo[1,2], Enos Abdelaziz Madaye[3], Abakar Naminou[3], Monique Léchenne[1,2], Aurélie Tschopp[4], Service Kemdongarti Naissengar[3], Timo Smieszek[5,6], Jakob Zinsstag[1,2], Nakul Chitnis[1,2]

[1]Swiss Tropical and Public Health Institute, Socinstrasse 57, 4051 Basel, Switzerland

[2]University of Basel, Petersplatz 1, 4001 Basel, Switzerland

[3]Institut de Recherches en Elevage pour le Développement, BP 433, Farcha, N'Djamena

[4]Veterinary Public Health Institute, Vetsuisse Faculty, University of Bern, 3097 Liebefeld, Switzerland

[5]Modelling and Economics Unit, National Infection Service, Public Health England, NW9 5EQ London, UK

[6]MRC Centre for Outbreak Analysis and Modelling, Department of Infectious Disease Epidemiology, Imperial College School of Public Health, W2 1PG London, UK

This manuscript has been submitted to PLoS Neglected Tropical Diseases, February 2018

7.1 Abstract

Canine rabies transmission was interrupted in N'Djaména, Chad, following two mass vaccination campaigns. However, after nine months cases resurged with re-establishment of endemic rabies transmission to pre-intervention levels. Previous analyses investigated district level spatial heterogeneity of vaccination coverage, and dog density; and importation, identifying the latter as the primary factor for rabies resurgence. Here we assess the impact of individual level heterogeneity on outbreak probability, effectiveness of vaccination campaigns and likely time to resurgence after a campaign. Geo-located contact sensors recorded the location and contacts of 237 domestic dogs in N'Djaména over a period of 3.5 days. The contact network data showed that urban dogs are socially related to larger communities and constrained by the urban architecture. We developed a network generation algorithm that extrapolates this empirical contact network to networks of large dog populations and applied it to simulate rabies transmission in N'Djaména. The model predictions aligned well with the rabies incidence data. Using the model we demonstrated, that major outbreaks are prevented when at least 70% of dogs are vaccinated. The probability of a minor outbreak also decreased with increasing vaccination coverage, but reached zero only when coverage was near total. Our results suggest that endemic rabies in N'Djaména may be explained by a series of importations with subsequent minor outbreaks. We show that highly connected dogs hold a critical role in transmission and that targeted vaccination of such dogs would lead to more efficient vaccination campaigns.

7.2 Author summary

Rabies transmission between dogs and from dogs to humans can be interrupted by mass vaccination of dogs. Novel geo-referenced contact sensors tracked the contacts and locations of several hundred dogs in N'Djaména, the capital of Chad. With the data generated by the sensors we developed a contact network model for rabies transmission dynamics. The model results were validated with incidence data. The model explains the timing of vaccination campaigns and number of cases better than previous models. Highly connected dogs play a critical role in rabies transmission and targeted vaccination of these dogs would lead to more efficient vaccination campaigns.

7.3 Introduction

The viral disease rabies, transmitted between mammals through bites, is fatal following the onset of symptoms. Although human rabies can be prevented by appropriate post-exposure prophylaxis (PEP), approximately 60,000 people die annually from rabies, mainly in Africa and Asia, (Hampson et al., 2015). The main source of exposure for human rabies is the domestic dog, so vaccinating dogs is an effective way of reducing rabies transmission among dogs and from dogs to humans (Zinsstag et al., 2009, 2017).

Rabies is endemic in N'Djaména, the capital city of Chad, with an average incidence of one laboratory-confirmed infected dog per week (Léchenne et al., 2017). A deterministic model of rabies transmission predicted that mass vaccination of dogs would be sufficient to interrupt transmission for six years (Zinsstag et al., 2009). Vaccination campaigns in dogs were conducted in 2012 and 2013, with both campaigns exceeding 70% coverage(Léchenne et al., 2016b). Rabies transmission was interrupted in January 2014 after the second vaccination campaign (Zinsstag et al., 2017), but there was a resurgence of cases nine months later. Subsequent analyses considered reasons for the quick resurgence, including spatial heterogeneity of vaccination coverage, and dog density; underreporting of cases; and importation. Simulation results from a deterministic metapopulation model suggested that importation was the most likely reason for the case resurgence (Laager et al.). Although deterministic models can predict the effect of large scale vaccination campaigns and the overall population dynamics, they do not adequately capture effects of stochasticity in low level endemic settings. This becomes important towards the end of an elimination campaign or upon re-establishment after interruption of transmission (Smieszek et al., 2009). Previous models did not include fine scale heterogeneity at the individual level or the network structure of dog to dog contacts.

The importance of including host contact structure in infectious disease modelling has been highlighted in many studies (Newman, 2003; Pastor-Satorras et al., 2015; Silk et al., 2017). Theoretical analysis of epidemic processes on graphs has shown that the basic reproductive ratio not only depends on the expected value but also on the standard deviation of the degree distribution of the graph (Andersson, 1999) and that on scale-free networks diseases can spread and persist independently of the spreading rate (Pastor-Satorras and Vespignani, 2001). These theoretical insights led to better understanding of disease transmission dynamics for different diseases, including pertussis (Rohani et al., 2010), influenza (Barclay et al., 2014), severe acute respiratory syndrome (SARS) (Meyers et al., 2005), human immunodeficiency virus and acquired immune

deficiency syndrome (HIV/AIDS) (Morris and Kretzschmar, 1995) and gonorrhea (Yorke et al., 1978), and inspired novel control measures such as acquaintance immunization (Cohen et al., 2003), contact tracing (Kretzschmar et al., 1996) and ring vaccination (Greenhalgh, 1986; Müller et al., 2000).

Due to the substantial influence of network structure on disease transmission dynamics, many studies have collected data on host interactions. Human contact network models are generally established using contact diaries (Wallinga et al., 2006; Mossong et al., 2008; Smieszek, 2009), proximity loggers (Stehlé et al., 2011; Cattuto et al., 2010; Salathé et al., 2010; Machens et al., 2013), video recording (Rainey et al., 2014) or mobile phones (Read et al., 2012). Contacts have also been studied in a wide range of animal species. The most common method for measuring animal contacts is behavioral observation, but other methods such as radio tracking, Global Positioning System (GPS) trackers, proximity loggers or powder marking are also utilized (White et al., 2017).

In the past decades, several rabies models with host contact structure have been published. White et al. (1995) simulated fox movement pathways using home range size estimates, data from radio tracking and behavioral encounter observations to estimate contact probabilities for different seasons and fox densities. They found that the rabies front set off by an incursion of rabies into a healthy population moved more slowly than in a previous model of homogeneous fox populations. Including contact behavior in the model also resulted in a substantially higher predicted rabies control success rate. Hirsch et al. (2013) used data from 30 raccoons fitted with proximity loggers to assess properties of the raccoon contact network. Unlike in earlier radiotelemetry studies, they found a highly connected population and discussed possible implications of the social network on the spread of rabies. Reynolds et al. (2015) used proximity logger data from 15 raccoons to build a contact network model of 90 raccoons and simulate rabies spread. They studied the effects of seasonality, differences in vaccination coverage and impact of behavioral changes in infected raccoons on disease spread. Dürr and Ward (2015) used a contact network model of rabies transmission among owned free-roaming dogs in Australia to estimate the impact of a hypothetical rabies incursion from Indonesia. They differentiated transmission within households, between households and between communities. The probability of between household transmission was based on GPS data from 69 dogs, while between community transmission was estimated using questionnaire data. Johnstone-Robertson et al. (2017) developed a contact network model for rabies in the wild dog population in Australia. They constructed a function for dog contact probabilities, using a wide range of different values to generate contact networks and then implemented a rabies transmission model based on parameters from literature.

However, individual based models of dog rabies transmission in endemic settings are lacking, so this study equipped 300 dogs in N'Djaména with purpose developed geo-referenced contact sensors. This is the first study to collect contact data among dogs as well as the first to integrate contact data from such a large subset of an animal population into a rabies model. The individual based model of rabies transmission we developed includes distance between home locations and a degree distribution fit to a contact network structure of dogs in N'Djaména. We compared our model results to 2016 outbreak data from two quarters of N'Djamena. We examined the re-establishment probability of rabies over different vaccination coverage and compared outbreak

probability over time with rabies incidence in N'Djaména from 2012 to 2016. Finally, we investigated the role of individual heterogeneity among dogs and the effect of targeted vaccination strategies.

7.4 Materials and methods

Contact network data collection

Contact network data was collected in three districts of N'Djaména, Chad, using 300 geo-located contact sensors (GCS) developed specifically for this study. The devices contain Global Positioning System (GPS) modules to track the location and movements of dogs and Ultra-High-Frequency (UHF) technology sensors to measure close-proximity events between dogs. The GCS devices record locations at one minute intervals. For the contact recording, the devices broadcast beacons at one minute intervals and constantly scan for beacons ensuring that no contacts with durations of at least one minute will be missed. Close proximity events were defined as records with a received signal strength indicator (RSSI) of more than -75dBm. Static tests of the devices showed that, independently of the angle between two devices, all contacts closer than 25 cm are registered when signal strength is above that value (Figure 7.9).
Collars fitted with the devices were placed on free roaming domestic dogs in three city districts (Table 7.1, Figure 7.1) with different dog densities (low, medium and high), that were easily accessible. The zones were chosen to include urban and peri-urban areas. Data were collected during the dry season in December 2016. In the selected districts, all dog-owning households in a pre-defined area of 1km^2 were identified in order to capture as many of the contacts between dogs as possible, bearing in mind that only contacts between dogs that both wear a sensor can be captured. Dog owners were asked to enroll their pets. Only one dog owner refused to participate in the study. The GCS units remained on the dogs for 3.5 days. After retrieval of the GCS units, dogs were vaccinated against rabies. We excluded study zone 3 from the network analysis due to the low proportion of devices usable for analysis.
The data from the contact sensors were used to establish an empirical contact network, where the nodes correspond to the dogs and any two nodes are connected by an edge if at least one contact between the two dogs was registered. Figure 7.10 shows the number of edges in the empirical network during different subintervals of the study period.

zone	district	location	dog density	number of dogs	deployed devices	usable devices
1	6	urban	high	328	290	237
2	1	peri-urban	medium	94	80	66
3	8	urban	low	59	41	25

Table 7.1: Characteristics of the three study zones. The reason for the discrepancy between the number of dogs and the number of deployed devices is that some collars could not be attached because dogs resisted. In study zone 1 the number of deployed devices was also limited by the fact that we had only 300 devices at our disposal. The discrepancy between deployed and usable devices is due to broken or lost GCS units, battery failure or failure in the data downloading process.

Rabies cases data

Surveillance of canine rabies in N'Djaména consists of passive reporting of cases confirmed with an immunofluorescence antibody test (IFAT). In 2012, prior to the vaccination campaign, there

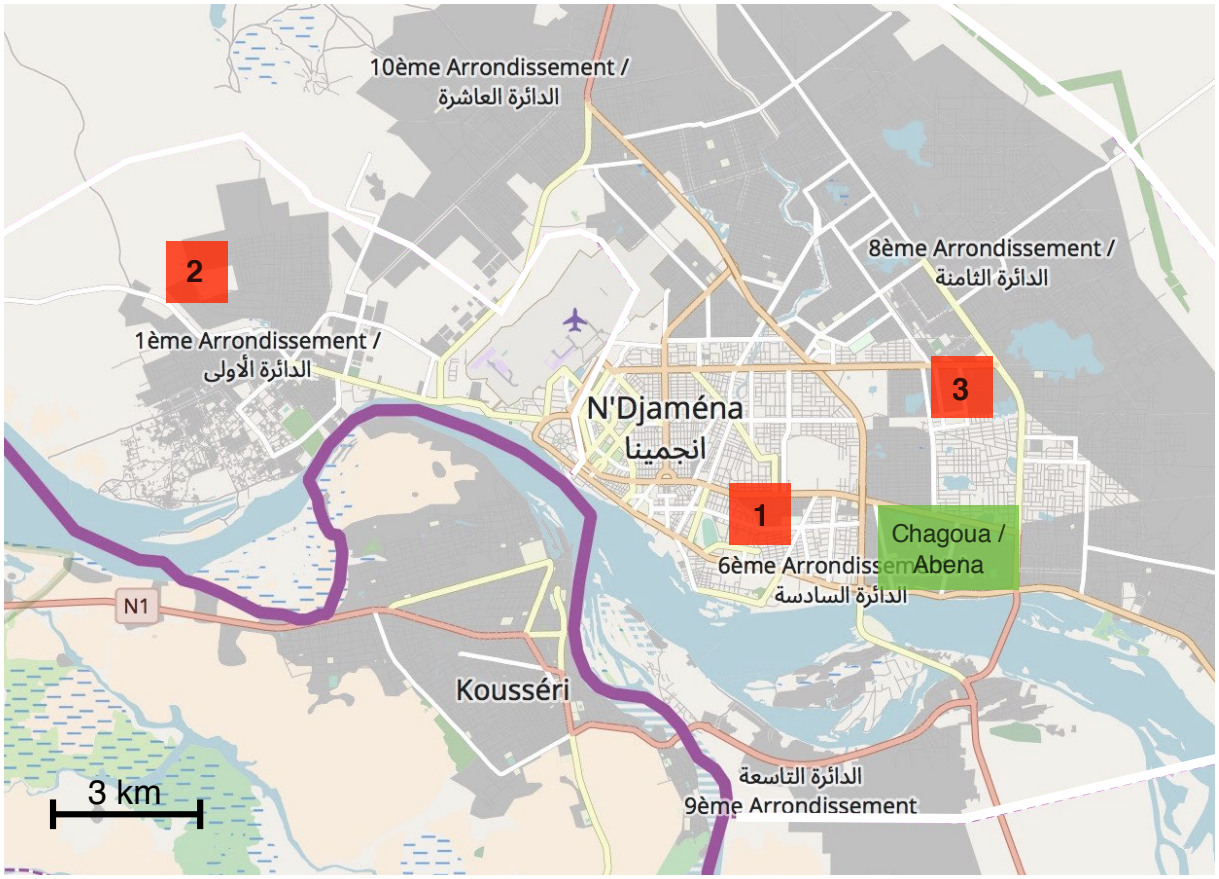

Figure 7.1: The location of the three study zones (red squares) and Chagoua and Abena quarters (green rectangle) in N'Djamena. The solid purple line denotes the border to Cameroun

was, on average, one case of dog rabies per week. After the vaccination campaigns in 2012 and 2013, no rabies cases were reported for nine months. In October 2014, new rabies cases were reported in district number 9, south of the Chari River. In January 2016, the first case north of the river was reported in the Chagoua quarter of district 6 (Figure 7.1). An additional 6 cases of dog rabies were reported in 2016 in Chagoua and the neighboring Abena quarter.

Dog population estimates

We simulated rabies incursion into Chagoua and Abena quarters to compare the model results to the outbreak data. Dog population estimates were derived from the 2012 mass vaccination campaign coverage assessment to determine the number of nodes in the network. A total of 2775 dogs were vaccinated during the 2012 campaign in Chagoua, Abena and the neighboring Dembe quarters(Léchenne et al., 2016b). A capture-mark-recapture model estimated vaccination coverage in that area at 67 %. In a second stage of the campaign, additional dogs were vaccinated in Chagoua, Abena and Dembe. During the latter stage, the proportion of dogs originating from Chagoua and Abena was assessed at 86% of dogs. Assuming that this proportion was the same in the first round, we estimated the dog population in Chagoua and Abena to total 3,500 dogs. This was confirmed through a household survey conducted after the vaccination campaign, which estimated the dog/human ratio to be 1/20. The proportion of ownerless dogs was between 8% and 15% (Léchenne et al., 2016b). The total human population in Chagoua and Abena was 72,000 people.

Network construction

We developed a spatially explicit network construction algorithm to expand the empirical contact network to a synthetic network with more nodes, which allows for more realistic simulations of rabies transmission. When applied to a set of nodes of the same size as the empirical network, this algorithm generated a network with a similar degree distribution. The outbreak probability and size of a rabies transmission model on the empirical and the synthetic network were similar, meaning we captured the features of the empirical network which are relevant for disease transmission in the construction algorithm.

The steps of the algorithm to create the synthetic network are described below. We first create a graph with n nodes and zero edges. The number of nodes n corresponds to the number of nodes in the empirical network. Each node is assigned a position consisting of x and y coordinates in a square. The coordinates are sampled using Latin Hypercube sampling. Any two nodes i and j are connected with a probability p_{ij} given by $p_{ij} = \exp(-\kappa\Delta_{ij})$, where Δ_{ij} is the Euclidean distance between node i and node j and κ is a scaling parameter. Next a proportion $1 - \tau$ of the nodes are selected uniformly at random. For each node i in that subset of nodes a number m is sampled from a Poisson distribution with mean λ. The node i is then connected to exactly m other nodes out of all the nodes in the graph. The probability of selecting node j into the m nodes is given by $\tilde{p}_{ij} = \frac{k_j}{\sum_{l=1}^{n} k_l}$, where k_j is the degree of node j and $\sum_{l=1}^{n} k_l$ is the sum of the degrees of all the nodes in the graph.

The three scaling parameters, κ, τ and λ are chosen such that the Kolmogorov distance between the degree distribution of the constructed network and the degree distribution of the empirical network is minimal. We minimize the Kolmogorov distance by using a gridsearch and confirm the results by minimizing a second metric, the χ^2 distance. The optimal values of the parameters κ, τ and λ for the two study zones are displayed in Table 7.2. Larger networks are constructed by choosing the desired number of nodes in the networks and following the steps described above with the optimal values for λ, τ and κ. The properties of the empirical and the synthetic networks are displayed in Table 7.3. When optimizing the parameters κ, τ and λ only the degree distribution of the two networks is taken into account. Therefore, other network properties such as clustering do not necessarily align between the synthetic and the empirical network.

		λ	τ	κ
Zone 1	Kolmogorov	24	0.75	25
	Chi-Square	23	0.75	25
Zone 2	Kolmogorov	7	0.7	10
	Chi-Square	6	0.7	11

Table 7.2: Optimal values for the three scaling parameters of the network construction algorithm for the two study zones. The optimal values minimize the distance between the degree distributions of the empirical and the simulated networks. The distance is calculated using the Kolmogorov or the Chi-Square metric.

Transmission model

We used an individual based transmission model to simulate the spread of rabies in a contact network. All nodes of the network are assigned a status; susceptible, exposed, infective or removed. Nodes infect adjacent nodes with a transmission rate β and progress from exposed to infectious and from infectious to removed with average transition periods σ and δ. For each infected dog the individual incubation period and infectious period is sampled from a Poisson

		empirical	synthetic				
			min	p25	p50	p75	max
Zone 1	nodes	237			237		
	edges	1739	1630	1756	1782	1812	1914
	density	0.0622	0.0582	0.0628	0.0637	0.0648	0.0684
	av. degree	14.68	13.8	14.8	15.0	15.3	16.2
	max. degree	64	39	46	48	50	67
	clustering	0.562	0.129	0.157	0.164	0.172	0.198
Zone 2	nodes	66			66		
	edges	272	238	280	292	305	365
	density	0.125	0.111	0.131	0.136	0.142	0.170
	av. degree	8.24	7.2	8.5	8.8	9.2	11.1
	max. degree	19	19	20	21	29	
	clustering	0.516	0.159	0.230	0.246	0.263	0.339

Table 7.3: Properties of the empirical and the synthetic contact networks for the two study zones. For the synthetic network five point summary statistics of 1000 runs of the construction algorithm are displayed.

distribution, with mean σ or δ, respectively. The model ignores birth and natural mortality. The parameter values are displayed in Table 7.4. The incubation period, σ, is chosen from recent literature (Singh et al., 2017) and fits with the observed time between cases in the incidence data from Chagoua and Abena. The duration of the incubation period is only marginally relevant for our simulations, because it only affects the outbreak duration and not the outbreak probability or size. The infectious period, δ, is chosen based on the assumption that a rabid dog in an urban setting would be killed earlier than a natural death from rabies. Our observation that more than two thirds of all samples tested at the rabies laboratory are positive supports the hypothesis that people are likely to recognize the symptoms of rabies since they are less likely to send non-rabid dogs for testing. If people recognise rabies they are more likely to kill rabid dogs. (Léchenne et al., 2017). The transmission rate is chosen using equation (7.1). We calculated the mean and variance of the empirical degree distribution, choosing the transmission rate such that R_0 is smaller or equal than 1. We reasoned that rabies is endemic in N'Djaména, with a constant low number of cases and no large outbreaks observed. The transmission rate choice is further supported by the comparison of the simulation results to the outbreak data from Chagoua and Abena.

	Description	Unit	Distribution	Range / Mean
σ	incubation period	time	Poisson	90
δ	infectious period	time	Poisson	2
β	transmission rate	time $^{-1}$	Uniform	[0.015, 0.02]

Table 7.4: Parameters of the rabies transmission model. Time is measured in days.

Network construction validation

We used an individual based transmission model to test whether the properties of the empirical and the reconstructed network lead to similar outbreak probability and size for different transmission rates. The results for 1000 simulation runs of this model on the empirical and the synthetic network are shown in Figure 7.2. We differentiate between minor outbreaks, which are outbreaks where more than one and less than one percent of the nodes gets infected, and major outbreaks, which are outbreaks where more than one percent of the nodes get infected. Incursions denote all outbreaks where more than one node gets infected and therefore include

both minor and major outbreaks. The figure suggests the construction algorithm performs well since the empirical and the simulated network yield similar results in outbreak probability and size. The values of the proportion of simulation runs with outbreaks correspond to the values of the average relative outbreak size, that is the sum of all the final outbreak sizes divided by the number of nodes in the network and the number of simulation runs. This is consistent with the theoretical result that the probability of a major outbreak and the relative size of such a major outbreak are equal (Britton et al., 2007). This holds despite the clustering of the synthetic network being higher than in a random graph due to the spatial component of the network construction algorithm. In Figure 7.2 the outbreak size increases steeply for transmission rate values that are slightly larger than 0.02. This is consistent with the basic reproductive ratio R_0 given by

$$R_0 = p\left(\mu + \frac{\mathrm{var}(D) - \mu}{\mu}\right), \tag{7.1}$$

where p is the transmission probability given a contact and μ and var(D) are the expected value and the variance of the degree distribution (Britton et al., 2007). In the case of the described network R_0 takes the value of 1 if the transmission rate β is 0.02. Since major outbreaks are only possible when R_0 is greater than one, the observed increase of the average outbreak size for values of the transmission probability greater than 0.02 aligns well with the theoretical result, even though not all conditions are met in the case of the described networks.

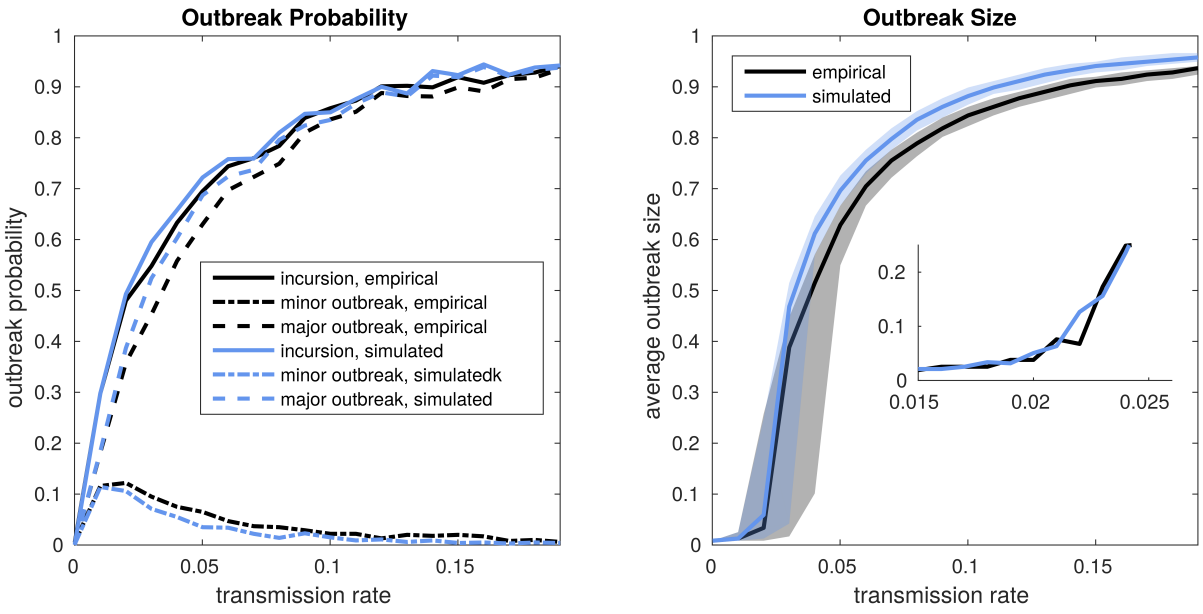

Figure 7.2: Outbreak probabilities and sizes of the transmission model on the empirical and the constructed network in study zone 1. In each simulation run, one randomly chosen dog is infected from the outside. The simulation ends when there is no more transmission. The incursion probability is the proportion of simulation runs where the number of infected dogs was greater than one. The probability of a minor outbreak is the proportion of simulation runs where more than one dog and less than 1 percent of the population get infected. The major outbreak probability is the proportion of simulation runs where more than 1 percent of the population get infected. The outbreak size is the cumulative proportion of infected dogs over the whole course of the infection. In the left panel the lines correspond to the mean over 1000 simulation runs for each value of the transmission rate. In the right panel the lines correspond to the median over 1000 simulation runs for each value of the transmission rate and the shaded area corresponds to the interquartile range.

7.5 Results

The empirical contact networks

In study zone 1, the network consisted of 237 nodes and 1739 edges, with an average degree of 15 and and maximal degree of 64. In zone 2, the network consisted of 66 nodes and 272 edges, with an average degree of 9 and a maximum degree of 20. In both zones, nearly all dogs were part of one connected component, that is a sub-graph where any two nodes are connected by a path. The network can be divided into communities using a modularity optimization algorithm (Blondel et al., 2008). This algorithm optimizes both, the number of communities and the assignment of each node to a specific community, such that the modularity, that is the density of links within communities compared to links between communities, takes the maximum possible value. When the network of study zone 1 is divided into communities using this algorithm it becomes visually obvious that communities mainly consist of dogs which live close together and do not frequently cross roads with traffic (Figure 7.3). This suggests, that roads with high traffic intensity constitute a functional barrier which substantially reduces contact between dogs residing on either side.

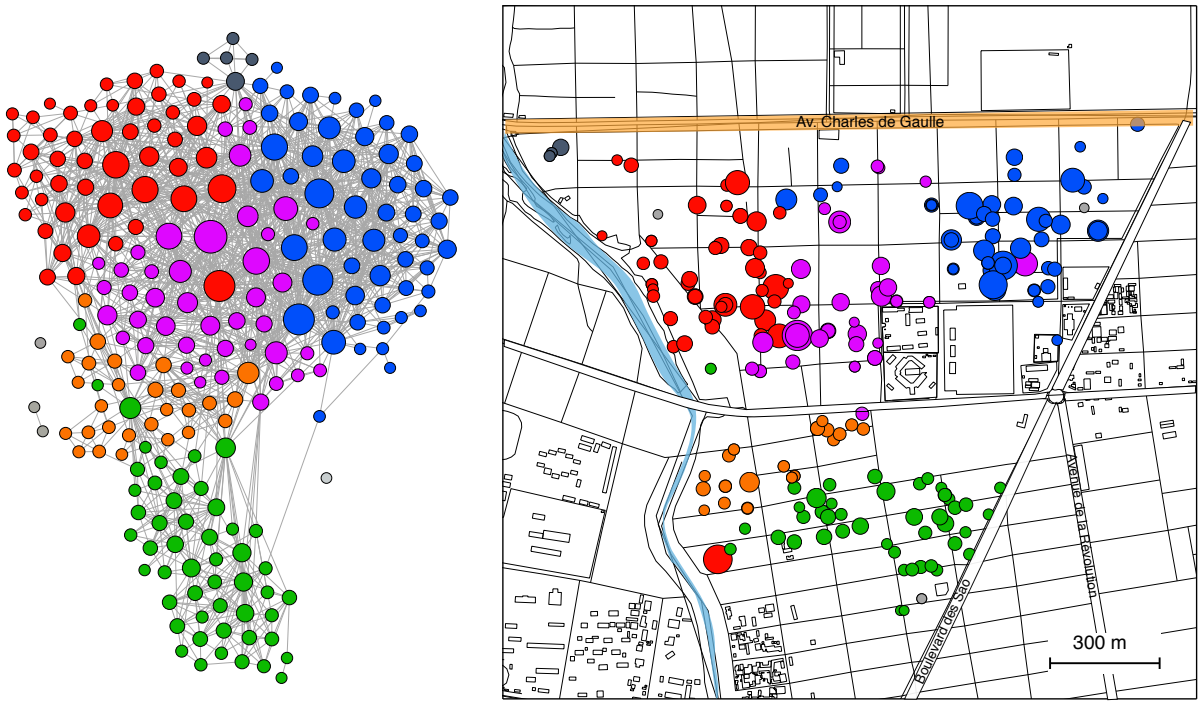

Figure 7.3: Contact network and home location of the 237 dogs in study zone 1. In the left panel each node corresponds to a dog. The size of the node is proportional to the degree of the node and the color corresponds to the community the node belongs to. Contacts between dogs are shown as grey lines. In the right panel each dot on the map corresponds to a home location of a dog. The colors correspond to the community in the network.

Comparing simulation results to outbreak data

Rabies was absent from the Chagoua and Abena quarters of N'Djaména for more than a year prior to the outbreak in 2016. The 7 cases were the first to occur north of the Chari River. Chagoua and Abena are virtually separated from other quarters to the west, north and east by main traffic roads and to the south by the Chari River. The area of these two quarters is approximately 4km^2, and the total number of dogs is estimated to be around 3,500. We simulate

the course of the infection after the incursion of one rabid dog. We found that in 450 out of 1000 simulations the chain of transmission was longer than 1, in other words additional dogs get infected. Among these chains of transmission the median of the cumulative incidence of all simulation runs aligns well with the cases observed in Chagoua and Abena (Figure 7.4). This suggests that the transmission rate in our model is a reasonable choice and that our simulations yield realistic results. Since rabies is often underreported, the true number of cases is likely to be higher than the reported number of cases. We accounted for this in a sensitivity analysis on the reporting probability (Figure 7.11). We found that if more than 60% of the cases are reported, the median of the simulations does not differ more from the incidence data than with perfect reporting. The final outbreak sizes are shown in Figure 7.12.

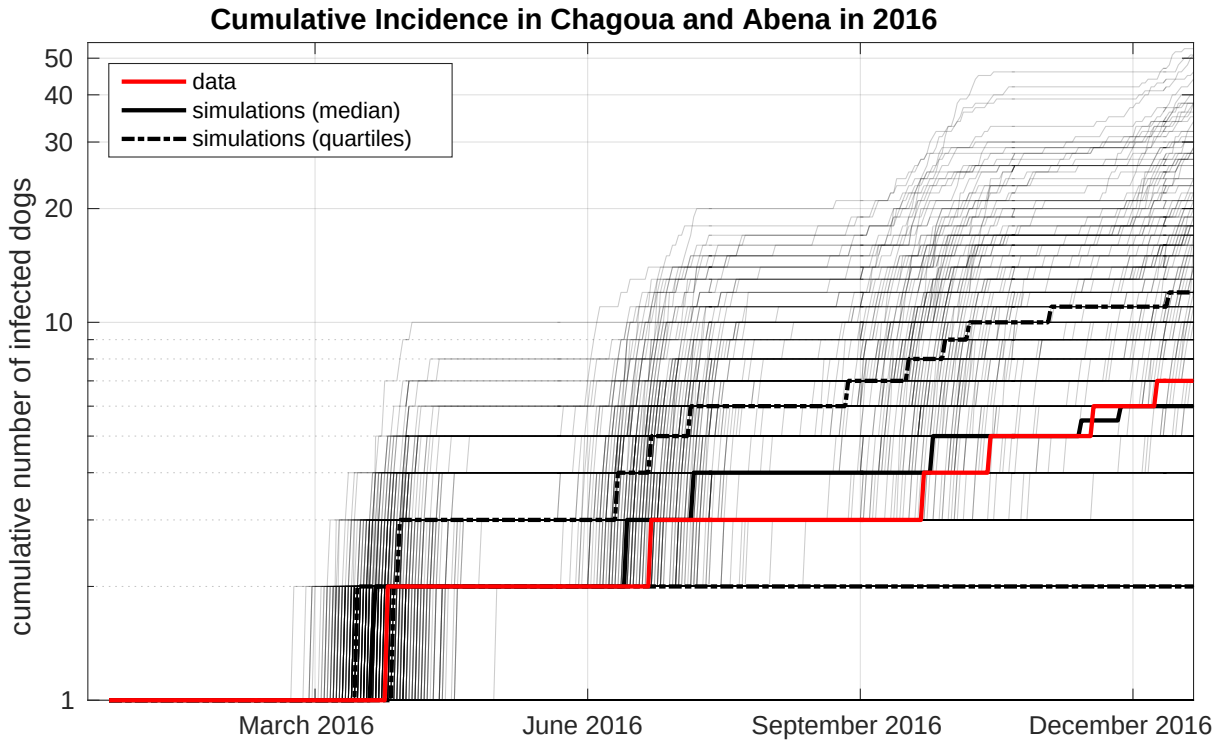

Figure 7.4: Incidence data and simulation results for the quarters Chagoua and Abena in 2016. The red line is the cumulative number of confirmed rabies cases. The black lines show median and quartiles the cumulative number of cases in simulation runs where the number of rabid dogs was greater than 1. Individual simulation runs are displayed as gray lines.

Outbreak probability, size and duration for different vaccination coverages

To assess the impact of vaccination coverage on the outbreak probability and size after the introduction of one rabid dog, we constructed a network with a large number of nodes. We considered a 4×4 kilometer square and a dog population with the same density as the dog population in study zone 1, which yields a network with 4930 nodes. We ran rabies incursion simulations on that network. The outbreak probabilitiy, size and duration across different vaccination coverage are shown in Figure 7.5. The probability of a major outbreak, defined as more than 1% of the dog population becoming infected, is substantially reduced when vaccination coverage is above 70%. The probability of minor outbreaks also decreases with vaccination coverage, but only reaches zero with nearly complete vaccination coverage. Even though a minor outbreak, by definition, could affect up to 1% of the population (50 dogs) the simulated average outbreak size is, in fact, very low. This is consistent with the theoretical result that the final number

of infected nodes converges to a two point distribution. A proportion of simulation runs stays close to zero whereas the other proportion ends up near the major outbreak size (for an example see Figure 7.13). The minor outbreaks, therefore, only capture the short chains of transmission. These chains include, on average, 5 dogs and last approximately 20 weeks, yielding an average number of one infected dog per month which aligns well with the observed endemic situation in N'Djaména (Léchenne et al., 2017).

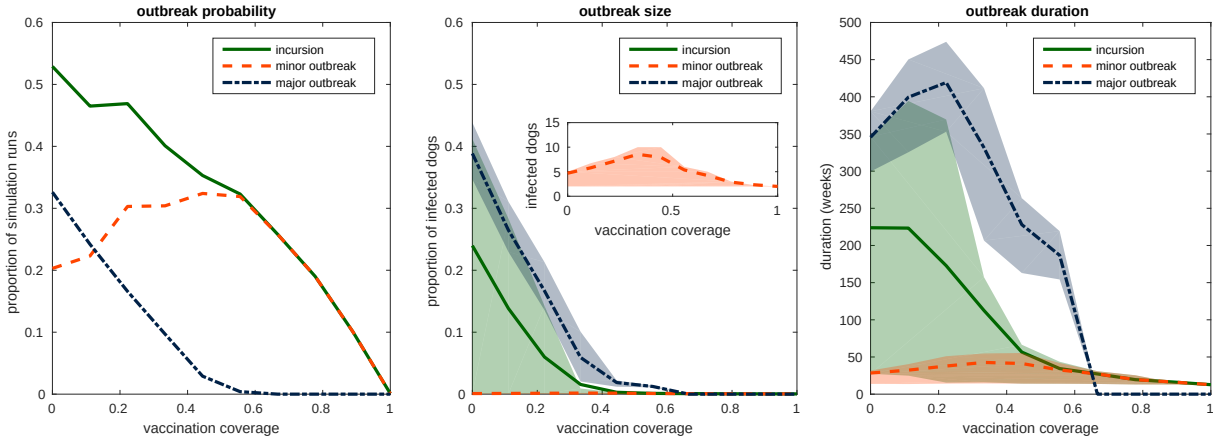

Figure 7.5: Outbreak probability, size and duration on a network of 4930 dogs for different vaccination coverages. In each simulation run, a proportion of the dogs is randomly assigned the status vaccinated and one randomly chosen susceptible dog is infected from the outside. The simulation ends when there is no more transmission. Simulation runs where more than one dog gets infected are classified as incursion. Simulation runs where more than one dog and less than 1% of the population get infected are classified as minor outbreaks. Simulation runs where more than 1% of the population gets infected are classified as major outbreaks. Incursions include minor and major outbreaks. The outbreak probability is the proportion of simulation runs with outbreaks. The outbreak size is the cumulative proportion of infected dogs over the whole course of the infection. The outbreak duration is the number of weeks until the last infected dog dies. In the left panel the lines correspond to the mean over 1000 simulation runs for each value of the vaccination coverage. In the center and the right panel the lines correspond to the mean over 1000 simulation runs for each value of the vaccination coverage and the shaded areas correspond to the interquartile ranges. The axis of the indented figure in the center panel are the same as in the surrounding figure.

Time to resurgence

After the vaccination campaigns in 2012 and 2013, no rabies cases were reported north of the Chari River until October 2014. We used a deterministic model (Zinsstag et al., 2017) to estimate vaccination coverage over time and the contact network model to calculate outbreak probability for the respective coverage. Comparing these probabilities with the incidence data (Figure 7.6) showed that the first case after the vaccination campaigns could not establish a chain of transmission because the probability for a major outbreak was very low at that time. Later, in February 2016, the respective probability was higher which could explain the subsequent cases.

Comparing vaccination strategies

We used the empirical contact network from zone 1 to compare different types of vaccination strategies. Dogs can be vaccinated at random or in a targeted way, based on the contact network structure among the dogs or based on the movements of the dogs. We considered four different ways of targeting dogs: (i) vaccination in order of the degree centrality of the nodes, (ii) vaccination in order of the betweenness centrality of the nodes, (iii) vaccinating each node with a probability that is linearly proportional to the average distance the corresponding dog spent away from the home location of the owner and (iv) vaccinating each node with a probability

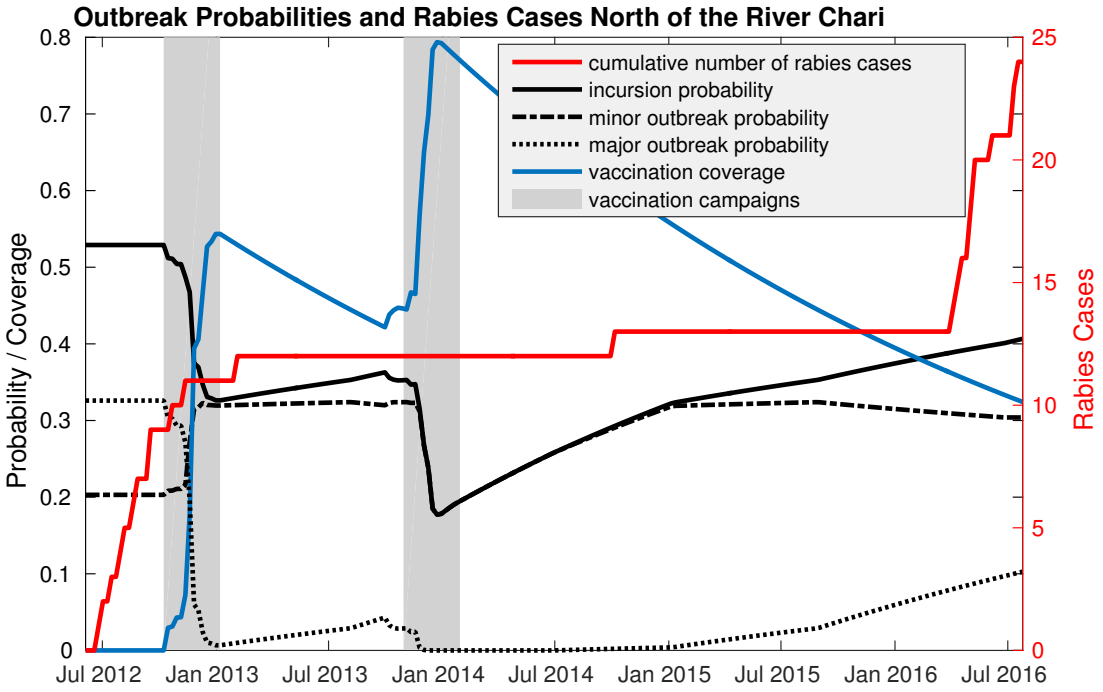

Figure 7.6: Outbreak probabilities and rabies cases north of the river Chari from 2012 and 2016. For each week the vaccination coverage was calculated using a deterministic transmission model. Vaccination coverages were then translated to outbreak probabilities using the contact network model.

that is linearly proportional to the area covered by the corresponding dog, where the area was estimated by fitting a minimal convex polygon to the GPS locations of the dog. The outbreak probability and size for each type of vaccination and different coverages are shown in Figure 7.7. Consistent with previous findings (Albert et al., 2000; Smieszek and Salathé, 2013) we observed that targeted vaccination reduces the outbreak probability and size more than random vaccination. Targeting nodes by degree yields a lower outbreak probability and size than targeting nodes by betweenness. The betweenness centrality of a node i is the proportion of shortest paths between any pair of nodes in the network that pass through node i. Nodes with high betweenness centrality are therefore part of many short paths between nodes, which is why removing them affects the global network structure and reduces the size of the largest component, while targeting nodes by degree operates on a local level and reduces the total number of edges more rapidly. In our case, chains on average are short, so the local structure is more important than the global structure. Vaccination based on movement also reduces the outbreak probability and sizes.

Sensitivity Analysis

We conducted a Partial Rank Correlation Coefficient sensitivity analysis (Wu et al., 2013) to assess the impact of the network construction and transmission model parameters on the model output, with ranges as displayed in Figure 7.5. The results are shown in Figure 7.8. The most sensitive parameter is τ, a scaling parameter of the network construction algorithm. For low values of τ, a large proportion of nodes are sampled to connect both to spatially close nodes and any other node in the network. These nodes have a higher degree and betweenness centrality

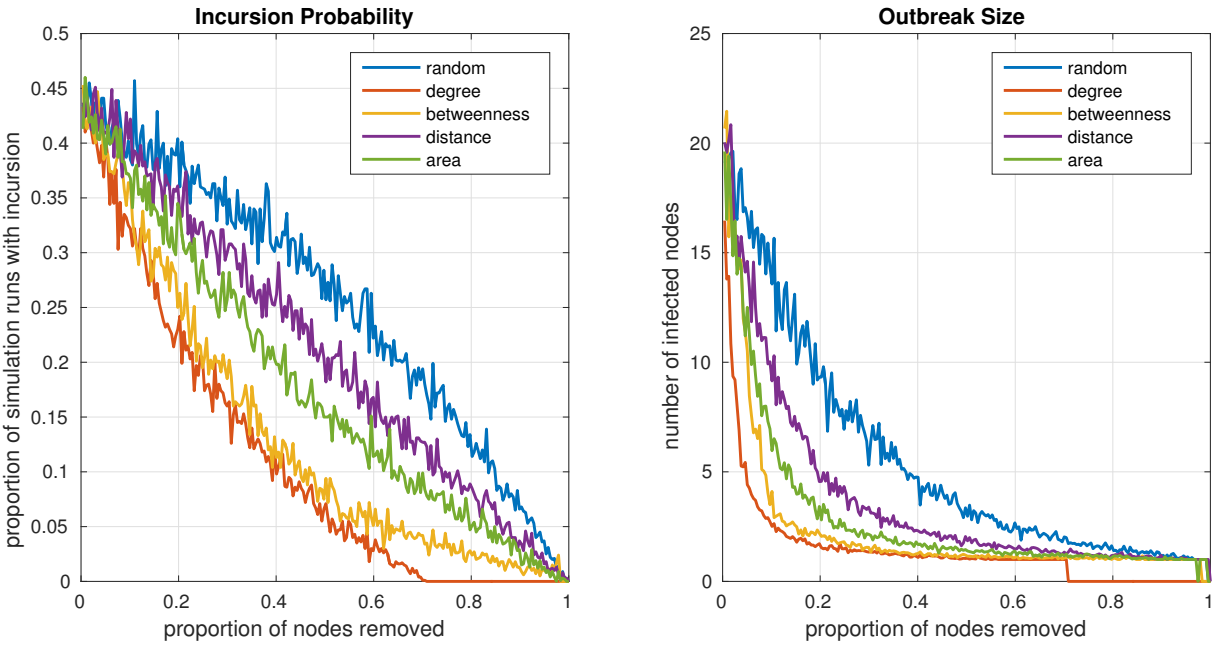

Figure 7.7: Outbreak probability and size for random and targeted vaccination and different coverages. For each coverage a fraction of nodes is considered as immunized and therefore removed from the network. These nodes are chosen either randomly (blue lines), in descending order of degree (red lines) or descending order of betweenness (yellow line). To simulate the effect of oral vaccination, the probability of a node being immunized was chosen to be linearly proportional to the average distance from the home location (purple line) or the area of the minimal convex polygon fitted into the gps logs (green line). The centrality values of the nodes are recalculated after each node removal. For each strategy and coverage 1000 simulation runs are conducted.

than the other nodes in the network, resulting in an overall larger outbreak size and duration. The remaining two network construction parameters, κ and λ, do not have a large effect on the model output. Among the parameters of the transmission model the infectious period, δ, is most sensitive. Since the model ignores birth and natural mortality, the incubation period σ is only relevant for the outbreak duration and not for the outbreak size. A sensitivity analysis of the outbreak probability, size and duration for different vaccination coverages is shown in Figure 7.14 and Figure 7.15.

7.6 Discussion

This study used empirical contact data to develop a contact network model of dog rabies transmission. We validated the simulation results with 2016 outbreak data from N'Djaména. We used the model to compare the probability of rabies establishment after incursion across different vaccination coverage. We showed that vaccination coverage above 70% prevents major outbreaks, which is consistent with previous findings (Zinsstag et al., 2017).

In contrast to deterministic models, our individual-based model allowed us to investigate the whole possibility space of outbreak scenarios. Differentiating between minor and major outbreaks revealed that even though the probability of major outbreaks is very low for high vaccination coverage, minor outbreaks can still occur even at nearly complete vaccination coverage. These minor rabies outbreaks consist of approximately 5 dogs, which aligns well with current observations from N'Djaména (Léchenne et al., 2017). The endemicity of rabies in N'Djaména could be explained as a series of rabies introductions with subsequent minor rabies outbreaks, as has been observed in Bangui (Bourhy et al., 2016).

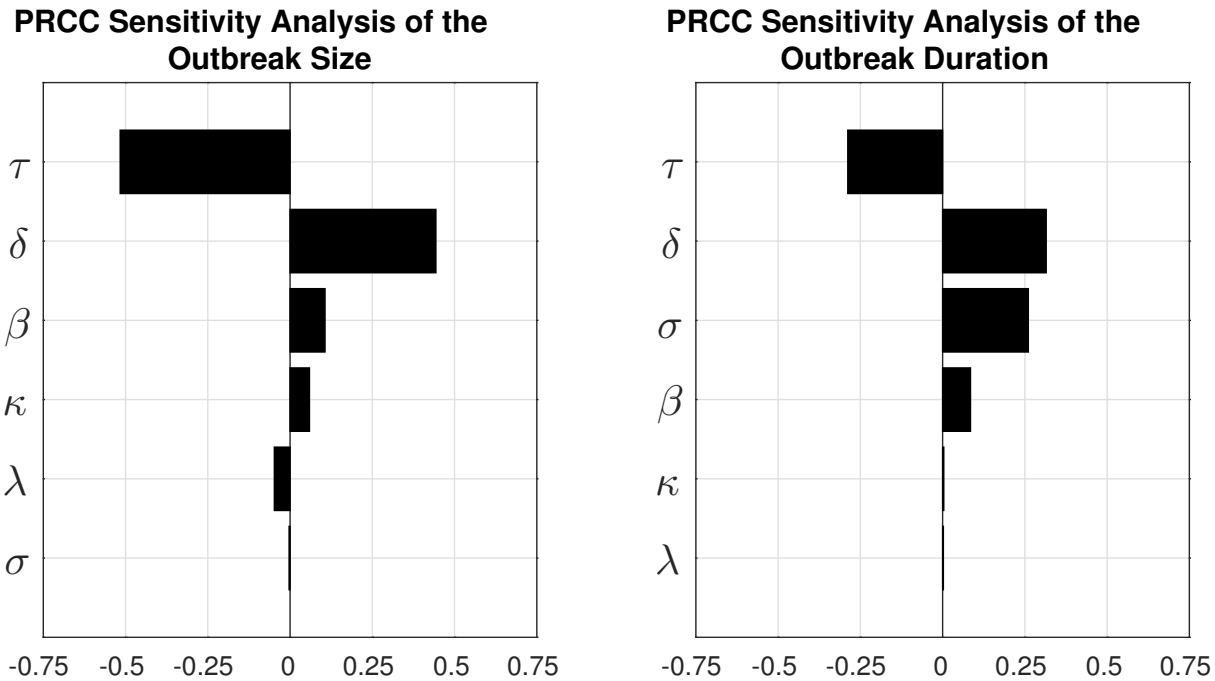

Figure 7.8: Partial Rank Correlation Coefficient sensitivity analysis of the outbreak size and outbreak duration. The parameter κ is a network construction parameter involved in the scaling of the spatial connection. The parameter τ is a network construction parameter that alters the proportion of far roaming dogs. The parameter λ is a network construction parameter that alters the mean number of peers of far roaming dogs. The parameter δ is the infectious period. The parameter σ is the incubation period. The parameter β is the transmission rate.

We showed that targeting dogs by degree centrality, betweenness centrality or based on their movement substantially increases the impact of vaccination. Targeted vaccination based on betweenness centrality does not perform better than targeted vaccination based on degree centrality. The observation that vaccination by degree performs as well as vaccination according to other network centralities is consistent with previous findings in humans (Smieszek and Salathé, 2013). The degree or betweenness centrality can only be assessed using expensive methods like the tagging with geo-located contact sensors conducted in this study. Such methods cannot be used in routine surveillance. We have shown that vaccination based on movement also reduces the outbreak probabilities and sizes. This might indicate that oral vaccination would be an effective intervention because dogs which cover a lot of territory would be more likely to encounter oral vaccine baits. Oral vaccination has been shown to effectively prevent rabies in dogs (Estrada et al., 2001) and is currently recommended by the WHO as a complementary measure to increase coverage in mass vaccination campaigns (WHO, 2018). Oral vaccination must be carefully planned with regard to biosafety, for example by assuring that vaccinators retrieve unconsumed baits (Smith et al., 2017). It has been successfully implemented to eliminate fox rabies in central Europe (Freuling et al., 2013). Further consideration of oral vaccination of dogs is warranted based on these results.

We observed a dog population where only a few dogs were not part of the largest component, similar to Hirsch et al. (2013), who used proximity loggers to reveal a highly connected population in raccons.

In contrast to the raccoon rabies model of Reynolds *et. al.* (Reynolds et al., 2015), which concluded that with vaccination coverage of 65% the probability of a large outbreak remains around 60 - 80%, we noted a substantial drop in the probability of a major outbreak. This might be due to the fact that, while raccoons remain infectious until death from rabies, we assumed

that dogs remain rabid for only two days on average because we hypothesized that in an urban setting a rabid dog would be killed by the community. Therefore, major rabies outbreaks could be prevented by rabies awareness and locally reactive interventions.

Unlike Dürr and Ward (2015) who found that even at a vaccination coverage of 70% approximately half the dog population dies from rabies, we found outbreak sizes of less than 1% of the population for high vaccination coverage. This might be due to the fact that Dürr *et al.* considered reactive vaccination after incursion rather than preventive vaccination.

There are several limitations to our study. Our simulations are based on the assumption that rabid dogs stay infective for two days on average, which does not consider the fact, that rabid dogs can be infectious for several days before they show symptoms. Previous models of rabies in wildlife indicated an effect of seasonality on outbreak sizes and durations. Collecting contact data at different times of the year is currently planned, and subsequent analyses will explore the impact of seasonality on contact rates. Dog contacts were only measured for a period of 3.5 days, the extent of battery life. While this observation window is longer than the average infectious period, we cannot be certain that the structure of the network would remain the same when measured for a longer time. Also, contacts with untagged owned dogs and unowned dogs (approx. 8% to 15% of the dog population) were not recorded. Furthermore, we did not include the change of behavior of a rabid animal. However, Reynolds et al. (2015) found that assuming a combination of paralytic and furious rabies in the population leads to little quantitative change in the outbreak size.

We found that major rabies outbreaks are unlikely when vaccination coverage is above 70%. Our results suggest that the endemicity of rabies in N'Djaména might be explained as a series of importations with subsequent minor outbreaks. Further investigation of determinants of dog roaming and contact behavior could inform potential targeted vaccination strategies.

7.7 Supporting information

Parameter	Description	Range	Type
κ	scaling of spatial connection	[20,30]	discrete
τ	proportion of far roaming dogs	[0.5, 1]	continuous
λ	mean number of peers of far roaming dogs	[20,30]	discrete
δ	infectious period	[1,7]	discrete
σ	incubation period	[7, 730]	discrete
β	transmission rate	[0.015, 0.02]	continuous

Table 7.5: Parameter ranges for the PRCC sensitivity analysis.

Acknowledgments

Calculations were performed at sciCORE (http://scicore.unibas.ch/) scientific computing core facility at University of Basel. The maps were generated using ©OpenStreetMap contributors. Katya Galactionova and Lisa Crump are greatly acknowledged for language editing.

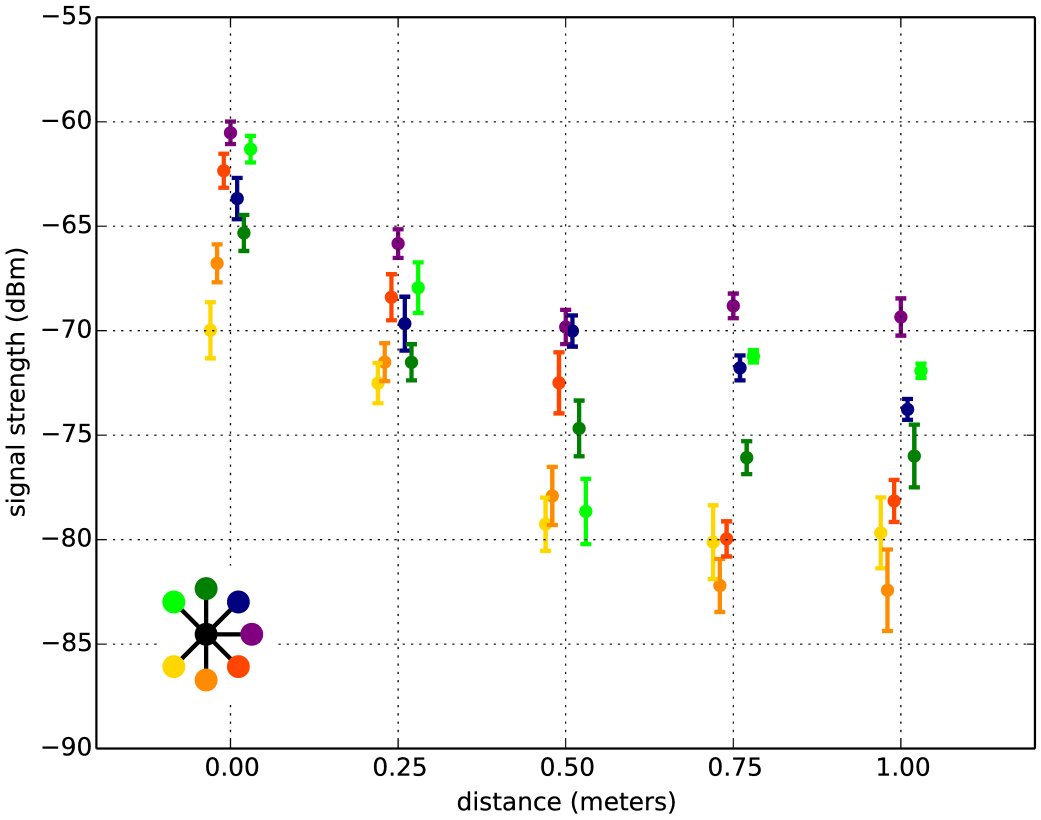

Figure 7.9: Signal strength of contacts between devices in a static test in N'Djaména. The devices were set up on the ground in a circular arrangement around a central device and contact were recorded for different distances over a period of 1 hour per distance. The colors correspond to different angles from the central device (black dot).

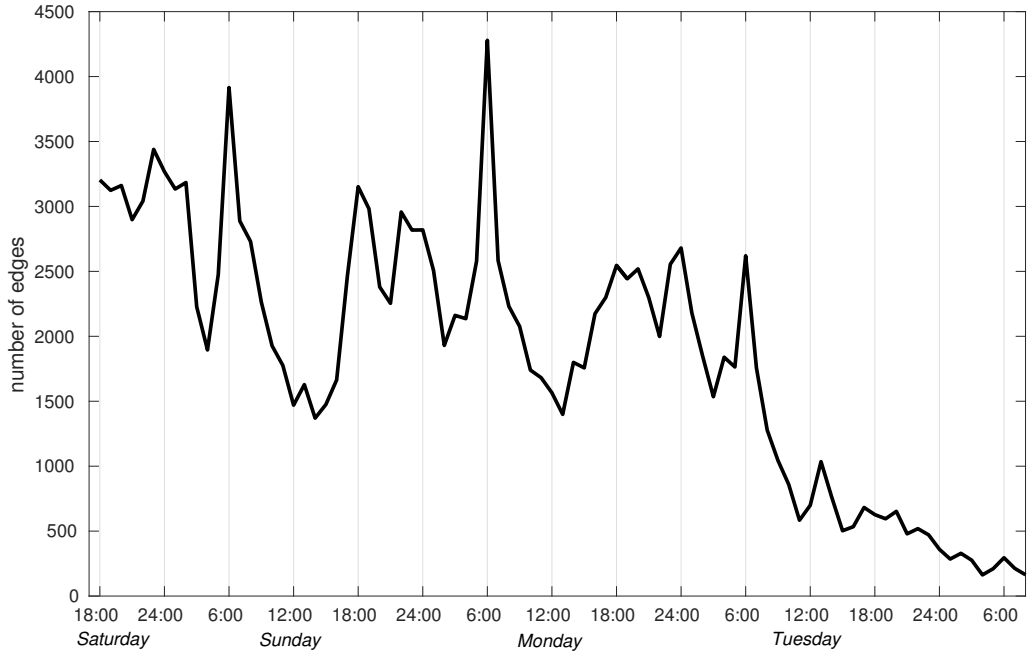

Figure 7.10: Contacts over time in study zone 1. For each 1 hour interval during the study period, ranging from Saturday 17:00 to Tuesday 7:00, the number of edges in the network is shown. The network for each 1 hour interval was constructed based on all contacts recorded during that interval and an edge was established if at least one contact between the two dogs was registered.

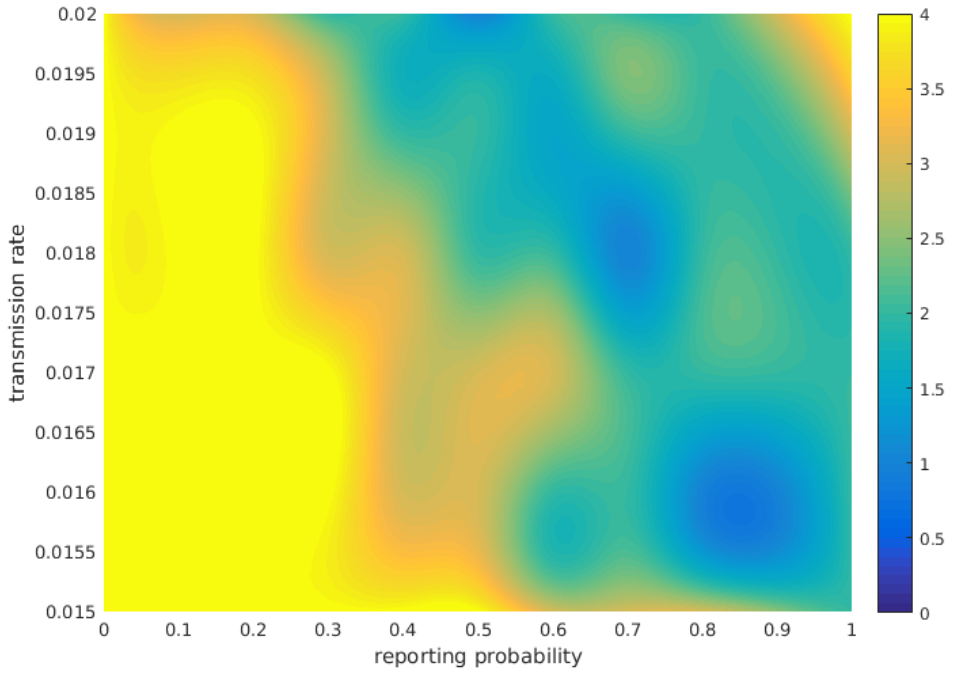

Figure 7.11: Sensitivity analysis of the simulation results for Chagoua and Abena on the probability of detecting rabid dogs. For each value of the transmission rate (ranging from 0.015 to 0.02 with steps of 0.01) 1000 simulation runs were conducted. Each case in the simulated incidence was randomly assigned as either reported or not reported for different values of the reporting probability (ranging from 0 to 1 with steps of 0.1). The color of each pixel corresponds to the maximum absolute difference between the median of the simulated reported cumulative incidence and the outbreak data.

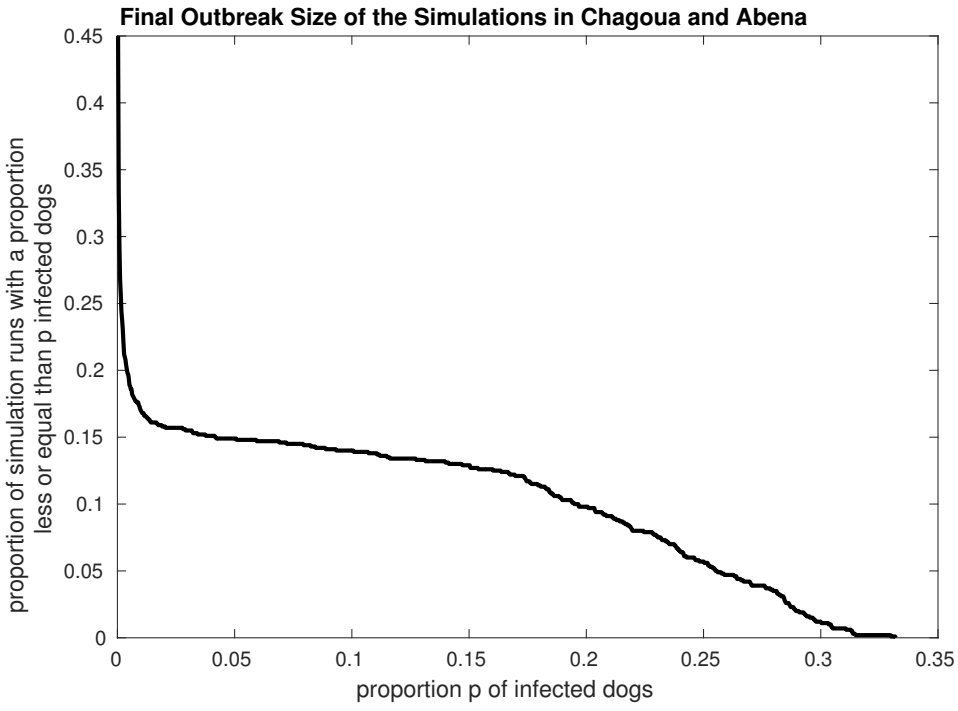

Figure 7.12: Final outbreak size of the simulations in the quarters Chagoua and Abena.

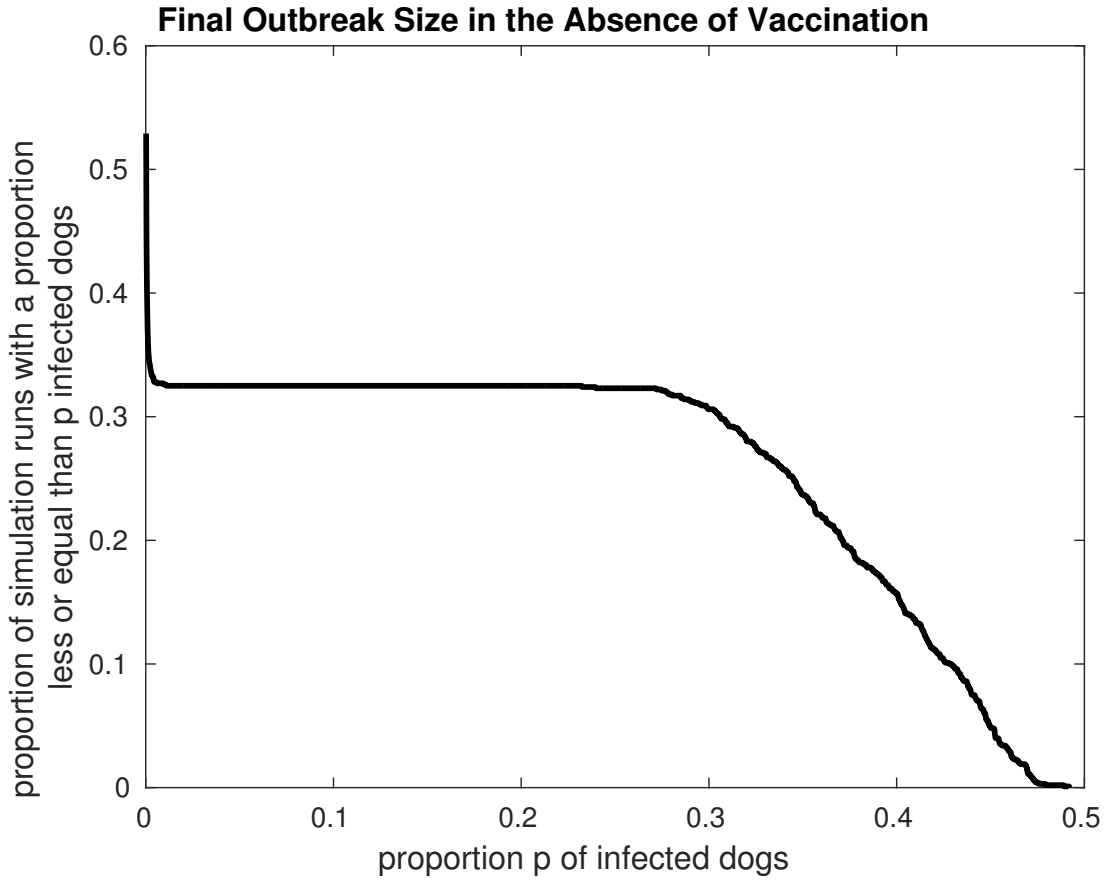

Figure 7.13: Final outbreak size of the simulations on a network of 4930 dogs, showing the two point distribution expected from theory.

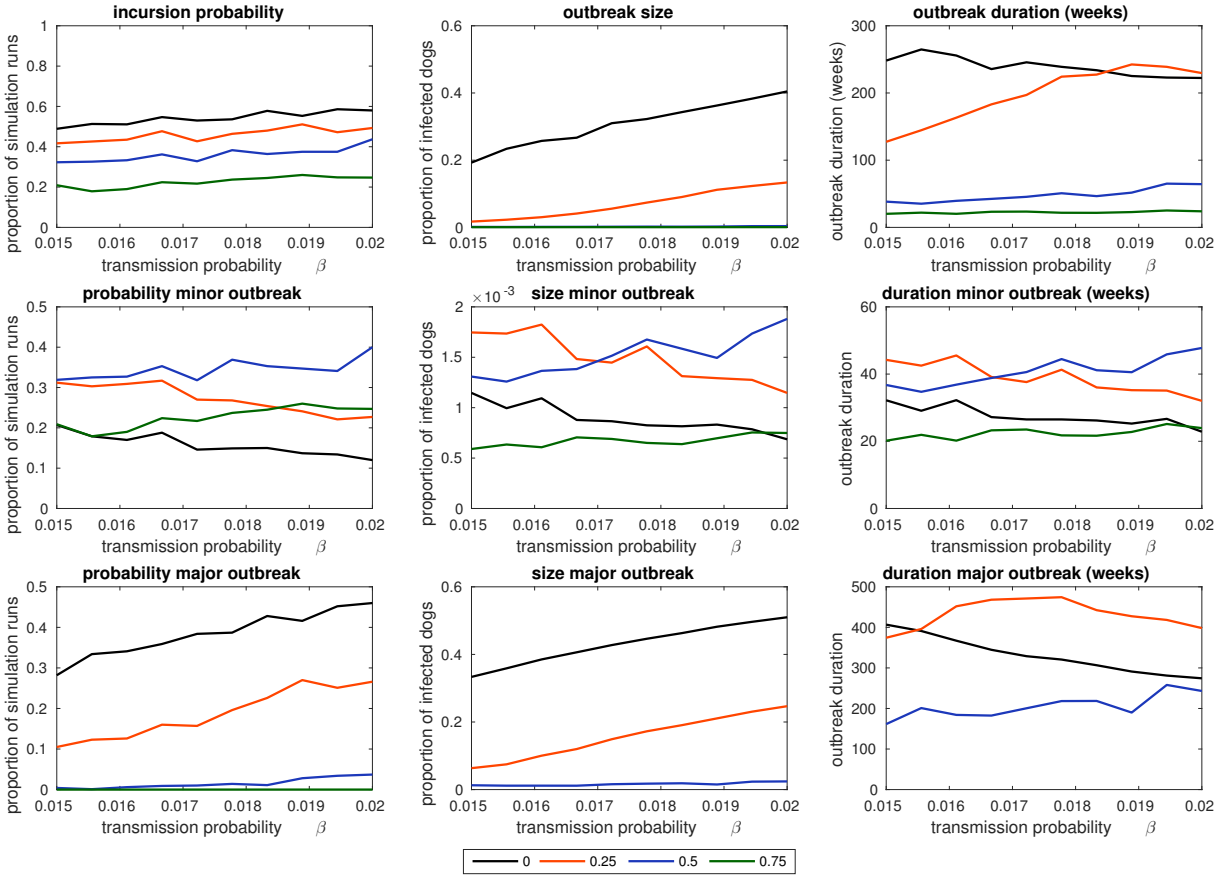

Figure 7.14: Sensitivity analysis of the outbreak probability, duration and size. The colors correspond to different vaccination coverages. For each vaccination coverage and parameter value the mean of 1000 simulation runs is shown. Simulation runs where more than one dog gets infected are classified as incursion. Simulation runs where more than one dog and less than 1% of the population get infected are classified as minor outbreaks. Simulation runs where more than 1% of the population gets infected are classified as major outbreaks. Incursions include minor and major outbreaks.

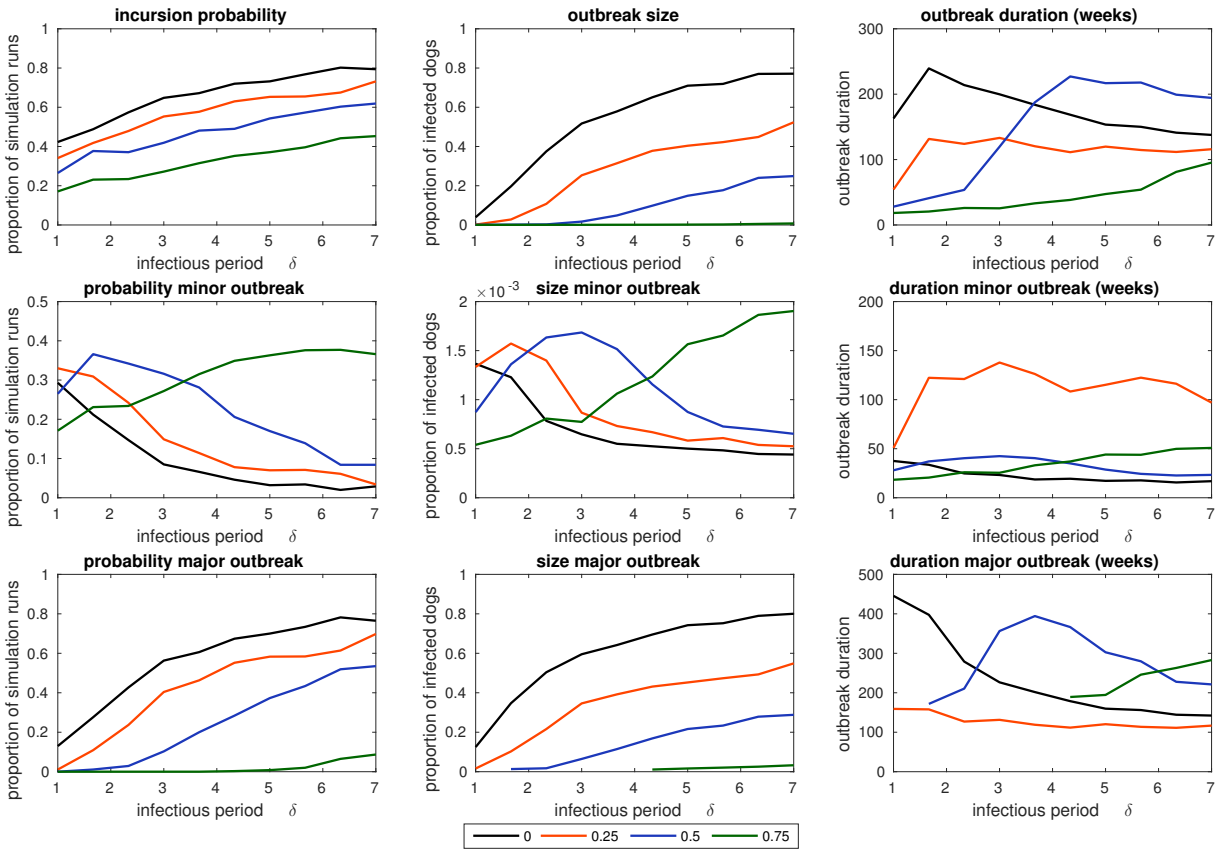

Figure 7.15: Sensitivity analysis of the outbreak probability, duration and size. The colors correspond to different vaccination coverages. For each vaccination coverage and parameter value the mean of 1000 simulation runs is shown. Simulation runs where more than one dog gets infected are classified as incursion. Simulation runs where more than one dog and less than 1% of the population get infected are classified as minor outbreaks. Simulation runs where more than 1% of the population gets infected are classified as major outbreaks. Incursions include minor and major outbreaks.

8. Discussion

8.1 Developing models for rabies transmission in N'Djamena

Confirming interruption of transmission

We calibrated a compartmental model for dog rabies in N'Djamena and used it to assess the impact of vaccination campaigns. Compartmental models represent the infection history of a disease with a number of compartments, such as susceptible or infective and describe the time dynamics of an epidemic with a system of ordinary differential equations. Infection is transmitted according to the mass action principle, which means that each individual is equally likely to infect any other individual. Despite their simplicity, such models are useful to investigate the dynamics of an infection over time and are widely used in rabies modelling (Kitala et al., 2002; Chen et al., 2015; Ruan, 2017; Fitzpatrick et al., 2014; Bilinski et al., 2016; Tohma et al., 2016). Because simple compartmental models are analytically tractable, basic quantities such as the force of infection, the basic reproductive ratio or endemic equilibria can be computed. We have shown that during the vaccination campaigns the effective reproductive ratio dropped below one. We compared the impact of population turnover and individual immunity loss on the increase of the effective reproductive ratio after the vaccination campaigns and found that population turnover contributes more to the increase than individual immunity loss.
Such deterministic models have a number of limitations. The random mixing assumption is not very realistic, because transmission is based on contacts and contacts are not necessarily random. Furthermore, the transitions between the compartments are mostly expressed in terms of the form $^{dC(t)}/_{dt} = -\rho C(t)$, where $C(t)$ is the proportion of individuals in a compartment at time t and $^{1}/_{\rho}$ is the mean time to transition. The proportion of individuals still in the compartment is given by $e^{-\rho t}$, which corresponds to an exponentially distributed waiting time. This is not always adequate, because for processes such as incubation a waiting time distributed symmetrically around the mean is more realistic. Also, because the state variables are continuous, infection can persist where a stochastic model would have yielded a die-out. The last point was addressed by implementing a stochastic version of the model with the Gillespie algorithm.

Comparing reasons for resurgence

To explain the resurgence of cases after the campaigns, we developed a metapopulation model. We incorporated spatial heterogeneity by dividing the city into patches, with an ordinary differential equation model in each patch. This relaxes the homogeneous mixing assumption to a certain extent, because transmission is more likely to happen within a patch than between patches. We have derived upper and lower bounds for the basic reproductive ratio of the metapopulation system. Spatial heterogeneity or underreporting alone could not explain the resurgence in cases. We found that importation is the most likely reason for the resurgence and estimated that an importation of one latently infected dog every six weeks would be enough to sustain transmission in N'Djamena. The stochastic implementation of the model confirmed the results

of the deterministic model. We also explored the hypotheses that the rabies incidence observed in N'Djamena is not the result of endemic rabies transmission but caused by a series of small outbreaks subsequently contained by an increased death rate of rabid dogs due to raised rabies awareness. Even though we were able to reproduce the observed rabies incidence with a deterministic model with an incidence dependent rabies death rate, a stochastic or individual based model would be more suitable to further investigate this hypothesis.

Investigating consequences of importation

Because importation seems to be the most likely reason for the resurgence in cases, we investigated the chains of transmission triggered by imported cases. When a case is introduced into a disease free population, individual heterogeneity and stochasticity substantially influence the further course of transmission. We therefore developed a stochastic, individual based model. This has the additional benefit that individuals can transition from one state to the next according to any waiting time distribution, which relaxes the exponential waiting time assumption of the deterministic models. In order to realistically reproduce the contact heterogeneity at individual level, we used data from 300 geo-located contact sensors to build a network of 5000 dogs. Since there is no established method for expanding a network to a network with more nodes, we have developed and validated a network construction algorithm. In this algorithm, contacts between dogs are established based on the spatial distance between their home locations. Furthermore, a proportion of dogs connects to other dogs independently of spatial distance with a probability that is proportional to the number of connections a dog already has. This mechanism is known as preferential attachment and has been used to describe contact networks among humans. The network construction algorithm therefore heuristically approximates dog to dogs contacts as a combination of a spatial and a social component. It is surprising how well this algorithm reproduces the empirical network. We have calibrated the transmission rate such that the simulation results correspond to outbreak data from two quarters in N'Djamena. We have shown that 70% coverage prevents major but not minor outbreaks. Combining the coverage assessment from the first model and the network model we have found a possible explanation for the timing of the resurgence. Targeting dogs with many contacts could substantially increase the effect of vaccination.

8.2 Implications for rabies control and elimination

Strategies adopted by rabies programs in general

There are four main technologies advocated for combating rabies in humans, each of which might be deployed in different ways.

Pre-exposure prophylaxis in humans has been recommended in places with high dog bite incidence, incomplete rabies control in the animal reservoir and limited access to immunoglobulin (Kessels et al., 2017; WHO, 2013). Introducing pre-exposure prophylaxis into the routine childhood immunization programme has been suggested for highly endemic areas (Durrheim et al., 2015b). However, such a strategy alone cannot prevent deaths from rabies because even with pre-exposure prophylaxis two doses of post-exposure prophylaxis are required in case of a bite by an infected animal.

Post-exposure prophylaxis in humans can effectively prevent rabies deaths but does not reduce transmission. However, a strategy of scaling up access to post-exposure prophylaxis to reach the goal of zero rabies deaths by 2030 is facing the challenge of an adequate risk assessment. Rabies exposures form a small proportion of the overall number of dog bites (Léchenne et al., 2017; Undurraga et al., 2017). Therefore, treating all dog bite cases as potential rabies exposures would result in post-exposure prophylaxis demands that would be not only very expensive but also possibly not procurable. Shortages occurred during the rabies elimination demonstration project in Tanzania (Mpolya et al., 2017). This was despite the substantial vaccine savings achieved by changing from intramuscular to intra-dermal administration of post-exposure prophylaxis (Hampson et al., 2011). To reduce vaccine demand new bite case management strategies have been investigated (Undurraga et al., 2017). These involve delaying post-exposure prophylaxis while observing the behaviour of the dog, but are currently neither implemented in this setting nor recommended by WHO (WHO, 2013).

Dog vaccination is a way of fighting rabies at its source. Dogs can be vaccinated parentally or orally, and vaccination can be organised as a routine service or via mass campaigns. The WHO currently recommends oral vaccination of dogs only as a complementary measure to increase coverage of mass vaccination campaigns (WHO, 2018, p. 79). Mass dog vaccination campaigns have been proven to be feasible also in low resource settings (Léchenne et al., 2016b) and to reduce human exposure (chapter 5). But while dog mass vaccination campaigns have been advocated under the assumption of being more cost-effective than post-exposure prophylaxis alone (Zinsstag et al., 2009), the actual costs can be substantially higher. In N'Djamena, the demand for post-exposure prophylaxis was not affected by the decreasing incidence of dog rabies cases (Léchenne et al., 2017). Furthermore, dog vaccination campaigns without dog population management have been criticized as unsustainable (Franka et al., 2013). In the absence of dog population management, population turnover quickly reduces vaccination coverage and reintroduction from surrounding areas (chapter 6) or spillovers from wildlife reservoirs threaten the gains of mass dog vaccination campaigns.

The fourth strategy is hence vaccination of reservoir hosts, as has proven effective with oral vaccination of foxes in Western Europe (Freuling et al., 2013) and foxes, coyotes and raccoons in North America (Slate et al., 2009).

Dog rabies elimination in Chad

The WHO framework for eliminating dog-mediated human rabies by 2030 promotes dog vaccination as the most cost-effective way of preventing rabies. Consequently, Anyiam et al. (2017) advocate for eliminating rabies in Chad through mass vaccination of dogs. They argue that covering the whole of Chad with mass vaccination campaigns of dogs one or two times is feasible and cost-effective and claim that this will lead to dog rabies elimination at an estimated cost of 28 million Euros over ten years. However, this approach disregards two major challenges: prevention of re-establishment and surveillance.

Firstly, the high population turnover of dogs leads to a considerable decrease of vaccination coverage over time (chapter 5). Therefore, the gains of a countrywide mass vaccination campaign are threatened by re-establishment of rabies. A large-scale vaccination campaign should

therefore not be guided by political, but rather by geographical boundaries. As we have shown with the network analysis, even traffic roads can constitute a barrier for dog to dog contacts (chapter 7). The rabies elimination demonstration project in Tanzania took advantage of natural boundaries such as rivers, mountains and highways when defining the intervention zone (Mpolya et al., 2017). It would therefore be beneficial, to first identify a bounded region where rabies can be eliminated locally and only then scale up to a countrywide elimination campaign. Following countrywide vaccination a buffer zone with ongoing vaccination has to be established, similar to the vaccination belt in eastern Europe (Müller et al., 2015). Furthermore, as coverage decreases, re-introduction from wildlife has to be prevented. In South Africa it is likely that black jackals are capable of sustaining rabies cycles (Zulu et al., 2009). After eliminating rabies from the dog population in northeastern Mexico, rabies was re-introduced into dogs through a coyote-dog contact in 2011 (Velasco-Villa et al., 2017). Therefore, sustainable mass vaccination campaigns need to account for additional efforts by either maintaining the vaccination coverage at high levels through repeated vaccination, as recommended in the rabies elimination demonstration project in Tanzania (Mpolya et al., 2017), or prevention of re-introduction through vaccination belts and control of rabies in the wildlife reservoir.
Secondly, even though vaccinating dogs reduces human exposure, this will only translate to a reduction of post-exposure prophylaxis need if a region can be reliably considered rabies-free. In the absence of information on the status of the dog, a bite has to be considered as a potential rabies exposure. Unless an effective surveillance system assures a region to be rabies free, some amount of post-exposure prophylaxis will always be necessary.

Rabies control in N'Djamena

Since elimination is unlikely in the short term, rabies control in N'Djamena requires post-exposure prophylaxis for humans, but such a rabies control program should be complemented by dog vaccination. Controlling rabies in the dog population has the advantage that the subsequent exposure reduction applies to all persons equally. The barriers that can hinder the timely administration of post-exposure prophylaxis like lack of awareness, low socio-economic class, distance to a health facility or stock-outs at the health facilities (Hampson et al., 2008) do not apply to dog vaccination. Vaccinated dogs protect humans regardless of their socio-economic status.

Dog vaccination procedures include the following possible options: mass vaccination campaigns, continuous vaccination by veterinarians, oral vaccine baits and reactive vaccination.
(a) *mass vaccination campaigns*
The mass vaccination campaigns in 2012 and 2013 were conducted under the assumption that cities are sources of rabies transmission and that the surrounding areas due to their low dog densities are not able to sustain transmission. With this premise, mass vaccination campaigns aimed at reaching a high coverage to interrupt transmission. The initial cost of such an effort pays off if once elimination is achieved no further efforts are required. The basic assumption of this approach has been challenged by Bourhy et al. (2016) where it was shown that rabies is not self-sustaining in the city of Bangui but rather occured via a series of introductions with short chains of transmission and subsequent extinctions. It is likely that it was also importa-

tion that caused the new cases in N'Djamena(chapter 6). This changes the framework of mass vaccination campaigns because the primary goal is no longer achieving a peak in coverage but rather to maintain a high enough coverage to prevent incursions from establishing local chains of transmission. Combining a homogeneous model to describe changes in coverage over time and a contact network model to determine incursion probabilities for different coverages, we find that annual vaccination campaigns would be sufficient to prevent incursions. These results depend on the dog demography since population turnover is the main driver of coverage decrease.

(b) *continuous vaccination of dogs by veterinarians*

Having a dog vaccinated by a veterinarian could be part of a concept of responsible dog ownership. This approach has the advantage of maintaining coverage at a certain level continuously. Furthermore, possibly this would lead to an overall healthier dog population and therefore slow down the population turnover. Using a homogeneous model with importation as described in chapter 6 of this thesis we have estimated that continuous vaccination of 60 % of the dogs would lead to similar outcomes in terms of dog rabies cases and subsequent reduction of human exposure as yearly mass vaccination campaigns of 70% of the dogs. Distributing vaccination throughout the year could be beneficial because of a more stable coverage and less logistic efforts.

(c) *reactive vaccination*

In addition to suggesting that importation contributes to the rabies transmission in N'Djamena our analyses also indicate that roads with high traffic intensity constitute a barrier for contacts. So possibly rabies could also be controlled on a very local scale, by reactive vaccination of a quarter on incursion of a rabid dog. This would have the additional benefit of locally raising awareness to rabies at the time it is needed. The transmission dynamics are highly sensitive to the death rate of rabid dogs. Raised awareness could therefore also contribute to reduced transmission. As Townsend et al. (2013a) have pointed out, detection probabilities influence the effectiveness of different vaccination strategies. Using a spatially explicit stochastic model they find that for detection probabilities above 10% reactive vaccination is as effective in preventing outbreaks as proactive vaccination and that fewer dogs have to be vaccinated in the reactive intervention strategy. However, for lower detection probabilities the probability of controlling an outbreak decreases substantially. Therefore, reactive vaccination would require an effective surveillance system.

(d) *oral vaccination baits*

Our models indicated that targeted vaccination of dogs that move far from the house of their owners would reduce the outbreak probability substantially. This suggests that oral vaccination might be an effective intervention. Deploying baits in an urban context has to be carried out carefully. But given the substantial effect, a further investigation of this approach would be worthwhile especially because experiences with oral vaccination could later on be transferred to wildlife rabies control.

8.3 Future work

Because of the substantial effect of targeted vaccination it would be useful to further study the characteristics of dogs with many contacts. In case simple proxies for high degree dogs could be identified, this could possibly guide targeted vaccination of such dogs. Oral vaccination both of dogs and of potential reservoir hosts (neither of which was investigated in this thesis) might also be part of the best intervention package for settings like N'Djamena. Should implementation of oral vaccination be considered, a study on temperature durability and bait uptake could be conducted. Furthermore, the data from the contact sensors also include information on duration and frequency of the contacts. This could be used to construct a weighted graph and run outbreak simulations thereon. Since the contact network study has been repeated in the rainy season, a model that accounts for the contact behaviour in different seasons could inform optimal timing of vaccination campaigns. In terms of data collection most importantly the surveillance should continue to inform future models on the dynamics of rabies over time. Possibly, surveillance could even be expanded to the rural areas around N'Djamena. Also, since importation is the most likely reason for the resurgence of cases, the provenance of recent cases could be investigated. Furthermore, the dog demography has been an important element in all models. Since the short lifespan of dogs is an important driver of population turnover and possibly even importation, more information on the causes of death for dogs would be useful.

9. Conclusion

In this thesis we have developed deterministic, stochastic and individual based models of dog rabies transmission and calibrated the model parameters to data on dog demography, dog contact networks and rabies incidence in N'Djamena. The model development was guided by questions raised by two mass vaccination campaigns of dogs. Did the campaigns lead to an interruption of transmission? Which factors contributed to the decrease of vaccination coverage over time? Why did new cases appear only nine months after the campaigns? We used deterministic models to describe the overall population dynamics, stochastic models to study the interruption of transmission and an individual based model to simulate rabies incursions on a contact network. We found that most likely decreasing vaccination coverage due to population turnover combined with introduction of latent dogs from the surroundings of N'Djamena led to the re-establishment of rabies. This improved understanding suggests that vaccination campaigns will likely not lead to longer periods with no transmission unless importation of exposed dogs is reduced. Furthermore, we have shown that highly connected dogs hold a critical role in rabies transmission and that vaccinating such dogs, possibly by oral vaccination, could increase the effect of vaccination strategies. Vaccinating dogs is an effective and equitable way of reducing human exposure and should therefore be an inherent part rabies control programmes in endemic settings.

Bibliography

Albert, R., Jeong, H., and Barabasi, A. L. (2000). Error and attack tolerance of complex networks. *Nature*, 406(6794):378–382.

Anderson, R. M., Jackson, H. C., May, R. M., and Smith, A. M. (1981). Population dynamics of fox rabies in Europe. *Nature*, 289(2):765–770.

Andersson, H. (1999). Epidemic models and social networks. *The Mathematical Sicentist*, 24:128 – 147.

Andry, M. (1780). Recherches sur la rage. *Societe Royale de Medecine*.

Anisimova, M. and Gascuel, O. (2006). Approximate Likelihood-Ratio Test for Branches: A Fast, Accurate, and Powerful Alternative. *Systematic Biology*, 55(4):539–552.

Anyiam, F., Léchenne, M., Mindekem, R., Oussigéré, A., Naissengar, S., Alfaroukh, I. O., Mbilo, C., Moto, D. D., Coleman, P. G., Probst-Hensch, N., and Zinsstag, J. (2016). Cost-estimate and proposal for a development impact bond for canine rabies elimination by mass vaccination in chad. *Acta Tropica*.

Anyiam, F., Lechenne, M., Mindekem, R., Oussigéré, A., Naissengar, S., Alfaroukh, I. O., Mbilo, C., Moto, D. D., Coleman, P. G., Probst-Hensch, N., and Zinsstag, J. (2017). Cost-estimate and proposal for a development impact bond for canine rabies elimination by mass vaccination in Chad. *Acta Tropica*, 175(Supplement C):112 – 120. Ecohealth: An African Perspective.

Arriola, L. and Hyman, J. M. (2009). *Sensitivity Analysis for Uncertainty Quantification in Mathematical Models*, pages 195–247. Springer Netherlands, Dordrecht.

Bano, I., Sajjad, H., Shah, A., Leghari, A., Mirbahar, K. H., Shams, S., and Soomro, M. (2016). A review of rabies disease, its transmission and treatment. *Journal of Animal Health and Production*, 4:140–144.

Barclay, V. C., Smieszek, T., He, J., Cao, G., Rainey, G., Gao, H., Uzicanin, A., and Salathé, M. (2014). Positive network assortativity of influenza vaccination at a high school: Implications for outbreak risk and herd immunity. *PLOS ONE*, 9(2):1–11.

Begon, M., Bennett, M., Bowers, R. G., French, N. P., Hazel, S. M., and Turner, J. (2002). A clarification of transmission terms in host-microparasite models: numbers, densities and areas. *Epidemiol. Infect.*, 129(1):147–153.

Beyer, H. L., Hampson, K., Lembo, T., Cleaveland, S., Kaare, M., and Haydon, D. T. (2011). Metapopulation dynamics of rabies and the efficacy of vaccination. *Proceedings of the Royal Society of London B: Biological Sciences*, 278(1715):2182–2190.

Bilinski, A. M., Fitzpatrick, M. C., Rupprecht, C. E., Paltiel, D., and Galvani, A. (2016). Optimal frequency of rabies vaccination campaigns in Sub-Saharan Africa. *Proceedings of the Royal Society of London B: Biological Sciences*, 283(1842).

Blondel, V. D., Guillaume, J.-L., Lambiotte, R., and Lefebvre, E. (2008). Fast unfolding of communities in large networks. *Journal of Statistical Mechanics: Theory and Experiment*, 2008(10):P10008.

Bogel, K., Moegle, H., Knorpp, F., Arata, A., Dietz, K., and Diethelm, P. (1976). Characteristics of the spread of a wildlife rabies epidemic in Europe. *Bull. World Health Organ.*, 54(4):433–447.

Bouckaert, R., Heled, J., Kühnert, D., Vaughan, T., Wu, C.-H., Xie, D., Suchard, M. A., Rambaut, A., and Drummond, A. J. (2014). BEAST 2: A Software Platform for Bayesian Evolutionary Analysis. *PLOS Computational Biology*, 10(4):1–6.

Bourhy, H., Nakouné, E., Hall, M., Nouvellet, P., Lepelletier, A., Talbi, C., Watier, L., Holmes, E. C., Cauchemez, S., Lemey, P., Donnelly, C. A., and Rambaut, A. (2016). Revealing the micro-scale signature of endemic zoonotic disease transmission in an african urban setting. *PLOS Pathogens*, 12(4):1–15.

Britton, T., Janson, T., and Martin-Löf, A. (2007). Graphs with specified degree distributions, simple epidemics, and local vaccination strategies. *Advances in Applied Probability*, 39(4):922948.

Cao, Y., Gillespie, D. T., and Petzold, L. R. (2006). Efficient step size selection for the tau-leaping simulation method. *The Journal of Chemical Physics*, 124(4):044109.

Castillo-Neyra, R., Brown, J., Borrini, K., Arevalo, C., Levy, M. Z., Buttenheim, A., Hunter, G. C., Becerra, V., Behrman, J., and Paz-Soldan, V. A. (2017). Barriers to dog rabies vaccination during an urban rabies outbreak: Qualitative findings from Arequipa, Peru. *PLOS Neglected Tropical Diseases*, 11(3):1–21.

Cattuto, C., den Broeck, W. V., Barrat, A., Colizza, V., Pinton, J. F., and Vespignani, A. (2010). Dynamics of person-to-person interactions from distributed RFID sensor networks. *PLoS ONE*, 5(7):e11596.

Chan, M. (2015). Opening address at a conference on the Global elimination of dog-mediated human rabies: the time is now. Technical report, World Health Organization.

Charron, D. F. (2012). Ecosystem approaches to health for a global sustainability agenda. *EcoHealth*, 9(3):256–266.

Chen, J., Zou, L., Jin, Z., and Ruan, S. (2015). Modeling the Geographic Spread of Rabies in China. *PLOS Neglected Tropical Diseases*, 9(5):1–18.

Chitnis, N., Hyman, J. M., and Cushing, J. M. (2008). Determining Important Parameters in the Spread of Malaria Through the Sensitivity Analysis of a Mathematical Model. *Bulletin of Mathematical Biology*, 70(5):1272.

Cleaveland, S., Lankester, F., Townsend, S., Lembo, T., and Hampson, K. (2014). Rabies control and elimination: a test case for one health. *Veterinary Record*, 175(8):188–193.

Cohen, R., Havlin, S., and ben Avraham, D. (2003). Efficient immunization strategies for computer networks and populations. *Phys. Rev. Lett.*, 91:247901.

Coleman, P. G. and Dye, C. (1996). Immunization coverage required to prevent outbreaks of dog rabies. *Vaccine*, 14(3):185 – 186.

Cunningham, G. (1997). Deliver me from evil: Mesopotamian incantations 2500-1500 BC.

Darkaou, S., Cliquet, F., Wasniewski, M., Robardet, E., Aboulfidaa, N., Bouslikhane, M., and Fassi-Fihri, O. (2017). A Century Spent Combating Rabies in Morocco (1911-2015): How Much Longer? *Front Vet Sci*, 4:78.

Darriba, D., Taboada, G. L., Doallo, R., and Posada, D. (2012). jModelTest 2: more models, new heuristics and parallel computing. *Nat. Methods*, 9(8):772.

Diekmann, O., Heesterbeek, J., and Roberts, M. (2010). The construction of next-generation matrices for compartmental epidemic models. *Journal of The Royal Society Interface*.

Drews, G. (2015). *Bakterien - ihre Entdeckung und Bedeutung für Natur und Mensch*. Imprint: Springer Spektrum, Berlin, Heidelberg, 2., berarb. u. aktualisierte aufl. 2015 edition.

Drummond, A. J., Ho, S., Phillips, M., and Rambaut, A. (2006). Relaxed phylogenetics and dating with confidence. *PLOS Biology*, 4(5).

Dürr, S., Meltzer, M. I., Mindekem, R., and Zinsstag, J. (2008a). Owner valuation of rabies vaccination in dogs, Chad. *Emerging Infect. Dis.*, 14:16501652.

Dürr, S., Meltzer, M. I., Mindekem, R., and Zinsstag, J. (2008b). Owner valuation of rabies vaccination of dogs, Chad. *Emerging Infect. Dis.*, 14(10):1650–1652.

Dürr, S., Naíssengar, S., Mindekem, R., Diguimbye, C., Niezgoda, M., Kuzmin, I., Rupprecht, C. E., and Zinsstag, J. (2008c). Rabies diagnosis for developing countries. *PLOS Neglected Tropical Diseases*, 2(3):1–6.

Dürr, S. and Ward, M. P. (2014). Roaming behaviour and home range estimation of domestic dogs in Aboriginal and Torres Strait Islander communities in northern Australia using four different methods. *Preventive veterinary medicine*, 117(2):340–357.

Dürr, S. and Ward, M. P. (2015). Development of a Novel Rabies Simulation Model for Application in a Non-endemic Environment. *PLOS Neglected Tropical Diseases*, 9(6):1–22.

Durrheim, D., Rees, H., Briggs, D., and Blumberg, L. (2015a). Mass vaccination of dogs, control of canine populations and post-exposure vaccination - necessary but not sufficient for achieving childhood rabies elimination. *Tropical Medicine and International Health*, 20.

Durrheim, D. N., Rees, H., Briggs, D. J., and Blumberg, L. H. (2015b). Mass vaccination of dogs, control of canine populations and post-exposure vaccination necessary but not sufficient for achieving childhood rabies elimination. *Tropical Medicine and International Health*, 20(6):682–684.

Estrada, R., Vos, A., DeLeon, R., and Mueller, T. (2001). Field trial with oral vaccination of dogs against rabies in the Philippines. *BMC Infect. Dis.*, 1:23.

Fahrion, A. S., Taylor, L. H., Torres, G., Müller, T., Dürr, S., Knopf, L., de Balogh, K., Nel, L. H., Gordoncilloand, M. J., and Abela-Ridder, B. (2017). The Road to Dog Rabies Control and Elimination-What Keeps Us from Moving Faster? *Front Public Health*, 5:103.

Fitzpatrick, M., Hampson, K., and Cleaveland, A. (2014). Cost-effectiveness of canine vaccination to prevent human rabies in rural Tanzania. *Annals of Internal Medicine*, 160(2):91–100.

Fooks, A. R., Banyard, A. C., Horton, D. L., Johnson, N., McElhinney, L. M., and Jackson, A. C. (2014). Current status of rabies and prospects for elimination. *The Lancet*, 384(9951):1389 – 1399.

Fracastoro, H. (1546). *Von den Kontagien, den kontagiösen Krankheiten und deren Behandlung*. Johann Ambrosius Barth.

Franka, R., Smith, T. G., Dyer, J. L., Wu, X., Niezgoda, M., and Rupprecht, C. E. (2013). Current and future tools for global canine rabies elimination. *Antiviral Research*, 100(1):220 – 225.

Freuling, C. M., Hampson, K., Selhorst, T., Schröder, R., Meslin, F. X., Mettenleiter, T. C., and Müller, T. (2013). The elimination of fox rabies from europe: determinants of success and lessons for the future. *Philosophical Transactions of the Royal Society B: Biological Sciences*, 368(1623).

Gastaut, H. and Miletto, G. (1955). Interpretation physiopathogenique des symptomes de la rage furieuse. *Rev. Neurol*, 92:5–25.

Gillespie, D. T. (1977). Exact Stochastic Simulation of Coupled Chemical Reactions. *The Journal of Physical Chemistry*, 81(25):2340–2361.

Gomez-Alonso, J. (1998). Rabies: A possible explanation for the vampire legend. *Neurology*, 51:856–9.

Greenhalgh, D. (1986). Optimal control of an epidemic by ring vaccination. *Communications in Statistics. Stochastic Models*, 2(3):339–363.

Guindon, S., Dufayard, J.-F., Lefort, V., Anisimova, M., Hordijk, W., and Gascuel, O. (2010). New Algorithms and Methods to Estimate Maximum-Likelihood Phylogenies: Assessing the Performance of PhyML 3.0. *Systematic Biology*, 59(3):307–321.

Guindon, S. and Gascuel, O. (2003). A Simple, Fast, and Accurate Algorithm to Estimate Large Phylogenies by Maximum Likelihood. *Systematic Biology*, 52(5):696–704.

Hadorn, G. H., annd S. Biber-Klemm, H. H.-R., Grossenbacher, W., Joye, D., Pohl, C., Wiesmann, U., and Zemp, E. (2008). The emergence of transdisciplinarity as a form of research. In Hadorn, G. H., Hoffmann-Reim, H., Biber-klemm, S., Grossenbacher, W., Joye, D., Pohl, C., Wiesmann, U., and Zemp, E., editors, *Handbook of Transdisciplinary Research*, page 1939. Springer.

Hampson, K., Abela-Ridder, B., Brunker, K., Bucheli, T. M., Carvalho, M., Caldas, E., Changalucha, J., Cleaveland, S., Dushoff, J., Gutierrez, V., , A. R. F., Hotopp, K., Haydon, D. T., Lugelo, A., Lushasi, K., Mancy, R., Marston, D., Mtema, Z., Rajeev, M., Montebello, D., Gonzalez, R., Rysava, K., Rocha, S. M., Sambo, M., Sikana, L., Vigilato, M., and Vilas, V. D. R. (2016). Surveillance to establish elimination of transmission and freedom from dog-mediated rabies. *Cold Spring Harbor Labs Journals*.

Hampson, K., Cleaveland, S., and Briggs, D. (2011). Evaluation of cost-effective strategies for rabies post-exposure vaccination in low-income countries. *PLOS Neglected Tropical Diseases*, 5(3):1–11.

Hampson, K., Coudeville, L., Lembo, T., Sambo, M., Kieffe, A., Attlan, M., Barrat, J., Blanton, J. D., Briggs, D. J., Cleaveland, S., Costa, P., Freuling, C. M., Hiby, E., Knopf, L., Leanes, F., Meslin, F.-X., Metlin, A., Miranda, M. E., Müller, T., Nel, L. H., Recuenco, S., Rupprecht, C. E., Schumacher, C., Taylor, L., Vigilato, M. A. N., Zinsstag, J., Dushoff, J., and on behalf of the Global Alliance for Rabies Control Partners for Rabies Prevention (2015). Estimating the Global Burden of Endemic Canine Rabies. *PLOS Neglected Tropical Diseases*, 9(4):1–20.

Hampson, K., Dobson, A., Kaare, M., Dushoff, J., Magoto, M., Sindoya, E., and Cleaveland, S. (2008). Rabies exposures, post-exposure prophylaxis and deaths in a region of endemic canine rabies. *PLOS Neglected Tropical Diseases*, 2(11):1–9.

Hampson, K., Dushoff, J., Bingham, J., Brckner, G., Ali, Y. H., and Dobson, A. (2007). Synchronous cycles of domestic dog rabies in sub-Saharan Africa and the impact of control efforts. *Proceedings of the National Academy of Sciences*, 104(18):7717–7722.

Hampson, K., Dushoff, J., Cleaveland, S., Haydon, D. T., Kaare, M., Packer, C., and Dobson, A. (2009). Transmission Dynamics and Prospects for the Elimination of Canine Rabies. *PLOS Biology*, 7(3):1–10.

Hemachudha, T., Ugolini, G., Wacharapluesadee, S., Sungkarat, W., Shuangshoti, S., and Laothamatas, J. (2013). Human rabies: neuropathogenesis, diagnosis, and management. *The Lancet Neurology*, 12(5):498 – 513.

Hirsch, B. T., Prange, S., Hauver, S., and Gehrt, S. D. (2013). Raccoon social networks and the potential for disease transmission. *PLOS ONE*, 8(10):1–7.

Jeltsch, F., Müller, M. S., Grimm, V., Wissel, C., and Brandl, R. (1997). Pattern formation triggered by rare events: lessons from the spread of rabies. *Proceedings of the Royal Society of London B: Biological Sciences*, 264(1381):495–503.

Jibat, T., Hogeveen, H., and Mourits, M. C. M. (2015). Review on dog rabies vaccination coverage in Africa: A question of dog accessibility or cost recovery? *PLOS Neglected Tropical Diseases*, 9(2):1–13.

Johnstone-Robertson, S. P., Fleming, P. J. S., Ward, M. P., and Davis, S. A. (2017). Predicted spatial spread of canine rabies in australia. *PLOS Neglected Tropical Diseases*, 11(1):1–21.

Kayali, U., Mindekem, R., Yémadji, N., Oussiguéré, A., Naissengar, S., Ndoutamia, A., and Zinsstag, J. (2003a). Incidence of canine rabies in N'Djaména, Chad. *Preventive Veterinary Medicine*, 61(3):227 – 233.

Kayali, U., Mindekem, R., Ymadji, N., Vounatsou, P., Kaninga, Y., Ndoutamia, A. G., and Zinsstag, J. (2003b). Coverage of pilot parenteral vaccination campaign against canine rabies in N'Djamena, Chad. *Bull. World Health Organ*, 81:739744.

Keller, J. P., Gerardo-Giorda, L., and Veneziani, A. (2013). Numerical simulation of a susceptible-exposed-infectious space-continuous model for the spread of rabies in raccoons across a realistic landscape. *Journal of Biological Dynamics*, 7(sup1):31–46. PMID: 23157180.

Kessels, J. A., Recuenco, S., Navarro-Vela, A. M., Deray, R., Vigilato, M., Ertl, H., Durrheim, D., Rees, H., Nel, L. H., Abela-Ridder, B., and Briggs, D. (2017). Pre-exposure rabies prophylaxis: a systematic review. *Bull. World Health Organ.*, 95(3):210–219.

Kitala, P. M., McDermott., J. J., Coleman, P. G., and Dye, C. (2002). Comparison of vaccination strategies for the control of dog rabies in Machakos District, Kenya. *Epidemiology and Infection*, 129(1):215222.

Klepac, P., Metcalf, J., Mclean, A., and Hampson, K. (2013). Towards the endgame and beyond: Complexities and challenges for the elimination of infectious diseases. *Philosophical transactions of the Royal Society of London. Series B, Biological sciences*, 368:20120137.

Kretzschmar, M., van Duynhoven, Y. T. H. P., and Severijnen, A. J. (1996). Modeling prevention strategies for gonorrhea and chlamydia using stochastic network simulations. *American Journal of Epidemiology*, 144(3):306–317.

Laager, M., Léchenne, M., Naissengar, K., Mindekem, R., Oussigére, A., Zinsstag, J., and Chitnis, N. A metapopulation model of dog rabies transmission in n'Djaména, chad. submitted.

Lakshmanan, N., Gore, T., Duncan, K. L., Coyne, M. J., Lum, M. A., and Sterner, F. J. (2006). Three-year rabies duration of immunity in dogs following vaccination with a core combination vaccine against canine distemper virus, canine adenovirus type-1, canine parvovirus, and rabies virus. *Veterinary therapeutics : research in applied veterinary medicine*, 7(3):223231.

Lankester, F., Hampson, K., Lembo, T., Palmer, G., Taylor, L., and Cleaveland, S. (2014). Implementing pasteur's vision for rabies elimination. *American Association for the Advancement of Science*, 345(6204):1562–1564.

Léchenne, M., Mindekem, R., Madjadinan, S., Oussiguéré, A., Moto, D. D., KemdongartiNaissengar, and Zinsstag, J. (2017). The importance of a participatory and integrated one health approach for rabies control: The case of N'Djamna, Chad. *Tropical Medicine and Infectious Disease*, 2(3).

Léchenne, M., Naissengar, K., Lepelletier, A., Alfaroukh, I. O., Bourhy, H., Zinsstag, J., and Dacheux, L. (2016a). Validation of a Rapid Rabies Diagnostic Tool for Field Surveillance in Developing Countries. *PLoS Negl Trop Dis*, 10(10).

Léchenne, M., Oussiguere, A., Naissengar, K., Mindekem, R., Mosimann, L., Rives, G., Hattendorf, J., Moto, D. D., Alfaroukh, I. O., and Zinsstag, J. (2016b). Operational performance and analysis of two rabies vaccination campaigns in N'Djamena, Chad. *Vaccine*, 34(4):571 – 577.

Lembo, T., Hampson, K., Kaare., M. T., Ernest, E., Knobel, D., Kazwala, R. R., Haydon, D. T., and Cleaveland, S. (2010). The feasibility of canine rabies elimination in africa: Dispelling doubts with data. *PLOS Neglected Tropical Diseases*, 4(2):1–9.

Machens, A., Gesualdo, F., Rizzo, C., E.Tozzi, A., Barrat, A., and Cattuto, C. (2013). An infectious disease model on empirical networks of human contact: bridging the gap between dynamic network data and contact matrices. *BMC Infect. Dis.*, 13:185.

Mayr, A., Eissnerand, G., and Mayr-Bibrack, B. (1984). *Handbuch der Schutzimpfungen in der Tiermedizin*. Verlag Paul Parey.

Mbilo, C., Léchenne, M., Hattendorf, J., Madjadinan, S., Anyiam, F., and Zinsstag, J. (2016). Rabies awareness and dog ownership among rural northern and southern Chadian communities - analysis of a community-based, cross-sectional household survey. *Acta Tropica*.

Meyers, L. A., Pourbohloul, B., Newman, M. E., Skowronski, D. M., and Brunham, R. C. (2005). Network theory and SARS: predicting outbreak diversity. *J. Theor. Biol.*, 232(1):71–81.

Mindekem, R., Kayali, U., Yemadji, N., Ndoutamia, A., and Zinsstag, J. (2005a). Impact of canine demography on rabies transmission in N'Djamena, Chad. *Mdecine tropicale : revue du Corps de sant colonial.*, 65:53–58.

Mindekem, R., Kayali, U., Yemadji, N., Ndoutamia, A. G., and Zinsstag, J. (2005b). La démographie canine et son importance pour la transmission de la rage humaine á N'Djaména. *Med Trop (Mars)*, 65(1):53–58.

Mindekem, R., Léchenne, M., Madjadinan., A. S., Schindler, C., Doumagoum, D. M., Alfaroukh, I., and Zinsstag, J. (2017a). Démographie canine et couverture vaccinale spontanée contre la rage á n'djaména, tchad. submitted.

Mindekem, R., Léchenne, M., Naissengar, K. S., Oussiguéré, A., Kebkiba, B., Moto, D. D., Alfaroukh, I. O., Ouedraogo, L. T., Salifouand, S., and Zinsstag, J. (2017b). Cost description and comparative cost efficiency of post-exposure prophylaxis and canine mass vaccination against rabies in N'Djamena, Chad. *Frontiers in Veterinary Science*, 4:38.

Mindekem, R., Léchenne, M. S., Naissengar, K. S., Oussiguéré, A., Kebkiba, B., Moto, D. D., Alfaroukh, I. O., Ouedraogo, L. T., Salifou, S., and Zinsstag, J. (2017c). Cost description and comparative cost efficiency of post-exposure prophylaxis and canine mass vaccination against rabies in N'Djamena, Chad. *Frontiers in Veterinary Science*, 4:38.

Moore, S. M. and Hanlon, C. A. (2010). Rabies-specific antibodies: Measuring surrogates of protection against a fatal disease. *PLOS Neglected Tropical Diseases*, 4(3):1–6.

Morris, M. and Kretzschmar, M. (1995). Concurrent partnerships and transmission dynamics in networks. *Social Networks*, 17(3):299 – 318. Social networks and infectious disease: HIV/AIDS.

Morters, M. K., Restif, O., Hampson, K., Cleaveland, S., Wood, J. L., and Conlan, A. J. (2013). Evidence-based control of canine rabies: a critical review of population density reduction. *J Anim Ecol*, 82(1):6–14.

Mosimann, L., Traoré, A., Mauti, S., Léchenne, M., Obrist, B., Véron, R., Hattendorf, J., and Zinsstag, J. (2017). A mixed methods approach to assess animal vaccination programmes: The case of rabies control in bamako, mali. *Acta Tropica*, 165:203 – 215. The Fate of Neglected Zoonotic Diseases.

Mossong, J., Hens, N., Jit, M., Beutels, P., Auranen, K., Mikolajczyk, R., Massari, M., Salmaso, S., Tomba, G. S., Wallinga, J., Heijne, J., Sadkowska-Todys, M., Rosinska, M., and Edmunds, W. J. (2008). Social contacts and mixing patterns relevant to the spread of infectious diseases. *PLOS Medicine*, 5(3):1–1.

Mpolya, E. A., Lembo, T., Lushasi, K., Mancy, R., Mbunda, E. M., Makungu, S., Maziku, M., Sikana, L., Jaswant, G., Townsend, S., Meslin, F.-X., Abela-Ridder, B., Ngeleja, C., Changalucha, J., Mtema, Z., Sambo, M., Mchau, G., Rysava, K., Nanai, A., Kazwala, R., Cleaveland, S., and Hampson, K. (2017). Toward elimination of dog-mediated human rabies: Experiences from implementing a large-scale demonstration project in southern tanzania. *Frontiers in Veterinary Science*, 4:21.

Mtema, Z., Changalucha, J., Cleaveland, S., Elias, M., Ferguson, H. M., Halliday, J. E. B., Haydon, D. T., Jaswant, G., Kazwala, R., Killeen, G. F., Lembo, T., Lushasi, K., Malishee, A. D., Mancy, R., Maziku, M., Mbunda, E. M., Mchau, G. J. M., Murray-Smith, R., Rysava, K., Said, K., Sambo, M., Shayo, E., Sikana, L., Townsend, S. E., Urassa, H., and Hampson, K. (2016). Mobile Phones As Surveillance Tools: Implementing and Evaluating a Large-Scale Intersectoral Surveillance System for Rabies in Tanzania. *PLOS Medicine*, 13(4):1–12.

Müller, J., Schonfisch, B., and Kirkilionis, M. (2000). Ring vaccination. *J Math Biol*, 41(2):143–171.

Müller, T., Demetriou, P., Moynagh, J., Cliquet, F., Fooks, A., Conraths, F., Mettenleiter, T., and Freuling, C. (2012). Rabies elimination in Europe: a success story. In AR, F. and T, M., editors, *Rabies control: towards sustainable prevention at the source*, page 3144. Oxford University Press, Paris, France.

Müller, T., Freuling, C. M., Wysocki, P., Roumiantzeff, M., Freney, J., Mettenleiter, T. C., and Vos, A. (2015). Terrestrial rabies control in the European Union: Historical achievements and challenges ahead. *The Veterinary Journal*, 203(1):10 – 17.

Müller, T., Schröder, R., Wysocki, P., Mettenleiter, T., and Freuling, C. (2015). Spatio-temporal use of oral rabies vaccines in fox rabies elimination programmes in Europe. *PLOS Neglected Tropical Diseases*, 9(8):1–16.

Murray, J. D., Stanley, E., and Brown, D. (1986). On the spatial spread of rabies among foxes. *Proceedings of the Royal Society of London*, 229(2):111–150.

Muthiani, Y., Traoré, A., Mauti, S., Zinsstag, J., and Hattendorf, J. (2015). Low coverage of central point vaccination against dog rabies in bamako, mali. *Preventive Veterinary Medicine*, 120(2):203 – 209.

Neilan, R. M. and Lenhart, S. (2011). Optimal vaccine distribution in a spatiotemporal epidemic model with an application to rabies and raccoons. *Journal of Mathematical Analysis and Applications*, 378(2):603 – 619.

Newman, M. E. J. (2003). The structure and function of complex networks. *SIAM Review*, 45(2):167–256.

Obrist, B., Iteba, N., Lengeler, C., Makemba, A., Mshana, C., Nathan, R., Alba, S., Dillip, A., Hetzel, M., Mayumana, I., Schulze, A., and Mshinda, H. (2007). Access to health care in contexts of livelihood insecurity: A framework for analysis and action. *PLOS Medicine*, 4(10):1–5.

Ou, C. and Wu, J. (2006). Spatial Spread of Rabies Revisited: Influence of AgeDependent Diffusion on Nonlinear Dynamics. *SIAM Journal on Applied Mathematics*, 67(1):138–163.

Pastor-Satorras, R., Castellano, C., Mieghem, P. V., and Vespignani, A. (2015). Epidemic processes in complex networks. *Rev. Mod. Phys.*, 87:925–979.

Pastor-Satorras, R. and Vespignani, A. (2001). Epidemic spreading in scale-free networks. *Phys. Rev. Lett.*, 86:3200–3203.

Rainey, J. J., Cheriyadat, A., Radke, R. J., Crumly, J. S., and Koch, D. B. (2014). Estimating contact rates at a mass gathering by using video analysis: a proof-of-concept project. *BMC Public Health*, 14(1):1101.

Read, J. M., Edmunds, W. J., Riley, S., Lessler, J., and Cummings, D. A. (2012). Close encounters of the infectious kind: methods to measure social mixing behaviour. *Epidemiol. Infect.*, 140(12):2117–2130.

Reynolds, J. J., Hirsch, J. J., Gehrt, S. D., and Craft, M. E. (2015). Raccoon contact networks predict seasonal susceptibility to rabies outbreaks and limitations of vaccination. *J Anim Ecol*, 84(6):1720–1731.

Rohani, P., Zhong, X., and King, A. A. (2010). Contact network structure explains the changing epidemiology of pertussis. *Science*, 330(6006):982–985.

Roy, A., Phares, T. W., Koprowski, H., and Hooper, D. C. (2007). Failure to open the blood-brain barrier and deliver immune effectors to central nervous system tissues leads to the lethal outcome of silver-haired bat rabies virus infection. *J. Virol.*, 81(3):1110–1118.

Ruan, S. (2017). Modeling the transmission dynamics and control of rabies in China. *Mathematical Biosciences*, 286:65 – 93.

Salathé, M., Kazandjieva, M., Lee, J. W., Levis, P., Feldman, M. W., and Jones, J. H. (2010). A high-resolution human contact network for infectious disease transmission. *Proc. Natl. Acad. Sci. U.S.A.*, 107(51):22020–22025.

Schwenk, A. J. (1986). Tight bounds on the spectral radius of asymmetric nonnegative matrices. *Linear Algebra and its Applications*, 75(1).

Silk, M. J., Croft, D. P., Delahay, R. J., Hodgson, D. J., Weber, N., Boots, M., and McDonald, R. A. (2017). The application of statistical network models in disease research. *Methods in Ecology and Evolution*, 8(9):1026–1041.

Singh, R., Singh, K. P., Cherian, S., Saminathan, M., Kapoor, S., Reddy, G. M., Panda, S., and Dhama, K. (2017). Rabies epidemiology, pathogenesis, public health concerns and advances in diagnosis and control: a comprehensive review. *Veterinary Quarterly*, 37(1):212–251. PMID: 28643547.

Slate, D., Algeo, T. P., Nelson, K. M., Chipman, R. B., Donovan, D., Blanton, J. D., Niezgoda, M., and Rupprecht, C. E. (2009). Oral rabies vaccination in north america: Opportunities, complexities, and challenges. *PLOS Neglected Tropical Diseases*, 3(12):1–9.

Smieszek, T. (2009). A mechanistic model of infection: why duration and intensity of contacts should be included in models of disease spread. *Theor Biol Med Model*, 6:25.

Smieszek, T., Fiebig, L., and Scholz, R. W. (2009). Models of epidemics: when contact repetition and clustering should be included. *Theoretical Biology and Medical Modelling*, 6(1):11.

Smieszek, T. and Salathé, M. (2013). A low-cost method to assess the epidemiological importance of individuals in controlling infectious disease outbreaks. *BMC Medicine*, 11(1):35.

Smith, D. L., Lucey, B., Waller, L. A., Childs, J. E., and Real, L. A. (2001). Predicting the spatial dynamics of rabies epidemics on heterogeneous landscapes. *Proceedings of the National Academy of Sciences of the United States of America*, 99(6).

Smith, T. G., Millien, M., Vos, A., Fracciterne, F. A., Crowdis, K., Chirodea, C., Medley, A., Chipman, R., Qin, Y., Blanton, J., and Wallace, R. (2017). Evaluation of immune responses in dogs to oral rabies vaccine under field conditions. *Vaccine*.

Stadler, T., Kühnert, D., Bonhoeffer, S., and Drummond, A. J. (2013). Birth–death skyline plot reveals temporal changes of epidemic spread in HIV and hepatitis C virus (HCV). *Proceedings of the National Academy of Sciences*, 110(1):228–233.

Stehlé, J., Voirin, N., Barrat, A., Cattuto, C., Isella, L., Pinton, J.-F., Quaggiotto, M., den Broeck, W. V., Régis, C., Lina, B., and Vanhems, P. (2011). High-resolution measurements of face-to-face contact patterns in a primary school. *PLOS ONE*, 6(8):1–13.

Steinbrecher, A. (2008). Fährtensuche: Hunde in der frühneuzeitlichen Stadt. *Traverse : Zeitschrift für Geschichte = Revue d'histoire*, 15(3).

Talbi, C., Holmes, E. C., de Benedictis, P., Faye, O., Nakouné, E., Gamatié, D., Diarra, A., Elmamy, B. O., Sow, A., Adjogoua, E. V., Sangare, O., Dundon, W. G., Capua, I., Sall, A. A., and Bourhy, H. (2009). Evolutionary history and dynamics of dog rabies virus in western and central Africa. *Journal of General Virology*, 90(4):783–791.

Talbi, C., Lemey, P., Suchard, M. A., Abdelatif, E., Elharrak, M., Jalal, N., Faouzi, A., Echevarría, J. E., Vazquez, S. M., Rambaut, A., Campiz, N., Tatem, A. J., Holmes, E. C., and Bourhy, H. (2010). Phylodynamics and human-mediated dispersal of a zoonotic virus. *PLOS Pathogens*, 6(10):1–10.

Tarantola, A. (2017). Four thousand years of concepts relating to rabies in animals and humans, its prevention and its cure. *Tropical Medicine and Infectious Disease*, 2(2).

Tohma, K., Saito, M., Demetria, C. S., Manalo, D. L., Quiambao, B. P., Kamigaki, T., and Oshitani, H. (2016). Molecular and mathematical modeling analyses of inter-island transmission of rabies into a previously rabies-free island in the Philippines. *Infection, Genetics and Evolution*, 38:22 – 28.

Townsend, S. E., Lembo, T., Cleaveland, S., Meslin, F. X., Miranda, M. E., Putra, A. A. G., Haydon, D. T., and Hampson, K. (2013a). Surveillance guidelines for disease elimination: A case study of canine rabies. *Comparative Immunology, Microbiology and Infectious Diseases*, 36(3):249 – 261. Special issue: One Health.

Townsend, S. E., Sumantra, I. P., Bagus, G. N., Brum, E., Cleaveland, S., Crafter, S., Dewi, A. P. M., Dharma, D. M. N., Dushoff, J., Girardi, J., Gunata, I. K., Hiby, E. F., Kalalo, C., Knobel, D. L., Mardiana, I. W., Putra, A. A. G., Schoonman, L., Scott-Orr, H., Shand, M., Sukanadi, I. W., Suseno, P. P., Haydon, D. T., and Hampson, K. (2013b). Designing Programs for Eliminating Canine Rabies from Islands: Bali, Indonesia as a Case Study. *PLOS Neglected Tropical Diseases*, 7(8):1–11.

Undurraga, E., Meltzer, M., Tran, C., Atkins, C., Etheart, M., Millien, M., Adrien, P., and Wallace, R. (2017). Cost-effectiveness evaluation of a novel integrated bite case management program for the control of human rabies, haiti 20142015. *The American journal of tropical medicine and hygiene*, 96.

Velasco-Villa, A., Escobar, L. E., Sanchez, A., Shi, M., Streicker, D. G., Gallardo-Romero, N. F., Vargas-Pino, F., Gutierrez-Cedillo, V., Damon, I., and Emerson, G. (2017). Successful strategies implemented towards the elimination of canine rabies in the Western Hemisphere. *Antiviral Research*, 143:1 – 12.

Wallinga, J., Teunis, P., and Kretzschmar, M. (2006). Using data on social contacts to estimate age-specific transmission parameters for respiratory-spread infectious agents. *Am. J. Epidemiol.*, 164(10):936–944.

Warrel, M. J. and Warrel, D. A. (2004). Rabies and other lyssavirus diseases. *The Lancet*, 363(9413):959 – 969.

Wasik, B. and Murphy, M. (2012). *Rabid*. Penguin Books.

Watts, D. J. and Strogatz, S. H. (1998). Collective dynamics of 'small-world' networks. *Nature*, 393(6684):440–442.

White, L. A., Forester, J. D., and Craft, M. E. (2017). Using contact networks to explore mechanisms of parasite transmission in wildlife. *Biol Rev Camb Philos Soc*, 92(1):389–409.

White, P. C. L., Harris, S., and Smith, G. C. (1995). Fox contact behaviour and rabies spread: A model for the estimation of contact probabilities between urban foxes at different population densities and its implications for rabies control in Britain. *Journal of Applied Ecology*, 32(4):693–706.

WHO (1957). Expert Committee on Rabies, Third Report. Technical report, World Health Organization.

WHO (2010). Rabies vaccines: WHO position paper-recommendations. Technical report, World Health Organization.

WHO (2012). Accelerating work to overcome the global impact of neglected tropical diseases a roadmap for implementation. Technical report, World Health Organization.

WHO (2013). WHO Expert Consultation on Rabies: Second Report. Technical report, World Health Organization.

WHO (2015). Global Elimination of Dog-Mediated Human Rabies: Report on the Global Rabies Conference. Technical report, World Health Organization.

WHO (2018). WHO Expert Consultation on Rabies: Third Report. Technical report, World Health Organization.

Willoughby, R. E. (2007). A cure for rabies? *Scientific American*, 296(4):88–95.

Wu, J., Dhingra, R., Gambhir, M., and Remais, J. (2013). Sensitivity analysis of infectious disease models: methods, advances and their application. *Journal of The Royal Society Interface*, 10(86).

Yorke, J. A., Hethcote, H. W., and Nold, A. (1978). Dynamics and control of the transmission of gonorrhea. *Sex Transm Dis*, 5(2):51–56.

Zinsstag, J. (2013). Towards a science of rabies elimination. *Infect. Dis. Poverty*, 22.

Zinsstag, J., Dürr, S., Penny, M. A., Mindekem, R., Roth, F., Gonzalez, S., Naissengar, S., and Hattendorf, J. (2009). Transmission dynamics and economics of rabies control in dogs and humans in an African city. *Proceedings of the National Academy of Sciences*, 106(35):14996–15001.

Zinsstag, J., Léchenne, M., Laager, M., Mindekem, R., Nassengar, S., Oussigre, A., Bidjeh, K., Rives, G., Teissier, J., Madjaninan, S., Ouagal, M., Moto, D. D., Alfaroukh, I. O., Muthiani, Y., Traoré, A., Hattendorf, J., Lepelletier, A., Bourhy, H., Dacheux, L., Stadler, T., and Chitnis, N. (2017). Vaccination of dogs in an african city interrupts rabies transmission and reduces human exposure. *Science Translational Medicine*, 9(421).

Zulu, G., Sabeta, C., and Nel, L. (2009). Molecular epidemiology of rabies: Focus on domestic dogs (Canis familiaris) and black-backed jackals (Canis mesomelas) from northern South Africa. *Virus Research*, 140(1):71 – 78.

List of Figures

List of Tables